



State of Wyoming
Department of Transportation

FINAL REPORT WY-1901F (Vol 1)



UPDATING AND IMPLEMENTING THE GRADE SEVERITY RATING SYSTEM (GSRs) FOR WYOMING MOUNTAIN PASSES (VOLUME 1)

By:

Department of Civil & Architectural Engineering
Wyoming Technology Transfer Center
University of Wyoming
1000 E. University Avenue, Dept. 3295
Laramie, Wyoming 82071

December 2018

DISCLAIMER

Notice

This document is disseminated under the sponsorship of the Wyoming Department of Transportation (WYDOT) in the interest of information exchange. WYDOT assumes no liability for the use of the information contained in this document.

WYDOT does not endorse products or manufacturers. Trademarks or manufacturers' names appear in this report only because they are considered essential to the objective of the document.

Quality Assurance Statement

The Wyoming Department of Transportation (WYDOT) provides high-quality information to serve government, industry, and the public in a manner that promotes public understanding. Standards and policies are used to ensure and maximize the quality, objectivity, utility, and integrity of its information. WYDOT periodically reviews quality issues and adjusts its programs and processes to ensure continuous quality improvement.

Copyright

No copyrighted material, except that which falls under the "fair use" clause, may be incorporated into a report without permission from the copyright owner, if the copyright owner requires such. Prior use of the material in a WYDOT or governmental publication does not necessarily constitute permission to use it in a later publication.

- **Courtesy** — Acknowledgment or credit will be given by footnote, bibliographic reference, or a statement in the text for use of material contributed or assistance provided, even when a copyright notice is not applicable.
- **Caveat for Unpublished Work** — Some material may be protected under common law or equity even though no copyright notice is displayed on the material. Credit will be given and permission will be obtained as appropriate.
- **Proprietary Information** — To avoid restrictions on the availability of reports, proprietary information will not be included in reports, unless it is critical to the understanding of a report and prior approval is received from WYDOT. Reports containing such proprietary information will contain a statement on the Technical Report Documentation Page restricting availability of the report.

Creative Commons:

The report is covered under a Creative Commons, CC-BY-SA license. When drafting an adaptive report or when using information from this report, ensure you adhere to the following:

Attribution — You must give appropriate credit, provide a link to the license, and indicate if changes were made. You may do so in any reasonable manner, but not in any way that suggests the licensor endorses you or your use.

ShareAlike — If you remix, transform, or build upon the material, you must distribute your contributions under the same license as the original.

No additional restrictions — You may not apply legal terms or technological measures that legally restrict others from doing anything the license permits.

You do not have to comply with the license for elements of the material in the public domain or where your use is permitted by an applicable exception or limitation.

No warranties are given. The license may not give you all of the permissions necessary for your intended use. For example, other rights such as publicity, privacy, or moral rights may limit how you use the material.

Technical Report Documentation Page

1. Report No. WY-1901F		2. Governmental Accession No.		3. Recipient's Catalog No.	
4. Title and Subtitle Updating and Implementing the Grade Severity Rating System (GSRS) for Wyoming Mountain Passes.				5. Report Date December 2018	
7. Author(s) Milhan Moomen (0000-0001-8324-7540), Dick Apronti (0000-0002-2072-2030), Amirarsalan Molan (0000-0002-8540-1174), Khaled Ksaibati (0000-0002-9241-1792)				6. Performing Organization Code	
9. Performing Organization Name and Address Department of Civil & Architectural Engineering Wyoming Technology Transfer Center University of Wyoming 1000 E. University Avenue, Dept. 3295 Laramie, Wyoming 82071				8. Performing Organization Report No.	
12. Sponsoring Agency Name and Address Wyoming Department of Transportation 5300 Bishop Blvd. Cheyenne, WY 82009-3340 WYDOT Research Center (307) 777-4182				10. Work Unit No.	
12. Sponsoring Agency Name and Address Wyoming Department of Transportation 5300 Bishop Blvd. Cheyenne, WY 82009-3340 WYDOT Research Center (307) 777-4182				11. Contract or Grant No. RS08(216)	
12. Sponsoring Agency Name and Address Wyoming Department of Transportation 5300 Bishop Blvd. Cheyenne, WY 82009-3340 WYDOT Research Center (307) 777-4182				13. Type of Report and Period Covered Final Report	
12. Sponsoring Agency Name and Address Wyoming Department of Transportation 5300 Bishop Blvd. Cheyenne, WY 82009-3340 WYDOT Research Center (307) 777-4182				14. Sponsoring Agency Code WYDOT	
15. Supplementary Notes WYDOT Technical Contact: Matt Carlson, P.E., State Highway Safety Engineer					
16. Abstract: The State of Wyoming like other western States is characterized by steep downgrades on mountainous highways. Such difficult terrain presents considerable crash risks to truck drivers inexperienced or unfamiliar with the landscape. Truck crashes on Wyoming mountain passes have been a cause for concern due to their devastating effect on lives and property. A major contributory factor to such truck crashes is brake failure. The risk of truck brake failure on downgrades is high due to the large amounts of heat energy generated during braking activity in such a difficult geometry. The Grade Severity Rating System (GSRS) was developed in the early 1980s to enhance truck safety on downgrades by recommending maximum safe descent speeds through Weight Specific Speed (WSS) signs. However, truck designs, brake and engine characteristics have changed during the intervening decades. This study updated the GSRS model to reflect current truck population characteristics. The updated GSRS model will engender driver compliance and confidence in the new recommended speeds, thereby improving mountain pass safety in Wyoming.					
17. Key Words Mountain Pass, Truck Crashes, GSRS, Updating,			18. Distribution Statement This document is available through the National Transportation Library; and the Wyoming State Library. Copyright © 2016. All rights reserved, State of Wyoming, Wyoming Department of Transportation, and University of Wyoming.		
19. Security Classif. (of this report) Unclassified		20. Security Classif. (of this page) Unclassified		21. No. of Pages 130	22. Price

Form DOT F 1700.7 (8-72) Reproduction of completed page authorized

SI* (MODERN METRIC) CONVERSION FACTORS

APPROXIMATE CONVERSIONS TO SI UNITS

Symbol	When You Know	Multiply By	To Find	Symbol
LENGTH				
in	inches	25.4	millimeters	mm
ft	feet	0.305	meters	m
yd	yards	0.914	meters	m
mi	miles	1.61	kilometers	km
AREA				
in ²	square inches	645.2	square millimeters	mm ²
ft ²	square feet	0.093	square meters	m ²
yd ²	square yard	0.836	square meters	m ²
ac	acres	0.405	hectares	ha
mi ²	square miles	2.59	square kilometers	km ²
VOLUME				
fl oz	fluid ounces	29.57	milliliters	mL
gal	gallons	3.785	liters	L
ft ³	cubic feet	0.028	cubic meters	m ³
yd ³	cubic yards	0.765	cubic meters	m ³
NOTE: volumes greater than 1000 L shall be shown in m ³				
MASS				
oz	ounces	28.35	grams	g
lb	pounds	0.454	kilograms	kg
T	short tons (2000 lb)	0.907	megagrams (or "metric ton")	Mg (or "t")
TEMPERATURE (exact degrees)				
°F	Fahrenheit	5 (F-32)/9 or (F-32)/1.8	Celsius	°C
ILLUMINATION				
fc	foot-candles	10.76	lux	lx
fl	foot-Lamberts	3.426	candela/m ²	cd/m ²
FORCE and PRESSURE or STRESS				
lbf	poundforce	4.45	newtons	N
lbf/in ²	poundforce per square inch	6.89	kilopascals	kPa

APPROXIMATE CONVERSIONS FROM SI UNITS

Symbol	When You Know	Multiply By	To Find	Symbol
LENGTH				
mm	millimeters	0.039	inches	in
m	meters	3.28	feet	ft
m	meters	1.09	yards	yd
km	kilometers	0.621	miles	mi
AREA				
mm ²	square millimeters	0.0016	square inches	in ²
m ²	square meters	10.764	square feet	ft ²
m ²	square meters	1.195	square yards	yd ²
ha	hectares	2.47	acres	ac
km ²	square kilometers	0.386	square miles	mi ²
VOLUME				
mL	milliliters	0.034	fluid ounces	fl oz
L	liters	0.264	gallons	gal
m ³	cubic meters	35.314	cubic feet	ft ³
m ³	cubic meters	1.307	cubic yards	yd ³
MASS				
g	grams	0.035	ounces	oz
kg	kilograms	2.202	pounds	lb
Mg (or "t")	megagrams (or "metric ton")	1.103	short tons (2000 lb)	T
TEMPERATURE (exact degrees)				
°C	Celsius	1.8C+32	Fahrenheit	°F
ILLUMINATION				
lx	lux	0.0929	foot-candles	fc
cd/m ²	candela/m ²	0.2919	foot-Lamberts	fl
FORCE and PRESSURE or STRESS				
N	newtons	0.225	poundforce	lbf
kPa	kilopascals	0.145	poundforce per square inch	lbf/in ²

TABLE OF CONTENTS

CHAPTER 1: INTRODUCTION.....	1
INTRODUCTION AND BACKGROUND OF DOWNGRADE TRUCK SAFETY	1
PROBLEM STATEMENT	2
STUDY OBJECTIVES	3
REPORT ORGANIZATION.....	3
CHAPTER 2: LITERATURE REVIEW	5
TRUCK SAFETY IN THE UNITED STATES.....	5
WYOMING TRUCK CRASH STATISTICS	6
PREVIOUS GSRS STUDIES.....	6
Bureau of Public Roads Rating System.....	7
Hykes Grade Rating System.....	7
Lill’s Grade Rating System.....	8
The FHWA Grade Severity Rating System	10
THE NEED TO UPDATE THE GSRS	14
Reduced Stopping Distance Requirements	16
TRUCK TYPES IN THE UNITED STATES.....	17
WEIGHT AND SPEED LIMITS IN THE STATE OF WYOMING.....	17
CHAPTER SUMMARY.....	20
CHAPTER 3: THE TRUCK DOWNGRADE BRAKING MODEL AND THE GSRS.....	23
THE GRADE DESCENT PROBLEM.....	23
THE BRAKE TEMPERATURE MODEL	25
Forces acting on a truck on a downgrade.....	25
Available Brake force.....	25
Engine Friction Power.....	26
TRUCK BRAKING SYSTEMS.....	27
Service Brakes.....	28
Retarders	30
INTEGRATION OF THE BRAKE TEMPERATURE EQUATION.....	31
IMPLICATIONS OF THE GSRS MODEL	36
Multi-grade Hills.....	49

CHAPTER 4: METHODOLOGY	51
TEST METHODOLOGY	51
TEST PROGRAM OVERVIEW	52
TEST VEHICLE PREPARATION.....	55
TEST DESCRIPTION.....	62
Site Selection and Traffic Control.....	62
Test Vehicle Preparation Tests.....	63
Main Field Tests.....	64
CHAPTER SUMMARY	67
CHAPTER 5: RESULTS	69
VEHICLE PREPARATORY TESTS	69
Brake Burnish Tests	69
Brake Balance Tests	69
FIELD TESTS TO UPDATE THE GSRS	70
Coast-down Tests (No Engine Braking)	70
Coast-down Testing to Determine Engine Braking.....	76
Cool-down Tests.....	78
Hill Descent Tests.....	81
Use of the Updated Brake Temperature Model.....	83
VALIDATION OF THE UPDATED BRAKE TEMPERATURE MODEL	85
WEIGHT SPECIFIC SPEED (WSS) SIGNS	88
Formulation of WSS Signs.....	90
Example of Weight and Speed Determination and Comparison of Maximum Speeds from the Modified GSRS (Old GSRS) and the Updated GSRS	91
USE OF RETARDERS.....	93
CHAPTER SUMMARY	94
CHAPTER 6: CONCLUSIONS AND RECOMMENDATIONS.....	97
CONCLUSIONS	97
Summary	97
RECOMMENDATIONS	99
FUTURE STUDIES	101
REFERENCES.....	103
APPENDIX 1: COAST-DOWN PLOTS	109

Coast-down Test Plots to Determine Drag Forces (Truck Loaded- No Jake Brake)..	109
Coast-down Test Plots to Determine Drag Force (Truck Unloaded-No Jake Brake).	111
Coast-down Test Plots to Determine Engine Brake Force (Truck Loaded - Full Jake)	112
Coast-down Test Plots to Determine Engine Brake Force (Truck Loaded – Half Jake)	114
APPENDIX 2: COOL-DOWN PLOTS	117
Extraction of Diffusivity Constant (K_1)	117
APPENDIX 3: HILL DESCENT PLOTS	121
Plots of Power into the Brakes	121
APPENDIX 4: MAXIMUM SAFE SPEED PLOT	125
APPENDIX 5: CASE STUDY 2	137
Case Study 2	137
APPENDIX 6: FIELD PICTURES	139
ACKNOWLEDGEMENTS	143

LIST OF FIGURES

Figure 1. Graph. Large Trucks and Passenger Vehicles Involved in Fatal Crashes Per 100 Million VMT, 1975-2014. (Data From Federal Motor Carrier Safety Administration, 2016).	6
Figure 2. Graph. Downgrade Truck Crashes on United States Highway 14.	7
Figure 3. Equation. Grade Ability Formula	8
Figure 4. Chart. Hykes Proposed Grade Rating System. (Hykes, 1963).	9
Figure 5. Chart. Lill’s Proposed Grade Severity Rating System. (Myers et al., 1981).	10
Figure 6. Picture. FHWA GSRS DOS Program Output. (Johnson et al., 1982a).	11
Figure 7. Picture. Example of a WSS Sign. (Johnson et al., 1982a).	12
Figure 8. Equation. Limiting Temperature.	12
Figure 9. Equation. Temperature Rise from Emergency Stopping.	12
Figure 10. Picture. Approximate Distribution of Drag Loss For a Typical Tractor Semitrailer on a Level Road. (Woodrooffe, 2014).	14
Figure 11. Photo. Examples of Aerodynamic Reduction Devices	16
Figure 12. Chart. United States’ Market Share of Heavy Duty Truck Models. (Statista.com, 2018).	18
Figure 13. Picture. Common Truck Configurations in the United States’ Heavy Vehicle Fleet. (FHWA, 2015).	19
Figure 14. Illustration. Bell-Mouthing of a Drum Brake. (Myers et al., 1981)	24
Figure 15. Illustration. Equilibrium of Forces during Descent. (Truck picture:www.topsimages.com, 2018).	26
Figure 16. Equation. Equilibrium of Forces.	26
Figure 17. Equation. Braking Force.	26
Figure 18. Equation. Friction Horsepower.	27
Figure 19. Equation. Empirical Horsepower Relationship.	27
Figure 20. Equation. Engine Drag Torque Calculation.	27
Figure 21. Picture. Typical Drum Brake. (Performance Review Institute, 2018).	29
Figure 22. Photo. Air Disc Brake. (Roberts, 2014).	30
Figure 23. Equation. Energy Balance.	31
Figure 24. Equation. Heat Transfer Relation.	32
Figure 25. Equation. First Order Brake Temperature Equation.	32
Figure 26. Equation. Horsepower into Brakes.	32
Figure 27. Picture. Bathtub Analogy of Brake Heat Transfer. (Bendix Spicer Foundation Brake LLC, 2011).	33
Figure 28. Equation. Brake Temperature Equation at Time (t).	34
Figure 29. Equation. Brake Temperature Equation at Distance (x).	34
Figure 30. Equation. Steady State Temperature.	34
Figure 31. Equation. Relation between Temperature Change and Power into Brakes.	35
Figure 32. Equation. Brake Temperature Equation for Non-Braking Intervals.	35
Figure 33. Graph. Variation of Length with Temperature. (Myers et al., 1981).	37
Figure 34. Graph. Variation of Grade with Temperature. (Myers et al., 1981).	37
Figure 35. Graph. Isotherms as a Function of Grade and Length. (Myers et al., 1981).	38
Figure 36. Graph. Variation of Weight and Temperature with Speed as a Parameter. (Myers et al., 1981).	39
Figure 37. Graph. Weight as a Function of Temperature and Speed. (Myers et al., 1981).	39

Figure 38. Graph. Isotherms as a Function of Weight And Speed. (Myers et al., 1981).	40
Figure 39. Graph. Variation of Brake Temperature with Speed. (Myers et al., 1981).	41
Figure 40. Graph. Variation of Brake Horsepower Absorption with Speed. (Myers et al., 1981).	41
Figure 41. Graph. Variation of Convective Heat Transfer Parameter with Speed. (Myers et al., 1981).	42
Figure 42. Graph. Steady State Brake Temperature. (Myers et al., 1981).	42
Figure 43. Graph. Exponential Variation of Steady-State Temperature. (Myers et al., 1981).	43
Figure 44. Graph. Brake Pressure Variation with Temperature. (Myers et al., 1981).	44
Figure 45. Equation. Limiting Temperature Constraint.	44
Figure 46. Equation. Steady State at Limiting Temperature.	45
Figure 47. Equation. Limiting Temperature at Bottom of Grade.	45
Figure 48. Equation. Relationship between Final and Limiting Brake Temperature.	46
Figure 49. Equation. Relation for Plotting Maximum Descent Speed Curves.	46
Figure 50. Graph. Maximum slopes for Vmax and grade length. (Myers et al., 1981).	47
Figure 51. Flowchart. GSRS Methodology.	51
Figure 52. Flowchart. GSRS Test Flow Chart	53
Figure 53. Photo. Test Truck.	56
Figure 54. Diagram. Instrumentation Layout.	58
Figure 55. Photo. Cab Controller Box	59
Figure 56. Photo. Signal Conditioning and Power Distribution Box.	59
Figure 57. Photos. Truck Instrumentation and Sensors	60
Figure 58. Photo. MICAS-X® Display. (Original Code Consulting, 2017).	61
Figure 59. Photo. MICAS-X® Plots. (Original Code Consulting, 2017).	61
Figure 60. Photo. Loading for Tests.	62
Figure 61. Photo. WYDOT Traffic Vehicles.	63
Figure 62. Plot. Brake Effectiveness during Burnish Tests.	69
Figure 63. Equation. Sum of Drag Forces Acting on a Truck.	70
Figure 64. Equation. Effective Mass.	70
Figure 65. Equation. Drag Force Equation.	70
Figure 66. Photo. © 2018 Google. Coast-down Test Track. (Google, 2018).	71
Figure 67. Velocity-Time Trace for Coast-down Run. (Truck Loaded – No Jake Brake)...	72
Figure 68. Photo. TruckSim 3D Visualization of a Coast-down Run. (Mechanical Simulation Corp., 2018).	73
Figure 69. Photo. Velocity-Time Trace Plot of a Coast-down Run from TruckSim. (Mechanical Simulation Corp., 2018).	74
Figure 70. Equation. Coastdown Calibration Curve.	74
Figure 71. Flowchart for Calibration Curve and Validation.	75
Figure 72. Equation. Calibrated Drag Force.	76
Figure 73. Equation. Determination of Engine Brake Force.	76
Figure 74. Equation. Engine Brake Force Determination.	77
Figure 75. Equation. Determining Horsepower into the Brakes.	77
Figure 76. Graph. Estimation of Brake Force.	77
Figure 77. Equation. Newton Cooling.	78
Figure 78. Equation. Modified Newton Cooling.	78

Figure 79. Equation. Relationship between K_1 and Truck Speed.	78
Figure 80. Graph. K_1 Extraction for $V = 0$ mph (Left Brakes).	79
Figure 81. Graph. Variation of K_1 with Speed (Left Brakes).	79
Figure 82. Graph. Variation of K_1 with Speed (Right Brakes).	80
Figure 83. Graph. Expression of K_1 for Brake System in Terms of Speed.	80
Figure 84. Equation. Correlation between Brake Temperature and Power into Brakes	81
Figure 85. Equation. Simplified Relation to Extract Brake Heating Constant (K_2).	81
Figure 86. Graph. Plot of Temperature Parameters versus Power into Brakes at 10 mph.	82
Figure 87. Equation. Relation Between (K_2) and Speed.	83
Figure 88. Graph. Variation of Heat Transfer Parameter ($1/K_2$) with Speed.	83
Figure 89. Equation. Determination of Maximum Descent Speed Plots.	84
Figure 90. Graph. Maximum Safe Speed as a Function of Grade Length and Steepness for Truck Weight 80,000 lb.	86
Figure 91. Graph. Grade Profile for Validation Test.	87
Figure 92. Graph. Comparison of Field and Predicted Brake Temperature from Validation Test.	88
Figure 93. Equation. Determining Number of Weight Intervals to be placed on WSS Sign.	90
Figure 94. Equation. Determination of Equivalent Weight Reduction Due to Retarder Use.	93
Figure 95. Graph. Velocity-Time Trace to Determine Drag Force Run 1 (Truck Loaded)	109
Figure 96. Graph. Velocity-Time Trace to Determine Drag Force Run 3 (Truck Loaded)	109
Figure 97. Graph. Velocity-Time Trace to Determine Drag Force Run 4 (Truck Loaded)	110
Figure 98. Graph. Velocity-Time Trace to Determine Drag Force Run 5 (Truck Loaded)	110
Figure 99. Plot. Velocity-Time Trace to Determine Drag Force Run 1 (Truck Unloaded)	111
Figure 100. Graph. Velocity-Time Trace to Determine Drag Force Run 2 (Truck Unloaded)	111
Figure 101. Graph. Velocity-Time Trace to Determine Engine Brake Force Run 1 (Truck Loaded)	112
Figure 102. Graph. Velocity-Time Trace to Determine Engine Brake Force Run 2 (Truck Loaded)	112
Figure 103. Graph. Velocity-Time Trace to Determine Engine Brake Force Run 3 (Truck Loaded)	113
Figure 104. Graph. Velocity-Time Trace to Determine Engine Brake Force Run 4 (Truck Loaded)	113
Figure 105. Graph. Velocity-Time Trace to Determine Engine Brake Force Run 5 (Truck Loaded)	114
Figure 106. Graph. Velocity-Time Trace to Determine Engine Brake Force Run 1 (Truck Loaded)	114
Figure 107. Graph. Velocity-Time Trace to Determine Engine Brake Force Run 2 (Truck Loaded)	115
Figure 108. Graph. K_1 Extraction for $V = 0$ mph (Right Brakes)	117

Figure 109. Graph. K_1 Extraction for $V = 20$ mph (Left Brakes)	118
Figure 110. Graph. K_1 Extraction for $V = 20$ mph (Right Brakes)	118
Figure 111. Graph. K_1 Extraction for $V = 30$ mph (Left Brakes)	119
Figure 112. Graph. K_1 Extraction for $V = 30$ mph (Right Brakes)	119
Figure 113. Graph. K_1 Extraction for $V = 45$ mph (Left Brakes)	120
Figure 114. Graph. K_1 Extraction for $V = 45$ mph (Right Brakes)	120
Figure 115. Graph. Plot of Temperature Parameters versus Power into Brakes at 21 mph	121
Figure 116. Graph. Plot of Temperature Parameters versus Power into Brakes at 31 mph	122
Figure 117. Graph. Plot of Temperature Parameters versus Power into Brakes at 36 mph	122
Figure 118. Graph. Plot of Temperature Parameters versus Power into Brakes at 50 mph	123
Figure 119. Graph. Maximum Safe Speed as a Function of Grade Length and Steepness for Truck Weight 95,000 lb	126
Figure 120. Graph. Maximum Safe Speed as a Function of Grade Length and Steepness for Truck Weight 90,000 lb	127
Figure 121. Graph. Maximum Safe Speed as a Function of Grade Length and Steepness for Truck Weight 85,000 lb	128
Figure 122. Graph. Maximum Safe Speed as a Function of Grade Length and Steepness for Truck Weight 75,000 lb	129
Figure 123. Graph. Maximum Safe Speed as a Function of Grade Length and Steepness for Truck Weight 70,000 lb	130
Figure 124. Graph. Maximum Safe Speed as a Function of Grade Length and Steepness for Truck Weight 65,000 lb	131
Figure 125. Graph. Maximum Safe Speed as a Function of Grade Length and Steepness for Truck Weight 60,000 lb	132
Figure 126. Graph. Maximum Safe Speed as a Function of Grade Length and Steepness for Truck Weight 55,000 lb	133
Figure 127. Graph. Maximum Safe Speed as a Function of Grade Length and Steepness for Truck Weight 50,000 lb	134
Figure 128. Graph. Maximum Safe Speed as a Function of Grade Length and Steepness for Truck Weight 45,000 lb	135
Figure 129. Photo. The ISX-15 Engine	139
Figure 130. Photo. Hyundai Van Trailer	139
Figure 131. Photo. Test Truck on a Weighing Scale	140
Figure 132. Photo. Technician Adjusting Air Pressure to Brakes	140
Figure 133. Photo. Truck Turning During Coast-down Testing	141
Figure 134. Photo. Cool-down Testing	141
Figure 135. Photo. Hill Descent Testing	142
Figure 136. Photo. Truck Brakes Cooling in between Testing	142

LIST OF TABLES

Table 1. Bathtub flow analogy vs. truck brake heating	34
Table 2. Summary of FHWA GSRS Model Parameters	36
Table 3. Test Types and Purpose of Tests	52
Table 4. Test Truck Specification.....	55
Table 5. Truck Instrumentation and Measured Parameters.....	56
Table 6. Test Locations.....	63
Table 7. Drag Terms from Field Coast-down Analysis.....	73
Table 8. Simulation Results for Loaded and Unloaded Test Weights	74
Table 9. Average Drag Coefficients from Field and Simulation Tests.....	76
Table 10. Comparison Simulation and Field Brake Temperatures	82
Table 11. Summary of Updated Temperature Model Parameters.....	84
Table 12. Summary of Validation Test and Results	88
Table 13. Maximum Truck Weights and Estimated Safe Speeds (Case Study 1 - Old GSRS)	91
Table 14. Maximum Truck Weights and Approximate Safe Speeds (Case Study 1 - Old GSRS)	92
Table 15. Maximum Truck Weights and Estimated Safe Speeds (Case Study 1 - Updated GSRS)	92
Table 16. Maximum Truck Weights and Approximate Safe Speeds (Case Study 1 - Updated GSRS)	92
Table 17. Effect of Retarder on Truck Weight	94
Table 18. Maximum Truck Weights and Estimated Safe Speeds (Case Study 2 - Old GSRS)	137
Table 19. Maximum Truck Weights and Approximate Safe Speeds (Case Study 1 - Old GSRS)	137
Table 20. Maximum Truck Weights and Estimated Safe Speeds (Case Study 2 - Updated GSRS)	138
Table 21. Maximum Truck Weights and Approximate Safe Speeds (Case Study 2 - Updated GSRS)	138

LIST OF ACRONYMS

AASHTO	American Association of State Highway and Transportation Officials
BHP	Brake Horsepower
BMCS	Bureau of Motor Carrier Safety
EPA	Environmental Protection Agency
FHP	Friction Horsepower
FHWA	Federal Highway Administration
FMVSS	Federal Motor Vehicle Safety Standards
GDP	Gross Domestic Product
GSR	Grade Severity Rating
GSRS	Grade Severity Rating System
GVW	Gross Vehicle Weight
IHP	Indicated Horsepower
ITS	Intelligent Transportation System
LCV	Longer Combination Vehicles
MICAS-X®	Multi-Instrument Control and Acquisition System-Extended
MUTCD	Manual on Uniform Traffic Control Devices
NHTSA	National Highway Traffic Safety Administration
NN	National Truck Network
SAE	Society of Automotive Engineers
USBPR	United States Bureau of Public Roads
VMT	Vehicle Miles Traveled
WSS	Weight Specific Speed
WYDOT	Wyoming Department of Transportation

CHAPTER 1: INTRODUCTION

This chapter begins with background information about truck safety on mountain passes. The problem statement and study objectives are also discussed. The chapter then presents the organization of the report and a chapter summary.

INTRODUCTION AND BACKGROUND OF DOWNGRADE TRUCK SAFETY

Mountain downgrades present enormous challenges to drivers of large trucks. Safely descending steep downgrades, which characterize mountain highways, require the use of the brake system to slow trucks down. Brake failure on downgrades is mostly attributed to excessive temperatures of the brake components. The continuous application of brakes on downgrades to slow heavy vehicles results in elevated brake temperatures. Brake components begin to distort and expand from brake linings while friction materials begin to lose their properties at high temperatures. This distortion has the potential to reduce the full surface-to-surface contact between the lining and the drum. This distortion, also referred to as bell-mouthing progressively decreases the braking efficiency. When this occurs, the driver is faced with three options; continuing down the hill and riding out the loss in braking efficiency, gambling on the residual braking power remaining, or attempting to stop completely to allow the brakes to cool. (Bowman, 1989). In situations where the residual horsepower is insufficient to control the speed to the end of the grade, or to bring the vehicle to a complete stop, then a runaway condition arises. Runaway events have devastating consequences to lives, property, and warrants the use of countermeasures to reduce their likelihood of occurrence.

The Bureau of Motor Carrier Safety (BMCS) carried out an investigation to identify causes of unusually severe truck crashes from 1973 to 1976. (Lill, 1977). A total of 496 crashes nationwide were identified for the study. The study found that 6 percent of the crashes were downgrade-related but that only a small portion of the crashes accounted for 40 percent of fatalities. Five primary factors were identified as being responsible for downgrade truck crashes. The factors were identified as:

- Failure to downshift on the grade, improper shifting, or the use of excessive speed (82 percent of the downgrade accidents).
- Drivers who were inexperienced or at least unfamiliar with the specific area (43 percent of the accidents).
- Inadequate signing for the downgrade (14 percent of the accidents).
- Defective truck brakes or improper brake adjustment (36 percent of the accidents).
- Indications of driver impairment such as the use of alcohol or fatigue due to excessive driving time (21 percent of the accidents).(Lill, 1977).

The conclusions from the investigation was that apart from the grade geometry, failure to downshift, and defective brakes appear to be the two primary factors in downgrade crashes. Inadequate signing and driver inexperience or impairment primarily cause failures to downshift and excessive speeding. These findings warranted the development of a Grade Severity Rating System (GSRS) and appropriate warning signs to aid drivers in choosing the correct speed and gear.(Myers et al., 1981). The GSRS cannot solve the problem of defective brakes or driver impairment but can aid drivers through the use of improved signing.

Grade information provided on warning signs by most states is based on the Manual on Uniform Traffic Control Devices (MUTCD). (FHWA, 2009). MUTCD recommends that hill signs be placed on the beginning of downgrades that may be hazardous for truck descent based on specified grade and length combinations. These signs are supplemented with appropriate legends where special characteristics exist. MUTCD recommends that mileage plaques should be used at one mile intervals to inform the driver of the length of the grade remaining for longer downgrades. However, the hill signs from the GSRS are general and do not give a complete picture of the downgrade.

The implementation of the GSRS and the accompanying weight specific speed (WSS) signs have proven to be effective in reducing the incidence of downgrade truck crashes due to brake failure. WSS signs are an improvement over conventional hill signs because they advise the driver on exactly what to do instead of just providing information, which requires analysis and decision-making. However, a few decades have passed since the GSRS was developed and implemented. Truck designs, brake, retarder and engine characteristics have changed markedly from the truck population which existed during the GSRS development. This warrants an update of the model and WSS signs.

This study was instituted to update the GSRS model to recommend maximum safe descent speeds which that will reduce the incidence of downgrade truck crashes attributed to brake failure on Wyoming mountain passes. The study consists of two main parts. The first involves reviewing, updating and validating the current Federal Highway Administration's (FHWA) Grade Severity Rating System (GSRS). The output from this task will be warning signs with advisory speeds for various truck weight categories (volume 1 of the report). The second task is a comprehensive evaluation of the current mountain pass warning system in Wyoming as well as the most current state of practice (volume 2 of the report). The most effective system of communicating the presence of hazardous downgrades and safe descent speeds to drivers is to be recommended by the study.

PROBLEM STATEMENT

The State of Wyoming is characterized by severe downgrades common to other western states. These downgrades are responsible for several truck crashes that have had a devastating consequence on lives and property due to the considerable dangers of driving on mountain passes. Downgrade truck crashes have been mainly attributed to brake failure that result from driver inexperience and unfamiliarity. The Wyoming Department of Transportation (WYDOT) has instituted several safety improvements to counter the incidence of downgrade truck crashes. However, these measures have failed to effectively arrest the problem. This study updated the FHWA's GSRS, that has been shown to reduce runaway truck crash occurrence on downgrades. An evaluation was also carried out of the current downgrade warning systems on Wyoming mountain passes. The recommendations from the study are aimed at reducing the incidence of truck crashes on Wyoming mountain passes, due to runaway truck crashes.

STUDY OBJECTIVES

The preceding discussion highlights the issue of downgrade truck crashes in Wyoming. It has been found that the GSRS has been effective in reducing the incidence of truck crashes on downgrades attributed to brake failure. The study aims to achieve two main goals. The first is to update the FHWA GSRS model to reflect the current truck population characteristics. Specifically, this will be achieved by carrying out field tests with an instrumented vehicle to update parameters in the GSRS model to account for the current characteristics of trucks in the United States fleet. The second objective of the study is to evaluate the effectiveness of the current warning system with regards to truck downgrade crashes. Different downgrade warning systems from intelligent transportation systems (ITS) have been reviewed as part of this study as well (volume 2 of the report). The output of this study is a recommendation of the best means of safely communicating downgrade information to truck drivers to reduce the incidence of runaway truck occurrence. Implementation of these recommendations will counter the occurrence and severity of downgrade truck crashes on Wyoming mountain passes.

REPORT ORGANIZATION

This report is organized into six chapters. The first chapter introduces truck safety on downgrades, problem statement, and study objectives. Chapter 2 is a review of literature on various subjects such as truck safety in the United States, previous studies on grade severity rating, the need to update the GSRS, truck types in the United States, weight and speed limits, among others. The third chapter discusses the truck downgrade braking model and the GSRS. The development of the brake temperature model, and its implications are also discussed in chapter 3. Chapter 4 describes the methodology adopted to achieve the objective of updating the parameters of the GSRS model. In chapter 5, the results of field tests and updated GSRS brake temperature model are discussed. The implementation of the GSRS and development of weight specific speed (WSS) signs are also presented in this chapter. Conclusions and recommendations for implementation of the study are offered in chapter 6.

CHAPTER 2: LITERATURE REVIEW

This chapter presents topics important to the need and development of the GSRS, starting with a brief discussion of truck safety in the United States and Wyoming. Previous studies on grade severity ratings are discussed along with their limitations. The chapter further discusses the need to update the GSRS in the light of improved truck designs, reduced engine friction, better tires and enhanced brakes. The chapter continues with a short description of truck types and their distribution in the United States. The chapter is concluded by looking at truck weight and speed limits in the United States in general and Wyoming.

TRUCK SAFETY IN THE UNITED STATES

Commercial vehicles play a critical role in the economy of the United States. The freight transportation industry employed 4.6 million people in 2014 and accounted for about 9.5 percent of the Nation's economic activity as measured by the gross domestic product (GDP). (U.S. Department of Transportation, 2015). According to the American Trucking Associations, trucks moved more than 10 billion tons of freight in 2015 and generated approximately \$730 billion in revenue; 81.5 percent of the Nation's freight bill. (American Truckers Associations, 2016). Approximately 11 million large trucks are registered in the country representing about 4.3 percent of the entire vehicle population. Large trucks traveled 288,306 million miles in 2013 out of a total 2,956,764 for all vehicles. (Federal Motor Carrier Safety Administration, 2014).

Truck safety has witnessed an improving trend over the past few decades. In 1979, large trucks were involved in 5.6 fatal crashes per 100 million vehicle miles traveled (VMT); the highest in five decades of data (Figure 1). By 2014, this had reduced to 1.3 fatal crashes per 100 million VMT representing a reduction of 77 percent. On the other hand, passenger vehicles had a fatality reduction of 65 percent, per 100 million VMT, within the same period. (Federal Motor Carrier Safety Administration, 2016). These overall decreases in truck-related fatalities is down to factors such as improved roads, improved truck braking systems, and an increased, uniform motorist information systems. (Bowman, 1989).

Despite these encouraging trends combined with the efforts of most motor carriers to operate responsibly, many motorists are wary of sharing the highway with large trucks. This is in part due to the relative larger sizes of large trucks in comparison to passenger vehicles. Owing to their size, large truck crashes have a greater likelihood of causing fatalities than do passenger vehicle crashes. (National Highway Traffic Safety Administration, 1991). In 2012, there were 30,800 fatalities nationwide, 3,702 (12 percent) of which involved trucks and buses that were deemed a sizeable contribution to fatalities in the United States. (Federal Motor Carrier Safety Administration, 2016). The majority of these truck related fatalities occur among occupants of other, generally much smaller, involved-vehicles rather than among truck occupants.

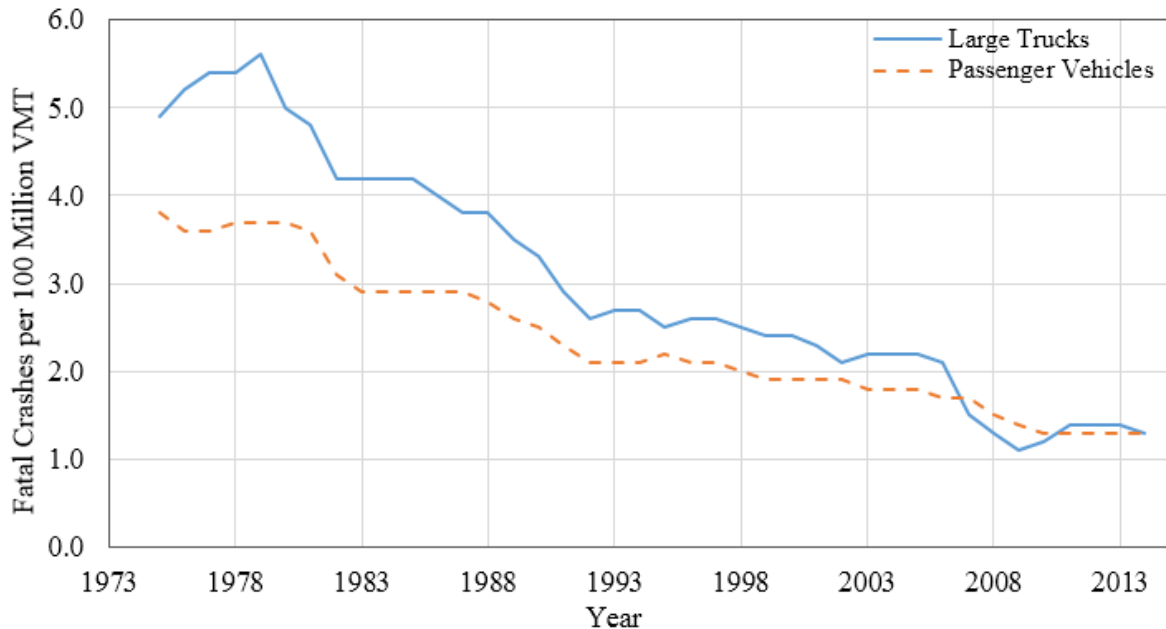


Figure 1. Graph. Large Trucks and Passenger Vehicles Involved in Fatal Crashes Per 100 Million VMT, 1975-2014. (Data From Federal Motor Carrier Safety Administration, 2016).

WYOMING TRUCK CRASH STATISTICS

Wyoming roads present significant challenges to truck drivers. Although many Wyoming highways pass through relatively, flat prairie areas, quite often, they traverse over mountainous highways characterized by difficult terrain. Such highways present challenges where unexpected or inexperienced drivers, ill-prepared to handle the severity of the mountainous road geometry get involved in crashes. Truck crashes on Wyoming mountain passes continue to pose significantly challenges to WYDOT despite several interventions undertaken. For instance, seven downgrade truck crashes attributable to brake failure were recorded on US-14 near Dayton, Wyoming from January to September 2014. (VanOstrand, 2014). This number was more than double the number of truck crashes from 2004 to 2014. In December 2015, a fatal crash was recorded on a section of US-14 despite a recent speed reduction to 40 miles per hour (mph). (Burr, 2015). The crash was attributed to brake failure and that points to the need to develop road signs with speed advisories targeting specific truck weights instead of general speed limit signs. Downgrade truck crashes have continued to increase despite several interventions. The truck crash trend on US-14 for a decade can be seen in Figure 2.

PREVIOUS GSRS STUDIES

Several measures including the use of grade severity rating systems have been instituted to reduce the risk of truck crashes on downgrades. The discussion below highlights some of the grade rating systems developed in the past to mitigate the downgrade crash problem.

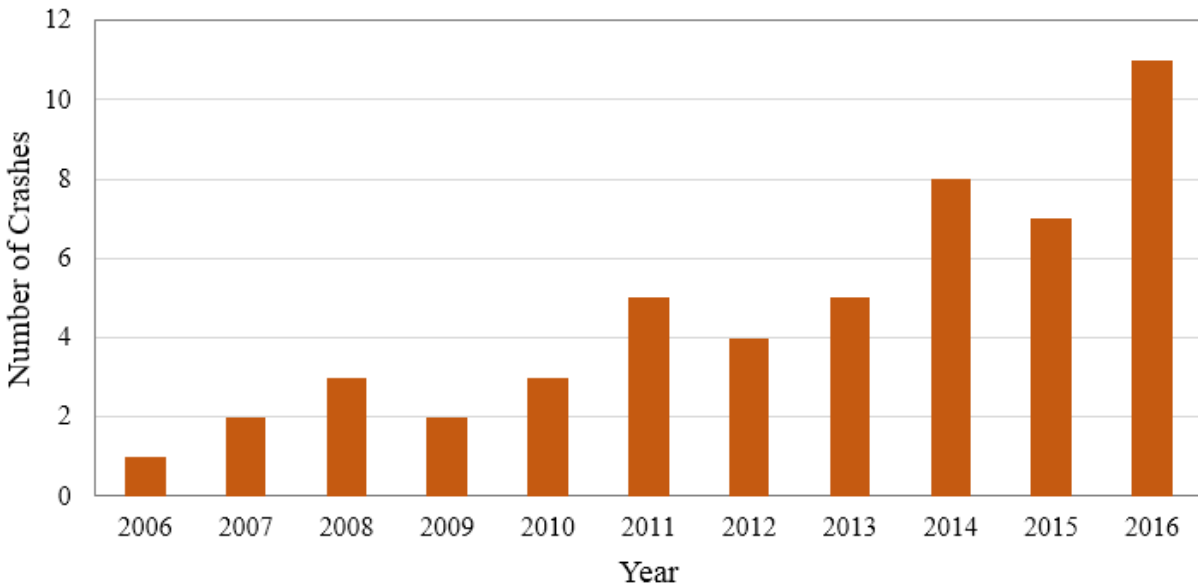


Figure 2. Graph. Downgrade Truck Crashes on United States Highway 14.

Bureau of Public Roads Rating System

One of the earliest grade rating systems was developed by the Bureau of Public Roads (BPR) in the 1950s. This was an arbitrary rating system for rating and posting grades. The BPR grading system combined the length and percent of grades to create a warning system. (Hykes, 1963). All grades within the Nation were surveyed and placed into three categories:

- Greater than 3 percent and greater than 10 miles long.
- Greater than 6 percent and greater than 1 mile long.
- Greater than 10 percent and greater than 1/5 mile long.

The warning categories were found to be haphazard and beset with a lot of variation within each category (Hykes, 1963). The system created considerable confusion for truck drivers.

Hykes Grade Rating System

The Hykes rating system was proposed in the 1960s as an improvement to the BPR rating system. An earlier study conducted by Fisher developed a system that rated brakes by their overall heat dissipation capacity expressed in horsepower. (Fisher, 1961). A model was developed that utilized horsepower rating to predict the downgrade performance abilities of commercial vehicles. A “grade ability formula” was developed using Fisher’s study along with additional field tests that helped determine the performance of vehicles on level and ascending grades. The “grade ability formula” is shown in the equation in Figure 3.

$$\theta = \frac{hp \times 37,500}{WV}$$

Figure 3. Equation. Grade Ability Formula.

where,

θ = the grade expressed in percent,

W = the weight of the vehicle in lb,

V = the speed of the vehicle,

hp = the horsepower available from all sources as a retarding or accelerating effect.

Hykes improved the “grade ability formula” to create a downhill energy equation that included the following grade retardation elements; brake horsepower, rolling resistance horsepower, chassis friction horsepower, air resistance horsepower, engine brake horsepower, and horsepower from the retarder. This improved equation made it possible to predict safe grades for a vehicle with certain characteristics and speed. Based on the improved equation, a typical truck with a gross weight of 40000 lb, frontal area of 80 square feet (sq. ft.), engine speed of 3200 revolutions per minute (rpm), and a descent speed of 30 mph was determined to be able to descend a 5.42 percent grade safely. (Hykes, 1963).

Highway tests were undertaken to validate the proposed grading system on a nine mile and 5 percent mountainous road. Vehicles with gross weights of 10,000, 20,000, 50,000, and 70,000 lb were rented or leased for the tests. Tests were conducted on each truck on the mountain grade in various gear ratios and vehicle speeds to determine the maximum safe speed of descent. Calculations were also made of the overall horsepower required in each descent.

The test results indicated a good correlation between the model’s ratings and single-unit vehicle performance. However, there was a difficulty in achieving good results using the tractor-trailer combinations because of: (1) trailer axle hop and bounce caused by the suspension type used, and (2) poor brake balance between tractor and trailer with the trailer brakes doing most of the braking and thus experiencing brake fade from overwork. The study recommended an improvement of the brake balance in tractor-trailer combinations to ensure conformance to regulations and to enable a more accurate prediction of safe downgrade descent speeds. The inability of the model to adequately predict safe speeds for tractor-trailer combinations resulted in Hykes recommending an alternative rating system that was not based on the Grade Ability Formula.

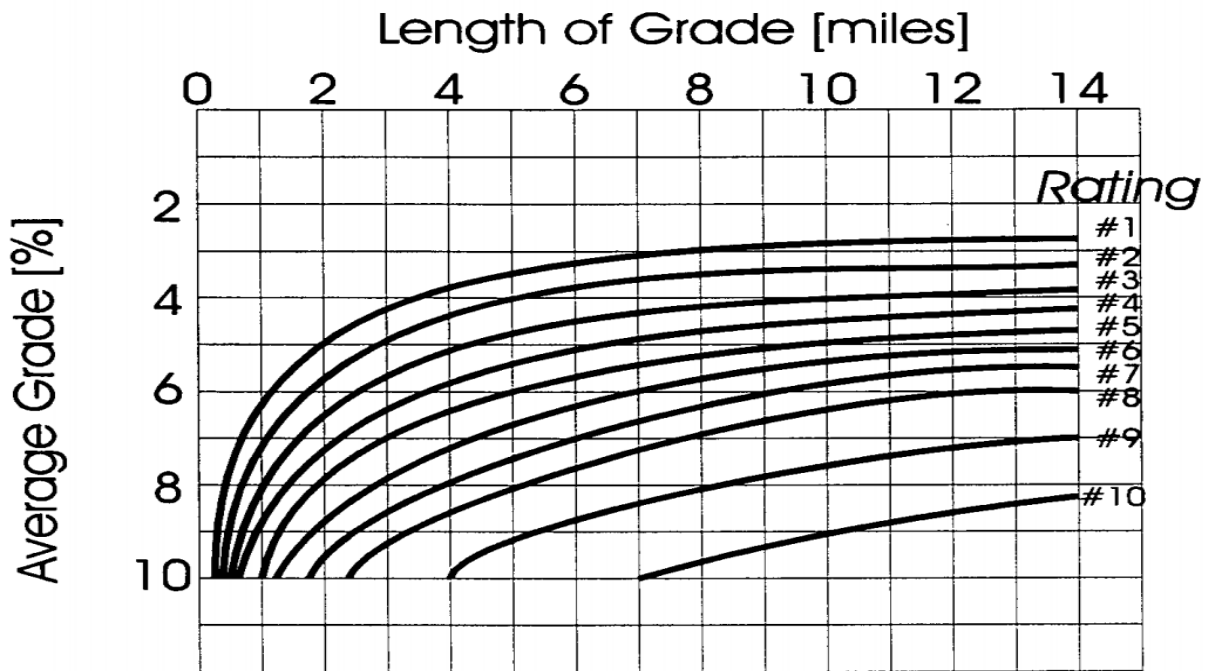
Hykes improved the BPR rating system by increasing the grade categories from three to ten. The new categories represented increasing levels of severity. The Hykes rating system is presented in © 1963 SAE.

Figure 4. Hykes still placed responsibility on drivers to use their experience and training to determine the appropriate gear and speed for descending a downgrade once they were given information of the grade’s rating.

Lill's Grade Rating System

Lill's grade rating system was proposed in 1975. (Lill, 1975). It introduced three important new ideas:

- The concept of rating hills by their effect on a representative truck.
- The inclusion of the effect of hill length through consideration of brake fade effects.
- The use of stopping distance criterion as a measure of available braking capacity.



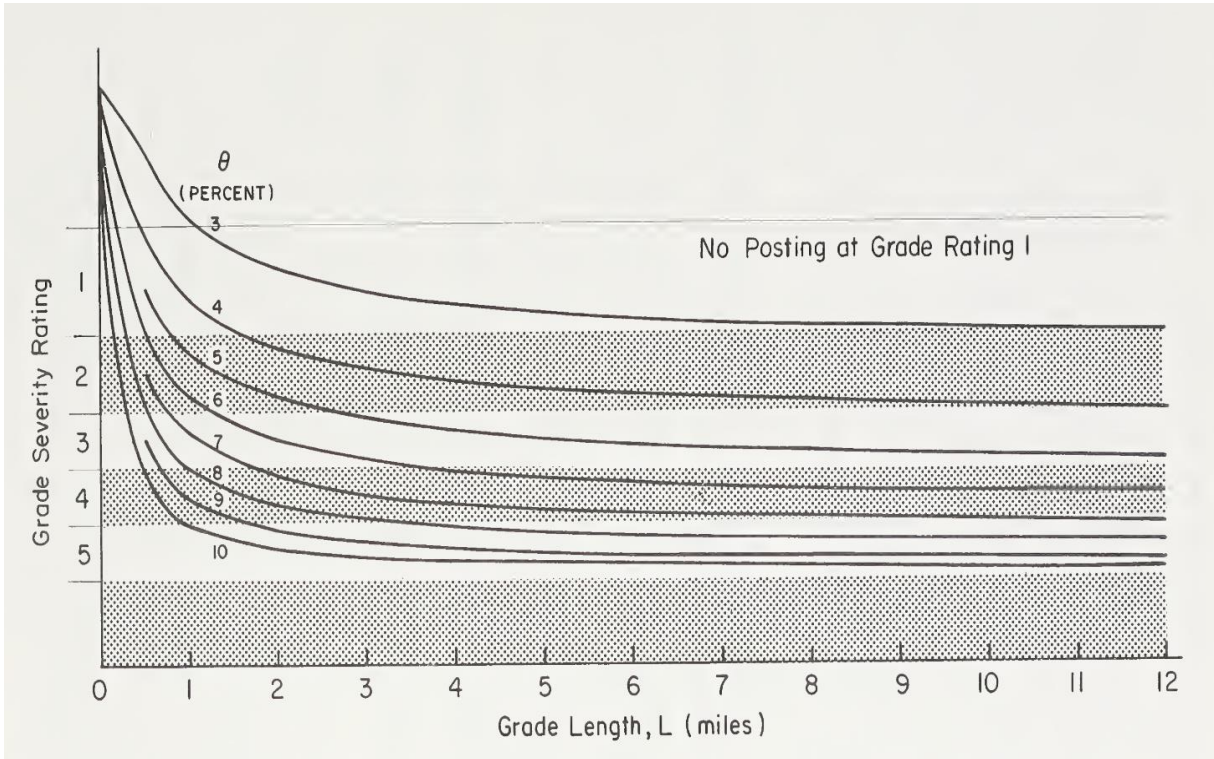
© 1963 SAE.

Figure 4. Chart. Hykes' Proposed Grade Rating System. (Hykes, 1963).

Lill's model was based on the work-kinetic energy equation applied to braking on a grade. The equation was used to solve for the descent speed that will allow stopping in a criterion distance. An important consideration for use in this model is the total retarding force that must include brake and non-brake terms. These were derived from a modification of the non-faded brake test results using brake fade factors developed by Hykes from temperature measurements during brake dynamometer tests. (Myers et al., 1981). Lill utilized the brake fade factor to introduce a brake equivalent time concept, which is defined as the hill descent time multiplied by the percent brake use. This analysis resulted in a maximum safe speed which allows stopping within his criterion of 250 ft. The stopping criterion varied with length and slope. Grade severity ratings were created corresponding to various speed bands, with high speed bands corresponding to least severe and low speed bands to most severe. Lill's grade severity rating system is shown in © 1981 FHWA.

Figure 5.

Lill's model had some limitations. First, the non-brake forces were considered constant whereas they are now known to be functions of velocity. Also, the brake fade factor is an empirical fit to specific test data and does not explicitly account for the effects of variables such as ambient temperature, initial temperature of the brakes, brake heat capacity and heat transfer characteristics. (Myers et al., 1981).



© 1981 FHWA.

Figure 5. Chart. Lill's Proposed Grade Severity Rating System. (Myers et al., 1981).

The FHWA Grade Severity Rating System

Investigations of severe truck crashes have identified that the development of a GSRS and appropriate warning signs to aid drivers in choosing the correct speed and gear with special emphasis on the inexperienced driver will mitigate the incidence of downgrade truck crashes. (Lill, 1977). This led to the development of the Federal Highway Administration (FHWA) GSRS model and the Weight Specific Speed (WSS) sign. The ultimate result of the GSRS is a roadside sign at the top of each hill that gives a recommended maximum descent speed (to be held constant for the entire grade descent) for each of several truck weight ranges. This concept is a major advancement in terms of grade descent safety because it tells drivers what to do directly, rather than giving them information that still requires evaluation under different loading conditions. (Johnson et al., 1982b).

Recognizing that brake temperature is a direct correlation of a vehicle's ability to stop, and thus, an inferential measure of safety, the GSRS was used to solve the "inverse problem". That is, what speed corresponds to a given final brake temperature (on a given hill, at a given weight,

etc.). This means that if a maximum safe final brake temperature is selected, then a maximum safe speed for a given loaded truck on any hill can be determined and signs can be erected to give drivers this information. (Johnson et al., 1982a). The implication is that, within the context of the temperature limit concept, the task of the driver is to control brake temperature during grade descent by choosing the correct speed and gear.

Development of the FHWA GSRS involved several tests on an instrumented 3-S2 5-axle truck. The tests were used to develop a model for estimating brake temperature at the bottom of the downgrade during descent. A DOS computer program was developed for the model to aid highway agencies in determining maximum descent speeds. Relevant inputs of the program required are truck weight (lb), speed (mph), downgrade length (miles) and downgrade percent. The program uses the information to generate the outputs of maximum safe descent speeds for different truck weights (see Figure 6).

MAXIMUM TRUCK WEIGHT (POUNDS)	MAXIMUM SAFE SPEED (MPH)	BRAKE TEMP. FROM DECLINE (F)	BRAKE TEMP. FROM EMERGENCY STOP (F)	TOTAL BRAKE TEMP. (F)	TOTAL TRAVEL TIME (MIN.)
70000	13	480	3	483	13.8
65000	17	488	5	493	10.6
60000	24	488	10	498	7.5
55000	32	482	17	499	5.6
50000	55	442	47	489	3.3

NOTE : INITIAL BRAKE TEMPERATURE = 150

Press 'C' to continue or 'O' for speeds with brake temperature between 500 °F and 530 °F :

© 1982 FHWA

Figure 6. Picture. FHWA GSRS DOS Program Output. (Johnson et al., 1982a).

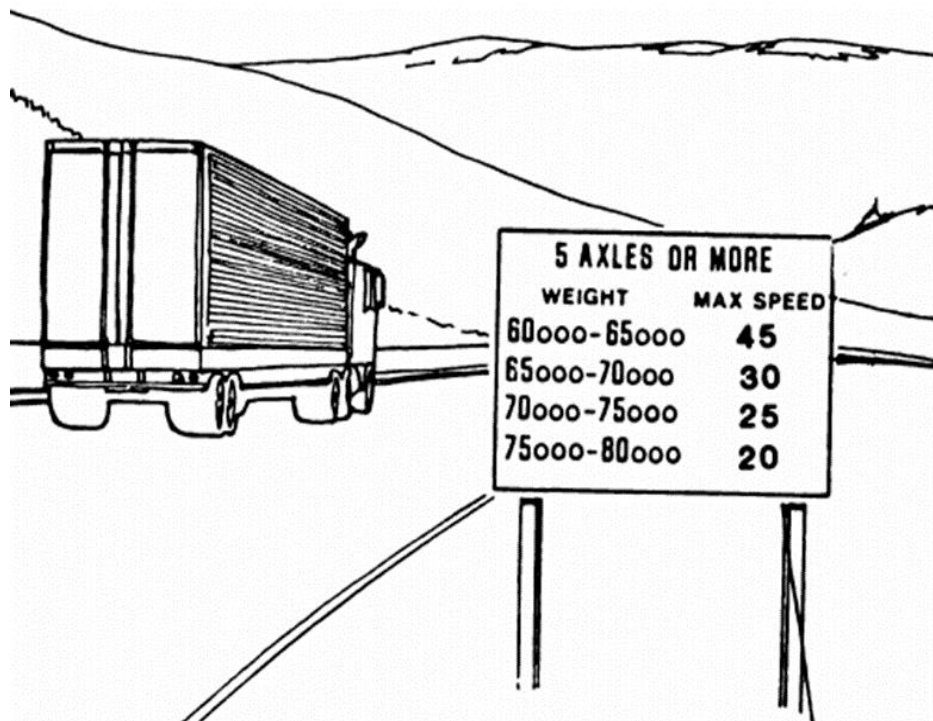
Generation of the maximum safe descent speeds allowed the development of WSS signs. WSS signs direct drivers on the allowable maximum speed to descend a downgrade based on the truck weight. An example of a WSS sign is shown in Figure 7.

Several validation tests were conducted after the development of the GSRS model and the WSS signs. These studies found that the WSS signs installed on downgrades are effective in reducing the incidence of truck runaways based on field validation of the GSRS model. (Bowman, 1989; Hanscom, 1985; Johnson et al., 1982b).

Apart from being used to estimate maximum safe truck descent speeds, the GSRS is also used to identify downgrades where there is a high likelihood of brake failure. (AASHTO, 2011). The

GSRs is also integral to identifying locations of truck escape ramps. (Abdelwahab and Morral, 1997; Larson, 1987). This is done by generating brake temperature profiles for dangerous downgrades and determining the locations along the downgrade where the brake temperature will exceed a critical value. The GSRs model is also used in crash analysis, especially for downgrades. (Glennon, 2018).

In the intervening decade after the development of the FHWA GSRs, some modifications were made to the model to factor in emergency stopping on a downgrade. (Johnson et al., 1982a). The maximum safe speed was redefined to be composed of two sources of brake heating; one being the heating from a steady grade, and heating from a sudden stop. The limiting brake temperature was also increased from 425°F to 500°F. (Johnson et al., 1982a). This value was based on the fade temperatures of brake linings, and a consideration of the typical degree of brake imbalance found on random trucks whose brake temperatures were measured.



© FHWA 1982.

Figure 7. Picture. Example of a WSS Sign. (Johnson et al., 1982a).

Johnson et al., 1982a, modified the GSRs model such that there would be adequate braking capacity to permit an emergency stop at the end of a decline without exceeding a maximum temperature of 500°F. (Johnson et al., 1982a). This temperature relationship is defined as (Figure 8):

$$T_{lim} = T_f + T_E$$

Figure 8. Equation. Limiting Temperature.

where,

T_{lim} = limiting brake temperature (500°F),

T_f = brake system temperature from maintaining constant velocity on the downgrade, and

T_E = temperature rise from performing an emergency stop.

The brake temperature increase due to an emergency stopping was expressed as (Figure 9) (Johnson et al., 1982a):

$$T_E = 3.11 \times 10^{-7} W V^2$$

Figure 9. Equation. Temperature Rise from Emergency Stopping.

where,

W = weight of truck (lb), and

V = speed of truck (mph).

Johnson et al., 1982a, analyzed the effect of retarders on the GSRS. The use of a retarder is assumed to be equivalent to carrying a lighter load as far as brake heating is concerned. That means brake heating on an 80,000 lb truck with a retarder may be the same as that of a 70,000 lb truck without a retarder.

Bowman and Coleman reviewed the weight boundary analysis conducted in the FHWA GSRS development. (Bowman and Coleman, 1989). The weight boundary is the maximum downgrade slope and length that can be descended by the different weight categories without exceeding the maximum brake temperature, including the temperature increase resulting from an emergency stop at the end of the grade. This was done as a result of the increase in maximum speed limits on highways from 55 to 65 mph, and the change in truck designs because of fuel conservation measures. (Bowman and Coleman, 1989). The previous weight boundary analysis undertaken by Myers et al. found that combinations of downgrade slope and length which would result in a possible runaway condition for vehicles 45,000 lb or less do not exist on major highways in the United States. (Myers et al., 1981). Bowman and Coleman concluded that when the effects of fuel conservation measures, the emergency stopping criteria and the higher highway speed limits are considered, a new weight limit of 35,000 lb is the safe weight below which runaway conditions are less likely to occur on United States highways. (Bowman and Coleman, 1989).

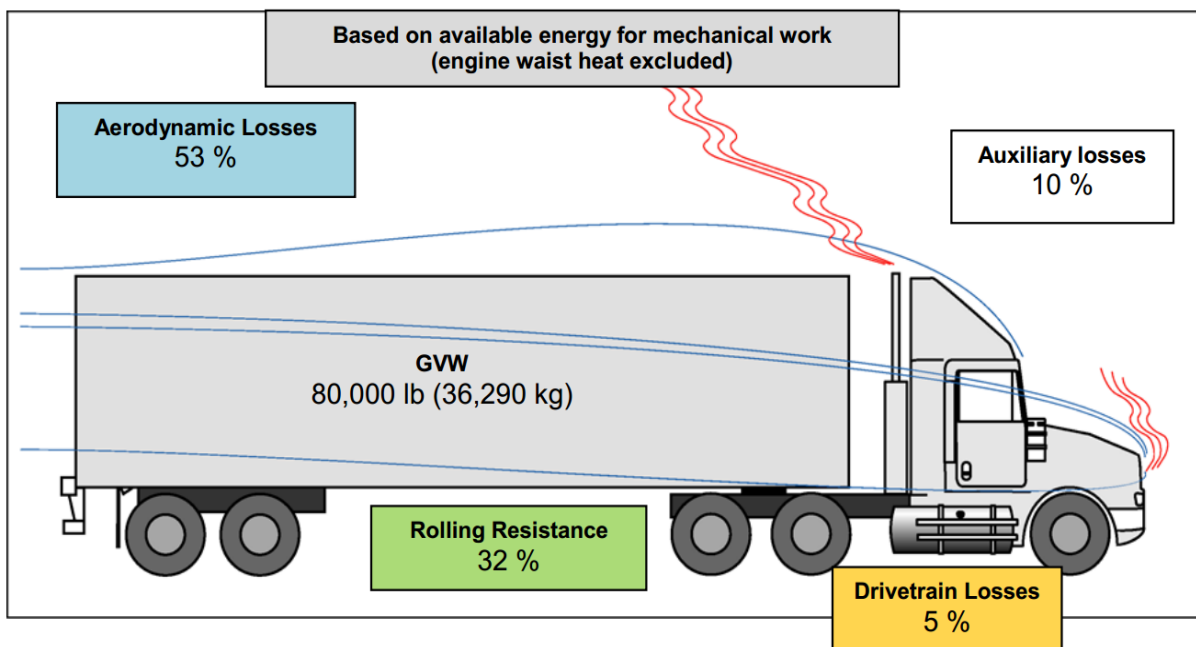
Highway agencies have taken advantage of the growth in technology to incorporate GSRS in some intelligent transportation system (ITS) projects. Several of the operational facilities identified in the literature include downhill truck warning systems located in Colorado, Oregon, West Virginia, British Columbia and Pennsylvania. (Eady et al., 2015; Robinson et al., 2002). These warning systems automatically weigh and classifying trucks as they approach a downhill section of the highway. Based on the weight and class measured, a safe descent speed is calculated with each truck receiving a vehicle-specific recommended safe descent speed on a variable message sign. The algorithm used for calculating the speeds are based on the GSRS mathematical model from FHWA. A study was conducted to determine the safety effectiveness of such a warning system. Data was collected on driver awareness and compliance of the downhill truck speed warning system installed on the westbound lanes of the Eisenhower Tunnel, on Interstate 70, in Colorado. (Janson, 1999). The study found that the warning system significantly reduced the truck descent speeds for most weight ranges above the 40,000 lb minimum to which the warning system responds.

THE NEED TO UPDATE THE GSRS

The FHWA GSRS model improved truck safety on downgrades. It marked a leap from previous grade severity rating systems because it tells the driver what to do directly, rather than giving him information that requires evaluation under different conditions. However, in the intervening decades since the GSRS was developed, there has been a radical change in the design of the typical truck. One main recommendation made on evaluating the safety effectiveness of the Eisenhower Tunnel downhill truck speed warning system was the need to revise the advisory speeds obtained from the GSRS algorithm. (Janson, 1999). This was because of the risk of the advisory speeds being too low and the danger of truck drivers ignoring the recommended speeds as unrealistic.

In 1989, a re-evaluation of the GSRS model was done by Bowman, which determined that some modifications of the GSRS model were required to account for the fuel conservation measures introduced for trucks almost a decade after the GSRS model was developed. (Bowman and Coleman, 1989). © 2014 UMTRI

Figure 10 shows some truck areas that have seen improvement and continue to be targeted for upgrading due to fuel conservation measures and emission standards.



© 2014 UMTRI

Figure 10. Picture. Approximate Distribution of Drag Loss For a Typical Tractor Semitrailer on a Level Road. (Woodrooffe, 2014).

The influence of fuel conservation measures on truck designs have included the lowering of aerodynamic drag of trucks by reducing frontal areas, using airfoils and streamlining of tractor designs. There has also been a general adoption of radial tires in place of the bias ply design used previously. These measures have reduced the non-braking forces available to retard truck motion thereby placing a greater load on brake systems. Additionally, the current truck braking system of most fleets in the United States have been updated to comply with the Federal Motor

Vehicle Safety Standard (FMVSS) rule of reducing stopping distance of trucks by 30 percent by the year 2013. (Bendix Spicer Foundation Brake LLC, 2011). In response, brake sizes have been increased and modifications made to comply with the rule. These improvements mean the current GSRS model is recommending maximum safe descent speeds for trucks that may be deemed too conservative and can lead to lower compliance.

In 1985, Kenworth introduced the aerodynamically designed T-600 model. This marked the industry's first serious attempt to incorporate aerodynamic improvements to truck tractors. (National Research Council, 2010). Aerodynamic improvements of trucks have roof deflectors, sleeper roof fairings, chassis skirts, air tabs, cab extenders among others (see

Figure 11). The use of aerodynamic technology on modern trucks reduces fuel consumption between two to ten percent with the use of different technologies. The corresponding aerodynamic drag improvement is between 6 to 20 percent. (National Research Council, 2010). Contemporary tractor areas have been aerodynamically optimized to reduce drag. As a result, drag coefficients have been reduced from about 0.9 and more to 0.6 currently. Aerodynamic truck improvements are still taking place with lower drag coefficients expected. Tesla has reported an aerodynamic drag coefficient of 0.36 for the Tesla semi electric truck in 2017. (Singh, 2017).

The adoption of radial tires by most transportation fleets has had consequences for fuel conservation and truck loading. Radial tires have lower diameters (2 inches) compared to typical tires. This has resulted in truck fleets having higher trailer boxes that can haul loads 2 inches higher while maintaining the required height restrictions. Radial tires also rotate faster by virtue of their smaller diameter compared to regular tires. This faster rotation leads to different brake-loading characteristics from regular tires, and subsequently, a change in the rate of kinetic energy absorption due to the faster rotation of these tires. Improved radial tires have lower internal friction which helps minimize operating temperatures and rolling resistance. (Bowman and Coleman, 1989). Such tires have been found to improve fuel savings of 6 percent and more compared to bias ply tires. (Goodyear Commercial Tire Systems, 2008). The incorporation of tandem tires in United States truck fleets has the effect of reducing contact pressure. This in turn has led to a reduction in energy consumption of trucks. (Woodrooffe, 2014).

Another important factor which provides resistance to forward motion of the truck is the engine friction. Engine friction has reduced markedly over the past decades. In 1974, a standard 290 horsepower (hp) engine absorbed approximately 113 hp, including the effects of driveline efficiency and accessory power. (Bowman and Coleman, 1989). A 300 hp engine produced in 1980 absorbed approximately 75 hp. Calculations from data supplied by a typical truck engine manufacturer, suggests a 450 hp engine manufactured in 2016 will absorb approximately, 60 hp of engine friction. Engine manufacturers have targeted reduced friction in bearings, valve trains and the piston-to-liner interface to improve efficiency. (National Research Council, 2010). Development of heavy duty oils have shown a lot of promise in reducing engine drag further. An example is the 10W-30 oil that has lower viscosity and would improve fuel consumption between 1 to 2 percent. (National Research Council, 2010).



© 2018 Kenworth.

a. Aerodynamically Designed Tractor. (Kenworth.com, 2018).



© 2015 FE.

b. Trailer Tail (Morgan, 2015).



© 2018 Truckinginfo.

c. Trailer Skirt.(Truckinginfo.com, 2018).



© 2015 FE.

d. Airtabs on Cab (Morgan, 2015).

Figure 11. Photo. Examples of Aerodynamic Reduction Devices

Reduced Stopping Distance Requirements

The National Highway Traffic Safety Administration (NHTSA) in a bid to reduce the gap between the stopping capability of passenger cars and trucks issued new braking standards for commercial vehicles. (Bendix Spicer Foundation Brake LLC, 2013). The reduced stopping distance requirement was defined as updates to Federal Motor Vehicle Safety Standards (FMVSS) 121. The updates require that the stopping distance of tractors traveling at 60 mph be reduced from 355 ft to 250 ft, a 30 percent reduction. The 30 percent reduction in stopping distance for the vast majority of commercial vehicles is envisaged to increase the safety of trucks. The final rule of the 30 percent stopping distance reduction was announced in July 2009 with transition to the new requirements occurring in two phases. The compliance dates were set for August 1, 2011, and August 1, 2013, depending on the vehicle type. A clear majority of

heavy trucks fell within the first compliance date. In response to the stopping requirements of FMVSS 121, most fleets have modified their tractor brakes. Steer axle brakes are now fitted with $16\frac{1}{2}$ x5 inches brake drums while drive-axles have stayed as $16\frac{1}{2}$ x7 inches. (Berg, 2014).

Daimler selected to install $16\frac{1}{2}$ x8 inch drums standard on drive axles for Freightliners and Western Stars. Truck manufacturers have also upgraded the brake chambers, linings and friction materials for both steer and drum axles. (For Construction Pros, 2012).

Air disc brakes are thought to stop trucks faster than drum brakes, and are likely to meet the FMVSS 121 reduced stopping distance requirement. (Bendix Spicer Foundation Brake LLC, 2013). However, the penetration of disc brakes into the United States' market has been slow. This has been attributed to the relatively higher initial costs of installing disc brakes and the familiarity of drum brakes to the United States truck fleets. However, disc brakes have been predicted to see a significant growth in the United States' market. In 2015, 12-15 percent of steer axles were fitted with disc brakes. This has been projected to increase to 35-40 percent by 2020, with the drive axles accounting for 25 percent of the market share. (Marsh, 2016). On trucks built by manufacturers such as Kenworth, and Peterbilt, air disc brakes are now standard on the steer axle. Air disc brakes are optional for other truck types such Mack, and Navistar.

TRUCK TYPES IN THE UNITED STATES

The United States' heavy duty truck market is dominated by seven truck types. These are International (Navistar), Freightliner (Daimler), Kenworth (Paccar), Volvo (Volvo), Mack (Volvo), Western Star (Daimler) and Peterbilt (Paccar). Figure 12 shows the market share of heavy duty trucks at the end of December, 2017. Freightliner has the highest percentage of trucks on United States' roads with a market share of 37.5 percent while Western Star has the lowest share of 2.7 percent.

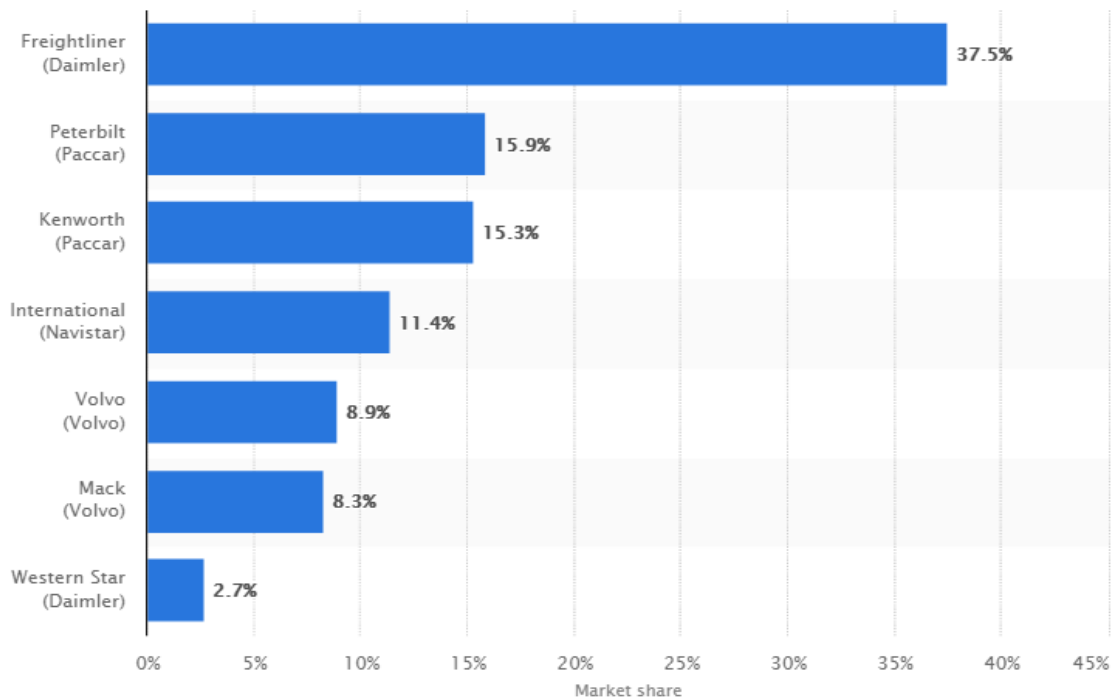
Freightliner and International dominate the day cab market of heavy trucks. About 44.4 percent of the day cab tractors on the market in 2015 were the Freightliner models and 41.1 percent were International. (Carr, 2015). The rest of the 14.5 percent market share was distributed among the five remaining models. International also dominated the sleeper cab market in the same year. About 50 percent of the sleeper tractors on the market were International models followed by Kenworth and Volvo, at 24 percent and 23 percent, respectively.

WEIGHT AND SPEED LIMITS IN THE STATE OF WYOMING

Truck weight and size limits are governed by state and Federal laws. Several of these laws were passed and amended over the last eight decades. The first Federal truck size and weight regulations, passed by Congress in 1956 as part of the National Interstate and Defense Highway Act limited combination trucks to an overall gross vehicle weight (GVW), of 73,280 lb. (FHWA, 2015). Single axle weights were restricted to a gross weight of 18,000 lb, with tandem axles being restricted to 32,000 lb. The 1956 Federal limits allowed an exception stating:

“Any state that allowed axle loads or gross vehicle weights in excess of the weight limits could continue to allow the higher state limits on interstate highways”. (FHWA, 2015).

This provision was referred to as the first “grandfather clause.”



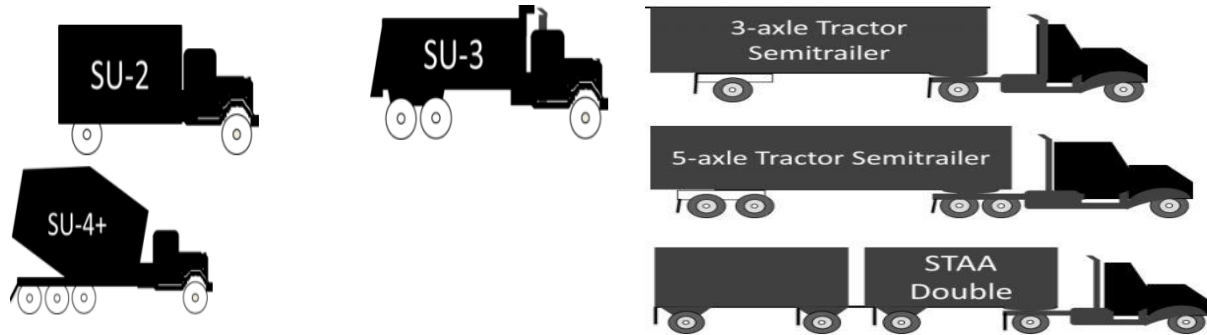
© 2018 Statista.

Figure 12. Chart. United States’ Market Share of Heavy Duty Truck Models. (Statista.com, 2018).

In 1974, a bill was passed by congress allowing states to increase weight limits on the interstate system to a maximum of 80,000 lb GVW and load limits to increase to 20,000 lb on single axles and 34,000 lb on a tandem axle. This increase was not a mandate and so was not instituted by some states on their interstate highways. (FHWA, 2015). In 1984, the Surface Transportation Assistance Act (STAA) imposed the Federal 80,000 lb limit as a mandate across the nation’s interstate highway system. The STAA also imposed length restrictions on truck tractor-semitrailer and truck tractor-semitrailer-trailer combinations on the national truck network (NN) or in transition between NN highways and terminals or service locations.

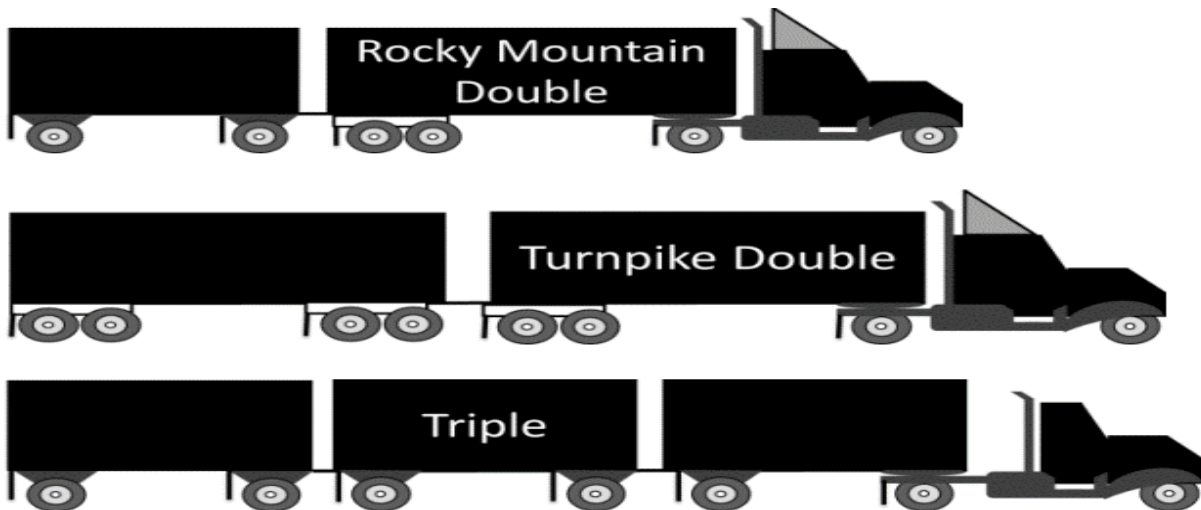
According to the Report to Congress on the Compilation of Size and Weight Laws, typical truck configurations on United States highways is classed into three groups. (FHWA, 2015). These are single-unit trucks, combination trucks, and longer combination vehicles (LCV). Single-unit trucks refer to vehicles where the power unit and vehicle chassis are permanently attached. These are mostly used for retail, construction, utilities and services. In 2012, single-unit trucks accounted for 39 percent of the vehicle miles traveled by all commercial trucks with a GVW exceeding 10,000 lb. (FHWA, 2015). Combination trucks are the most common freight carrying trucks on United States roads. They are five-axle tractor semitrailer combinations and are commonly referred to as the “18-wheeler.” Combination trucks account for 61 percent of all commercial vehicle miles traveled in the United States in 2012 along with LCVs. LCVs comprise three- and four- vehicle combinations that use at least one full-length trailer in the

combination (up to 48 ft.) or three shorter trailers. Three LCVs are predominant for this type of vehicle across the United States. They are the Rocky Mountain Doubles, Turnpike Doubles and Triples. Figure 13 shows common truck configurations on United States highways.



a. Single-unit trucks

Combination trucks



b. Longer combination vehicles

© 2015 FHWA.

Figure 13. Picture. Common Truck Configurations in the United States' Heavy Vehicle Fleet. (FHWA, 2015).

Different truck combinations and GVWs are allowed on Wyoming highways. The Wyoming grandfather provisions allow vehicles to operate up to 117,000 lb GVW on some routes in the states including the interstate system. All highways in the state allow single axles to be loaded to 20,000 lb GVW, tandem axles to 36,000 lb GVW, and triple axles to 42,000 lb GVW. (Wyoming Highway Patrol, 2018).

Speed limits on United States highways are set by state and local authorities. The maximum speed limits that can be established depend on whether the road is rural, urban interstate, or a non-interstate limited-access highway. In the mid-1970s, national maximum speed limits were

set by congress for all states, with compliance ensured by withholding Federal highway funds from states that maintained speed limits greater than 55 mph. (Wyoming Highway Patrol, 2014). Currently, states are allowed to set their own speed limits, with 41 states having speed limits of 70 mph or higher on portions of their highway system. In 2014, the Wyoming legislature increased speed limits up to 80 mph on about 500 miles of Wyoming rural interstate highways. This speed was allowed on portions of Interstates 25 (I-25), 80 (I-80) and 90 (I-90) from July 1, 2014. (Wyoming Highway Patrol, 2014). The maximum speed limit on urban freeways and interstates is 65 mph, while the speed limit on divided roads has been set at 70 mph. For undivided highways, the maximum speed limit is 70 mph while it has been set at 30 mph for residential areas. (WYDOT, 2016). Speed limits on undivided roads that traverse mountainous terrain are usually below 70 mph.

CHAPTER SUMMARY

This chapter presented a literature review as a basis for understanding the general concept of the GSRS, and an overview of truck safety in the United States and Wyoming. Previous grade rating systems were discussed along with their limitations.

Trucks play a vital role in the economy of the United States. Trucks serve as the main means of moving freight in the Nation and the industry employ millions of citizens. Though truck safety has witnessed an improving trend over the past decades, truck-related fatalities are still a cause for concern. Trucks are especially vulnerable to crashes on steep downgrades due to the risk of brake failure and truck runaway crashes. This is because the large amounts of energy generated by brakes to slow down trucks on downgrades increases the probability of a brake fade due to heating and ultimately, crashes due to runaway events. Therefore, mountainous terrain such as those which characterize some Wyoming roads presents significant challenges to truck drivers. Truck crashes on downgrades in the state attributed to brake failure are common. WYDOT has implemented safety interventions such as reduced speed limits but the truck crash problem persists.

A countermeasure to the incidence of truck crashes on downgrades has been the rating of grade severity. These severity ratings provide an indication of how hazardous a downgrade is and the need for truck drivers to take extra precaution in descending them. Previous grade severity rating studies have included the BPR, Hykes, and Lill's grade rating systems. Some of the previous rating systems were oversimplified and did not always take into account truck and environmental characteristics in the rating of grades.

The FHWA sponsored a study to develop a GSRS. The GSRS relies on a brake temperature model which predicts the brake system temperature at the bottom of the grade. This system was an improvement to previous GSRS. This is because truck and environmental factors, such as initial brake temperature, ambient temperature, brake cooling and heating factors, and downgrade characteristics were considered in the rating system. The output of the GSRS was a WSS sign that provided advisory descent speeds for different truck weight categories. This was an improvement over previous rating systems as it greatly simplified the driving task.

In the intervening decades since the GSRS was developed and implemented, truck designs, brake improvements, and reductions in retarding forces have necessitated updating the GSRS model.

The recommended descent speeds from the FHWA GSRS have been found to be conservative. There is a concern that this situation may result in truck drivers ignoring the speeds, thereby endangering safety on mountainous highways. An update to the GSRS to reflect the current truck population characteristics will lead to reasonable recommended speeds and likely compliance by the truck driving population.

CHAPTER 3: THE TRUCK DOWNGRADE BRAKING MODEL AND THE GSRS

This chapter presents the theoretical background and development of the GSRS. A review of the grade descent problem is first presented after which the brake temperature model is discussed. The chapter continues with an introduction of truck brake types and retarders. The chapter ends with a discussion of the physical implications of the GSRS along with the concept of maximum descent speeds on downgrades.

THE GRADE DESCENT PROBLEM

Overheating of brakes on downgrades is a major cause of runaway trucks. A runaway vehicle was defined by Johnson et al., 1982a as:

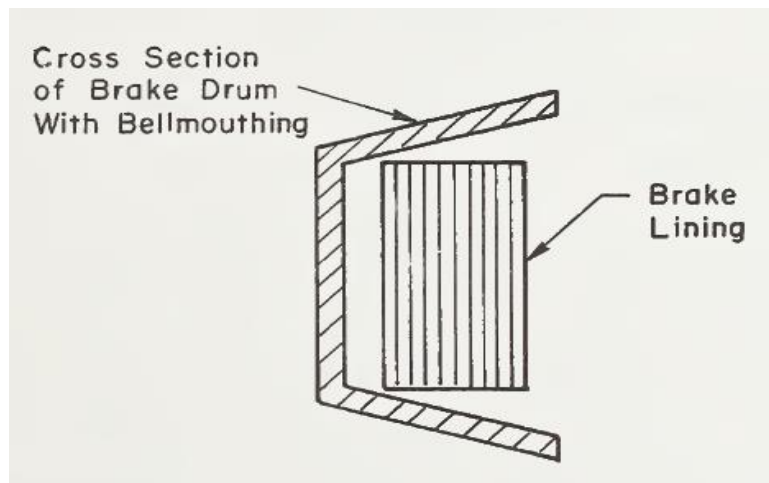
“A vehicle whose speed, headway, or directional control problems are aggravated by a downgrade to the extent that the chances for a crash are substantially increased for a given set of road, traffic, and environmental conditions”. (Johnson et al., 1982a).

Preventing a runaway on a grade requires choosing the correct speed/gear to maintain a safe margin of braking capacity, both for emergency stopping and to prevent runaways. While high speed is associated with runaway trucks on grades, it is not the only attribute since other factors (equipment, weather, or driver) can cause problems with control while negotiating a steep downgrade. (Bowman, 1989).

Severe downgrades generate large amounts of heat energy that must be absorbed by a truck's service brakes. The heat must be dissipated to prevent thermal energy building up in the brakes. Brake temperature rise produces a decreased brake efficiency known as “brake fade”. Truck brakes must therefore be able to dissipate more heat out of the brakes than is being generated to prevent brake fade. For example, a truck loaded to 80,000 lb descending a 6 percent grade at 50 mph requires an energy dissipation rate of about 350 hp. (Myers et al., 1981). If the heat rejection properties of the truck were less than 350 hp, brake temperature would rise continuously during the grade descent and could become critical on a long grade. As a contrast, the same 80,000 lb truck making a 0.45 g stop (on a level ground) from 50 mph requires 4,800 hp of heat to be dissipated, most of which will be accomplished by the brakes. However, because a 0.45 g stop will last for a short time (approximately 5 seconds), the temperature rise would not be critical. Brake fade progresses into truck runaways if the brake temperature continues to rise. (Johnson et al., 1982a).

There are different categories of brake fade. These are friction fade, fluid fade, domino fade, and mechanical fade. Friction fade refers to the reduction in friction at a friction surface. Friction fade is mostly prevalent in brake linings and increases with temperature. (Glennon, 1998). Fluid fade occurs when brake fluid overheats causing it to vaporize. This is common for cars and trucks from classes 1 to 6 that use hydraulic brake systems. Domino fade is characteristic of trucks with a brake imbalance (braking effort on some brakes higher than others). Brakes producing more braking effort heat up quickly and fade. The other brakes then receive a disproportionate amount of heat and also slowly fade, hence the domino effect. Mechanical fade is the primary mode of brake failure in grade descents and disproportionately affects drum brakes. (Myers et al., 1981). Application of the brake lining in a drum brake is outward toward

the rotating drum's friction surface. At elevated temperatures and large brake force applications, the drum begins to expand and distort. The expansion increases the brake diameter, away from the brake lining. This expansion can cause the brake lining to exceed the available shoe travel (even with automatic slack adjusters installed). Such a phenomenon can also occur at moderately high temperatures if the slack adjusters are not properly set. (Myers et al., 1981). The heating distortion of the drum leads to a situation known as "bell-mouthing" (© 1981 FHWA **Figure 14**). As the brakes heat, the "open" front of the drum expands more than the "closed" back of the drum. This flared opening of the drum causes it to resemble the shape of a bell (hence the name bell-mouthing). The result is a greatly reduced contact area between lining and drum leading to a degraded braking efficiency.



© 1981 FHWA

Figure 14. Illustration. Bell-Mouthing of a Drum Brake. (Myers et al., 1981)

Several studies and brake improvements have attempted to overcome the issue of brake fade and runaways on downgrades, but the problem persists. Analysis and prediction of brake fade is a difficult task because data are generally not available for specific brake systems. (Myers et al., 1981). The proprietary nature of truck data; the variability in characteristics from truck to truck and difficulties in the testing and analysis of friction brakes makes brake fade prediction difficult.

However, a generalized brake temperature model with the aim of preventing brake fade was developed based on an understanding of the basic physics of brake operation and fade by Myers et al., 1981. The basic concepts at play are two distinct aspects of the brake fade phenomena. The first is the relation of the brake system temperature and power into the brakes which are in turn dependent on the hill descent time history. Second, the relationship between braking friction force to the brake system temperature must be taken into account. Myers et al., 1981, argued that it was possible to develop a GSRs and gear selection model by considering only the relation of brake system temperature to hill descent time. Thus, a practical brake temperature model to predict brake temperatures on grades can be determined from basic energy balance considerations requiring only data that can be determined from relatively simple field tests. (Myers et al., 1981).

THE BRAKE TEMPERATURE MODEL

Brakes are energy converters and convert the kinetic and potential energy of a vehicle into heat energy using friction. Heat generation in vehicle brake systems is due to rubbing velocity between a pad and a rotor or a drum. Brakes are designed keeping in mind that the operating temperatures must be kept below a certain threshold. This is to ensure safe operation of brake components including pads or linings, rotors or drums, wheel cylinders or calipers, brake fluid, wheel bearings, axle and bearing seals, and lubricating oils or greases. (Limpert, 2011). Sound engineering analysis of brake temperatures are carried out using temperature models.

The brake temperature model of a truck on a downgrade may be derived by analyzing the energy transformations that occur during a grade descent. Energy transformations occur according to the law of conservation of energy, which asserts that the total amount of energy in the universe remains constant over time. Stated another way, energy can neither be created nor destroyed; it can only be transformed from one state to another. This fundamental rule is applicable to truck engines and brake systems. For a truck descending a grade, potential energy in the form of fuel is converted to mechanical energy; energy associated with motion by the engine and drivetrain. To slow the vehicle, it is the primary responsibility of the brakes to transform the mechanical energy into heat energy. This is achieved through the action of frictional shearing stresses in the disc/pad and lining interface.

Forces acting on a truck on a downgrade

Apart from the braking force (F_B), from the brake system, other non-brake forces act to slow a truck down. These are forces which retard truck motion on a downgrade but do not originate from the braking system. They are collectively known as “non-brake” forces (F_{NB}). They are:

- Aerodynamic drag
- Rolling Resistance drag
- Chassis friction, an
- Engine braking force.

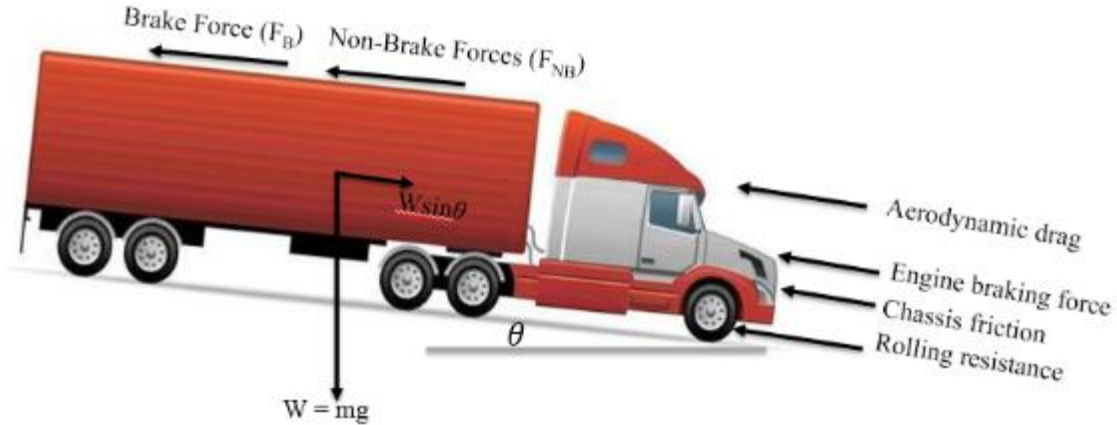
The first three forces are known together as drag forces. The three drag forces have been conveniently lumped into one because only the total drag is needed in computations for the brake temperature equation. The aerodynamic drag is due to the resistance of air to the motion of the truck on the grade. This drag is dependent on vehicle speed, wind and vehicle velocity, projected front area and ambient conditions. The rolling resistance drag refers to the frictional forces acting between the tires and the road. The rolling resistance drag is influenced by weight, coefficient of friction and marginally by vehicle speed. Chassis friction results from the resistance to motion by the chassis components. This is usually evaluated together with rolling resistance for trucks. (SAE Recommended Practice J1263, 2010). Engine braking force accounts for the resistance to motion arising from friction of the engine components and retarder use.

Available Brake force

The available brake force required to slow a truck on a downgrade can be evaluated by accounting for drag forces acting on the truck. The sum of drag forces on a truck on a downgrade

can be derived from simple mechanics. Consider a truck weighing W on a downgrade of slope θ (© 2015. YouTube (See Acknowledgements section)).

Figure 15).



© 2015. YouTube (See Acknowledgements section).

Figure 15. Illustration. Equilibrium of Forces during Descent. (www.topsimages.com, 2018).

The equilibrium of forces may be expressed as (Figure 16 and Figure 17):
Sum of forces in downgrade direction

$$= W \sin \theta - F_B - F_{NB}$$

Figure 16. Equation. Equilibrium of Forces.

$$F_B = W \sin \theta - F_{NB}$$

Figure 17. Equation. Braking Force.

The available braking force after accounting for the non-brake forces is supplied by the truck’s brake system. The brakes must have the capacity to generate the required torque to slow the truck. During grade descents, it is important for the truck brakes not to exceed a temperature that will cause expansion of drums or a reduction in the friction coefficient of linings and pads. Brake torques are known to drop to 30 percent of their cold levels for high temperatures. (Limpert and Andrews, 1987).

Engine Friction Power

Horsepower is commonly expressed as indicated horsepower (IHP) which is determined from the pressure in cylinders. There is a loss of horsepower due to friction in the engine resulting in a reduced power output. The horsepower that is actually delivered at the engine crankshaft is known as the brake horsepower (BHP). The energy loss due to friction for an internal combustion engine is therefore computed as the difference between the horsepower achieved by the expansion of combustion gasses in the cylinder (IHP) and the brake power extracted from the

engine (BHP). (James, 2012). Engines lose power generated due to the hydrodynamic stresses in lubrication films and metal-to-metal contact. In heavy duty diesel engines, friction losses are due to mechanical friction, pumping work and auxiliary system losses such as air conditioning, air compressor, alternator and the power steering pump. Friction power increases with increasing engine size and rotational speed; and is affected by lubricant type and temperature. (Sean, 2017). Engine friction horsepower (FHP) can be calculated if both brake power and indicated power values are known (Figure 18):

$$FHP = IHP - BHP$$

Figure 18. Equation. Friction Horsepower.

An empirical relationship relates torque to horsepower. This is expressed in the equation in Figure 19 :

$$Horsepower = \frac{Torque \times Engine \text{ rpm}}{5252}$$

Figure 19. Equation. Empirical Horsepower Relationship.

where, torque is measured in ft-lb. It is thus easy to convert torque to horsepower once engine rpm is known for the particular torque. For this study friction horsepower at an rpm of 1800 was considered since that is the rated engine speed at which the maximum torque corresponding to the maximum engine retardation is derived. (Jacobs Vehicle Systems, 2010). A formulation was established by Tetard et al., 1993 which relates engine speed, and cylinder displacement to engine drag torque for tractor engines of 12 and 15 liters displacement as (Figure 20). (Tetard et al., 1993):

$$C_m = (3.44N^2 - 3.25N + 9.40)Cyl + 30$$

Figure 20. Equation. Engine Drag Torque Calculation.

where,

C_m = the engine drag torque (Nm),

N (in thousands of rpm) = engine speed, and

Cyl = engine displacement in liters.

Engine friction horsepower can also be derived from coast-down tests with the gears engaged. Engine brake force from the two methods were compared for this study. Engine friction horsepower is enhanced by retarders which provide additional braking capability.

TRUCK BRAKING SYSTEMS

Due to its complex nature and potential for severe crashes during failure, truck braking technology has seen a lot of development over the past decades. Several systems have been developed but the outcome of a successful braking is still dependent on driver knowledge of his brake systems, experience and competence. Automotive braking relies upon the successful utilization of friction between a rotor, usually a cast iron drum or a disc and a fiber reinforced composite material. (Day, 1988).

Fundamental physical laws come to play in vehicle braking. Key among them is the law of conservation of energy. Potential energy from a vehicle in the form of fuel is converted to kinetic energy by the engine and drivetrain. To slow a vehicle down, brakes have to work against the kinetic energy. The kinetic energy of the moving vehicle is transformed to heat energy by the brake system of the vehicle. Thus, the most important aspect of any vehicle's braking system is its ability to generate the required torque to slow the vehicle, and then dissipate this heat into the atmosphere. (Bendix Spicer Foundation Brake LLC, 2011).

Trucks are usually installed with two braking systems: service (foundation) and auxiliary brakes. On long and very steep downhill grades, service brakes are susceptible to brake fade where they lose their effectiveness and can lead to a crash. Auxiliary brakes aid in slowing trucks in situations where additional brake horsepower is required.

Service Brakes

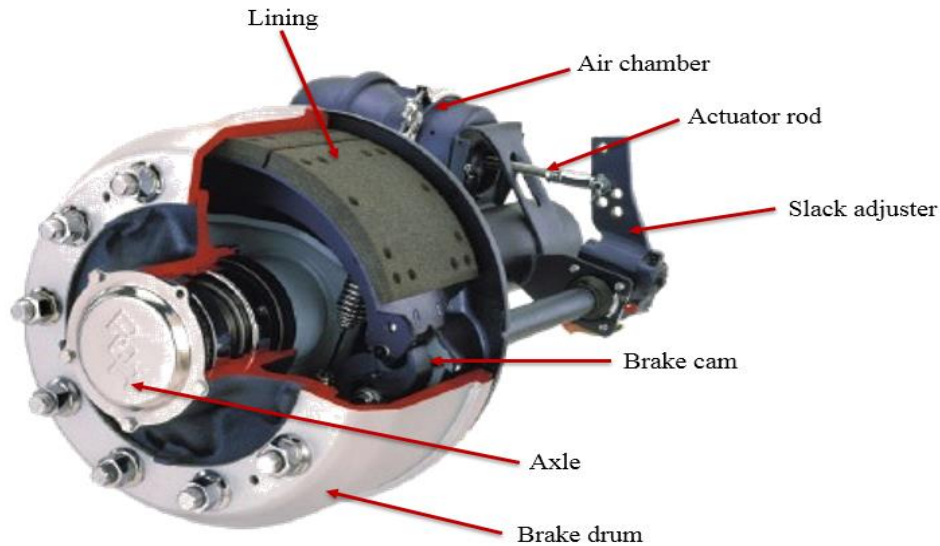
Service brakes function as the main braking system of large trucks and operate when the pedal is pressed. Braking is achieved by the braking system transmitting a force to the wheels, and by using friction which converts the kinetic energy of the vehicle to heat energy which is dissipated into the air. Service brakes are of two types; drum and disc brakes.

Drum Brakes

Drum brakes dominate the market of the trucking industry. About 90 percent of trucks have drum brakes fitted to their fleet. (Berg, 2014). Drum brake components are housed in a drum that rotates along with a wheel. Braking is accomplished by shoes which press against the drums to slow the wheel when a pedal is pressed. Fluid was previously used to transfer pressure to the brake shoes, but this has been replaced by air pressure. Drum brakes are known to be susceptible to brake fade and loss of braking effectiveness. © 2018 PRI (See Acknowledgements section).

Figure 21 shows the components of a drum brake.

Different designs of brake drums exist. S-Cam brakes are the most common type of drum brakes. Cam brakes are operated by applying a force from an air chamber or actuator. Due to their simple designs, relatively lightweight, and their relative low economic cost, S-cam brakes are used on approximately 95 percent of class 5-8 air braked trucks in North America. (Bendix Spicer Foundation Brake LLC, 2011). The other type of drum brake design is the wedge brake. These come in two types, the simplex and duplex. Wedge brakes can be actuated using hydraulic or air pressure. This type of brake is currently used overwhelmingly for special applications, such as on off-road or construction vehicles.



© 2018 PRI (See Acknowledgements section).

Figure 21. Picture. Typical Drum Brake. (Performance Review Institute, 2018).

Disc Brakes

For several decades, United States' companies have relied on the classic S-cam drum brakes for their fleets. However, changes in stopping distance laws have created the need to have better braking performance. (National Highway Traffic Safety Administration, 2009). This has led to fleets adopting alternate technologies including disc brakes. Disc brakes use a caliper to compress a pair of semi-metallic pads against a flat rotor to create friction that retards the motion of a wheel. Disc brakes provide better stopping, are less prone to be out-of-adjustment and are relatively resistant to brake fade. Heat dissipation is efficient in disc brakes with vented designs which makes it possible to maintain high braking performance in demanding conditions. (Bendix Spicer Foundation Brake LLC, 2011). Despite their advantages over drum brakes, disc brakes can also experience brake fade when overheated. (Trevorrow and Eady, 2010). The disc can warp due to varied thermal expansion of separate parts, which will result in less effective braking.

Disc brakes are used wide-spread in Europe. Though disc brakes are gaining popularity on the United States market, they are not quite as popular as drum brakes. When the FMVSS 121 stopping distance-rules for heavy vehicles were announced, it was expected that this will be a push for conversion from drum to disc brakes. However, this expectation has not been met. The lethargy in installing disc brakes has been due to costs, weight and existing infrastructure for drum brake manufacture that have existed for three or four decades. (Berg, 2014).

© 2014 CCJ.

Figure 22 shows an air disc brake.



© 2014 CCJ.

Figure 22. Photo. Air Disc Brake. (Roberts, 2014).

Retarders

Truck braking is achieved primarily through the use of the service brakes. Most trucks are equipped with retarders, also known as auxiliary brakes to provide additional braking power on downgrades. Four main retarders are in current use. These are:

- Engine compression (Jake) brake retarders.
- Exhaust retarders.
- Hydraulic driveline retarders.
- Electric driveline retarders.

Engine Compression (Jake) Brake Retarders

The engine brake was first developed by Clessie L. Cummins in 1931 after a near crash on a steep descent of the Cajon Pass on Old US-66 highway leading to San Bernardino, California. Engine brakes are by far the most popular retarders installed on trucks. Engine brakes function by converting the engine into an energy-absorbing air compressor. Specifically, a master-slave piston arrangement is used to open the cylinder exhaust valves near the top of the normal compression stroke, releasing the compressed cylinder charge to exhaust. (Cummins, 1966). As a result, there is a reduction in the pressure of compressed air to atmospheric conditions preventing the piston from going back down during the power stroke. This leads to a net power absorption by the engine during its operating cycle. (Myers et al., 1981).

Exhaust Retarders

The exhaust brake functions by using a valve installed on the engine exhaust system to restrict and hold back the engine exhaust. Exhaust restriction is achieved by either a butterfly or sliding-type valve. As this pressure increases, work spent by the piston compressing the air is not recovered when the exhaust valve of the cylinder is closed on the down stroke. The back pressure increases until the pressurized gas re-enters the cylinders on the down stroke, and also enters the intake manifold through the intake valve. (Fancher et al., 1981). This increases the back pressure inside the engine and slows the truck down. Exhaust retarders are known to offer only about half the retarding power of engine brakes but produce less noise, are easy to operate and are relatively inexpensive. (Wilson, 2000).

Hydraulic Driveline Retarders

Hydraulic retarders make use of the viscous drag forces between dynamic and static vanes in a fluid-filled chamber to achieve retardation. (Pandey et al., 2015). The retardation device is actuated by filling a chamber with fluid which resists a rotor movement. Heat is generated as the fluid is churned and removed by a cooling system. (Fancher et al., 1981). The degree of retardation is varied by adjusting the fill level of the chamber. Hydraulic retarders are quiet in relation to engine retarders, and do not produce axle lockup because they produce no torque at zero rpm. (Fancher et al., 1981).

Electric Driveline Retarders

Electric retarders convert mechanical energy to thermal energy by an electric eddy-current generator. Retardation is achieved by providing a retarding torque to a rotating component such as the propeller driveshaft, a drive axle differential or a trailer axle. This rotating component is attached to a steel disc that turns in the flux field of a set of fixed electro-magnets. Generated thermal energy is dissipated by cooling fins. Electric retarders are known to absorb high forces. However, electric retarders produce a torque proportional to speed at low rpm which implies that an electric retarder alone cannot bring the vehicle to rest. (Fancher et al., 1981).

INTEGRATION OF THE BRAKE TEMPERATURE EQUATION

The discussions above highlight the roles several factors play in the downgrade braking model. The section on brake types and function provides a good basis to develop the brake temperature equation. The following discussion presents the development of the brake temperature model as formulated by the FHWA study. Myers et al., 1981. As noted previously, brakes are energy converters and transform mechanical energy to heat energy. The thermal energy is absorbed by the brakes and then dissipated out to the environment by convection, radiation and conduction. This process can be represented as an energy balance equation (

$$\left(\begin{array}{c} \text{Rate of change of} \\ \text{internal energy} \\ \text{in brake system} \end{array} \right) = \left(\begin{array}{c} \text{Rate of conversion} \\ \text{of mechanical energy} \\ \text{to heat brake system} \end{array} \right) - \left(\begin{array}{c} \text{Rate of heat} \\ \text{transfer from} \\ \text{brake system} \end{array} \right)$$

Figure 23):

$$\left(\begin{array}{c} \text{Rate of change of} \\ \text{internal energy} \\ \text{in brake system} \end{array} \right) = \left(\begin{array}{c} \text{Rate of conversion} \\ \text{of mechanical energy} \\ \text{to heat brake system} \end{array} \right) - \left(\begin{array}{c} \text{Rate of heat} \\ \text{transfer from} \\ \text{brake system} \end{array} \right)$$

Figure 23. Equation. Energy Balance.

For simplicity, the energy balance equation above does not consider the spatial distribution of temperature in an individual brake or the distribution of braking effort among the brakes. The equation only accounts for the gross energy balance in the braking systems and is thus considered a “lumped parameter” model. The brake temperature attained during sustained braking may be analyzed from simple analytical solutions given that the braking power, cooling and braking times remain constant. For the lumped parameter model, the internal thermal energy

in the brakes is assumed to be proportional to the temperature with the total heat capacity $M_B C$, being the proportionality constant. Consideration of the rate at which mechanical energy is converted into thermal energy in the brakes is by the power input into the brakes, HP_B . Heat transfer from the brakes is by convection, conduction and radiation. However, it has been found that most heat transfer from the surface of the brakes is by convection into the surrounding airstream. (Murphy et al., 1971). The relatively small effects of conduction and radiation are lumped with the convection. The basic equation for the transfer of heat by convection is expressed as (Figure 24):

$$hA_c(T - T_\infty)$$

Figure 24. Equation. Heat Transfer Relation.

where,

h = film coefficient in lb/ft-°F,

A_c = effective heat transfer area of the brake ft²,

T = temperature of the brake drum in °F, and

T_∞ = ambient temperature in °F.

The above equation in Figure 24 is also referred to as the Newton cooling equation. Under the assumptions enumerated above, the energy balance equation (

$$\left(\begin{array}{c} \text{Rate of change of} \\ \text{internal energy} \\ \text{in brake system} \end{array} \right) = \left(\begin{array}{c} \text{Rate of conversion} \\ \text{of mechanical energy} \\ \text{to heat brake system} \end{array} \right) - \left(\begin{array}{c} \text{Rate of heat} \\ \text{transfer from} \\ \text{brake system} \end{array} \right)$$

Figure 23) may be written as a first order differential equation as shown in Figure 25. (Myers et al., 1981):

$$M_B C \frac{dT}{dt} = HP_B - hA_c(T - T_\infty)$$

Figure 25. Equation. First Order Brake Temperature Equation.

where,

M_B = brake mass in lb,

C = the specific heat capacity in ft-lb/slug, and all other symbols are as previously defined.

The equation in Figure 25 provides an analytic expression for brake temperature. For this equation, brake mass, the effective brake system area, and the specific heat capacity of the brake system are constants independent of speed. With an initial brake temperature specified, the equation may be considered as an initial value or Cauchy problem. To compute the amount of braking received by the braking system, an expression relating brake force and speed is used. This is expressed as (Figure 26):

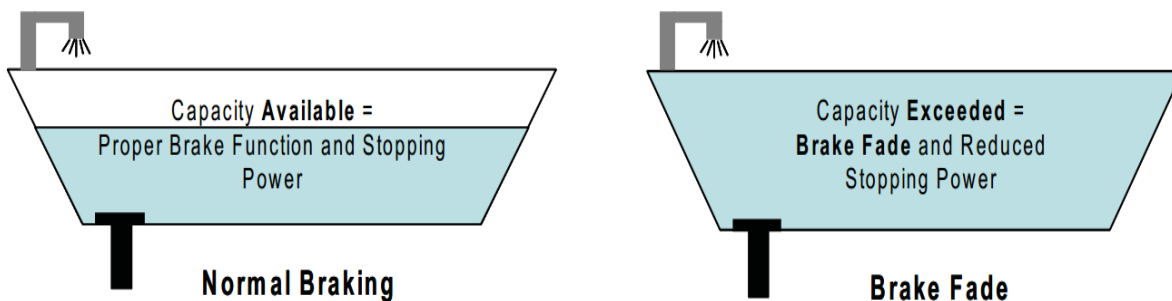
$$HP_B = \frac{F_B V}{375}$$

Figure 26. Equation. Horsepower into Brakes.

The use of the brake force in the temperature equation model assumes that the available brake force is just enough for the actual force required. This required brake force is as expressed in Figure 26. For the development of the brake temperature model, the temperature rise during a steady descent with no acceleration and a constant non-brake force (F_{NB}) are of interest. The slope of the downgrade(θ), braking force(F_B), and hence power into the brakes (HP_B) are also assumed constant. With HP_B constant, the brake temperature equation may be derived using standard techniques.

To better understand the mathematical formulation of the brake temperature, it is important to consider a physical analogy of the proffered solution (integration). The brake tab analogy on the generation and dissipation of thermal energy has been considered in this analogy. Two important factors are critical in the functioning of brake systems in generating and dissipating thermal energy; the amount of heat the system retains, commonly referred to as thermal capacity, and the rate at which this thermal energy is dissipated into the atmosphere. (Bendix Spicer Foundation Brake LLC, 2011). The bathtub analogy illustrates this point (© 2011 Bendix

Figure 27).



© 2011 Bendix

Figure 27. Picture. Bathtub Analogy of Brake Heat Transfer. (Bendix Spicer Foundation Brake LLC, 2011).

The amount of water the tub can hold is its capacity. For a brake system, the thermal capacity is mainly dependent on the size, shape, and material of the drum or rotor. The rate at which water flows into the tub from the faucet is equivalent to the rate that the brake system adds heat to its capacity during energy transformation to heat as the brakes are applied. As water fills the tub, the drain removes the water, preventing an overflow. In a steady state or equilibrium condition, water must be drained out of the tub at a rate just equal to the flow rate of water into the tub. This function is similar to a brake system's objective to dissipate heat at a rate that prevents brake fade. The steady input of power into the brakes will cause the temperature to rise until the temperature difference reaches an equilibrium, and the heat transfer out of the brakes just equals the power into the brakes. In situations where the drain is unable to match the rate at which water is being added, the tub will overflow. This is parallel to brake fade which occurs when the thermal capacity of the brake system has been exceeded leading the system to operate at a reduced effectiveness. From the bathtub analogy, it may be observed that a large tub implies that more water can be stored for a given depth. This implies that a high heat capacity or brake mass can store more thermal energy in the brake system for a given temperature level. A large drain orifice, and thus a higher discharge coefficient results in a high flow rate out of the tub, implying

that a lower head is required to balance a given input flow rate. Similarly, a high heat transfer coefficient reduces the temperature required to balance a given power input. This also means that the steady-state fluid level will be approached rapidly as the fluid will not rise high. A high brake heat transfer coefficient will cause the brake system to dissipate heat quickly and respond in time to brake power inputs and temperature rise because the low steady-state temperature will be approached quickly.

The analogous description in the bathtub flow and brake heating equivalents are summarized in Table 1. The concept of the bathtub may now be made quantitative by formally solving the brake temperature initial value problem.

Table 1. Bathtub flow analogy versus truck brake heating.

No.	Bathtub Flow	Truck Brake
1.	Water flow rate into bathtub	Rate of flow of energy (power) into brakes, HP_B
2.	Fluid head (depth)	Temperature difference, $T - T_\infty$
3.	Area of bathtub	Total effective heat capacity, $M_B C$
4.	Volume of water in tub	Internal energy, $M_B CT$
5.	Orifice discharge coefficient	Effective heat transfer coefficient, h
6.	Orifice area	Total effective heat transfer area, A_c
7.	Rate of water flow out of tub	Heat transfer rate, $hA_c(T - T_\infty)$

The differential equation (Figure 25) may then be integrated using standard techniques to derive the brake temperature equation. The brake temperature equation is defined as:

$$T(t) = T_o + [T_\infty - T_o + K_2 HP_B][1 - e^{-K_1 t}]$$

Figure 28. Equation. Brake Temperature Equation at Time (t).

where,

$K_1 = \frac{hA_c}{M_B C}$ is the inverse thermal time constant, and

$K_2 = \frac{1}{hA_c}$ is the inverse of the total heat transfer parameter.

Both expressions for K_1 , and K_2 can be expressed as functions of speed through the effective heat transfer coefficient (h). This formulation of the brake temperature equation was derived by Limpert, 1975. The reader is also referred to Myers et al., 1981 for details on the integration of the brake temperature equation. The temperature equation can be rewritten with a substitution for time, $t = x/V$ (Figure 29):

$$T(x) = T_o + [T_\infty - T_o + K_2 HP_B][1 - e^{-K_1 x/V}]$$

Figure 29. Equation. Brake Temperature Equation at Distance (x).

The equation in Figure 29 is appropriate for the analysis because the GSRS is often concerned with the brake temperature at some distance, x from the summit. As the distance becomes infinite, the exponential term $[1 - e^{-K_1x/V}]$ goes to 1 and the brake temperature reaches a steady-state value (Figure 30):

$$T_{ss} = T_{\infty} + K_2HP_B$$

Figure 30. Equation. Steady-State Temperature.

where,

T_{ss} = steady-state temperature in °F.

To assess the effect of HP_B and K_1 on brake temperature rise, an assumption is made that $T_o = T_{\infty}$. The equation in Figure 29 may then be rewritten as the ratio of power into the brakes divided by the total heat transfer coefficient $1/K_2 = hA_c$, all multiplied by an exponential factor. This gives:

$$T - T_{\infty} = \frac{HP_B}{hA_c} [1 - e^{-(hA_c/M_{BC})(x/V)}]$$

Figure 31. Equation. Relation between Temperature Change and Power into Brakes.

where, A_c = effective heat transfer area of the brake, ft². It may be observed from the equation in Figure 31, that all things being equal, increasing power into the brakes or reducing the heat transfer out of the brakes will increase brake temperature.

To sufficiently analyze brake system temperatures, it is useful to assess the physical significance of the brake temperature model parameters. Brake temperature in the temperature equation is considered as a “control variable” in that the driver attempts to control brake temperature to prevent brake fade. (Myers et al., 1981). In turn, the brake temperature may be controlled by speed and transmission gear, which are also control variables because they are controlled by the driver. For the grade geometry parameters slope and length which completely characterize any single grade hill, the temperature model assumes them to be constant. The parameters T_{∞} and T_o are thought of as environmental parameters which are characteristics of a downgrade site. However, T_o may also be considered a truck parameter. The parameter, T_o is largely determined by highway characteristics near the beginning of a downgrade site, and ambient conditions. In the development of the FHWA GSRS model, T_o was considered more as an environmental parameter, constant for all trucks. The remaining parameters, (W , K_1 , K_2 , F_{drag} , and HP_B) are specific to trucks but may be considered truck population truck variables, (excluding W) and are nominally constant from day to day for a specific truck. (Myers et al., 1981). However, truck weight, cannot be considered a population variable, in that it varies day to day for each specific truck, and is thus the truck variable.

Bowman, 1989, suggests that on substantial non-braking sections (including upgrades), the value of the grade should be set to zero. This accounts for the cooling that takes place during those

non-braking intervals. The cooling on such sections is also associated with a decrease in horsepower into the brakes as demonstrated in Figure 32:

$$HP_B = (-F_{drag}) \frac{V}{375} - HP_{eng}$$

Figure 32. Equation. Brake Temperature Equation for Non-Braking Intervals.

IMPLICATIONS OF THE GSRS MODEL

The implications of the GSRS model is presented in this section, as discussed by Myers et al., 1981. The FHWA GSRS model is based on the brake temperature model to predict brake temperatures during grade descent. Values of the parameters in the model were determined and validated by conducting field tests with a typical 3-S2 tractor semi-trailer combination (5-axle truck). The test truck was fitted with temperature sensors (thermocouples), installed in the brake linings, and an eight-channel recorder to measure the vehicle speed, engine speed, and brake application pressure during the tests. Three primary tests were conducted for the study; coast-down, cool-down and hill descent tests. The coast-down tests were undertaken to determine the non-brake forces acting on the truck. Cool-down and hill descent tests were conducted to assess the cooling and heating characteristics of the truck brakes by determining the thermal constants K_1 and K_2 respectively. Details of the tests are discussed in the methodology chapter. Table 2 shows a summary of the truck downgrade braking model parameters developed by Myers et al., 1981:

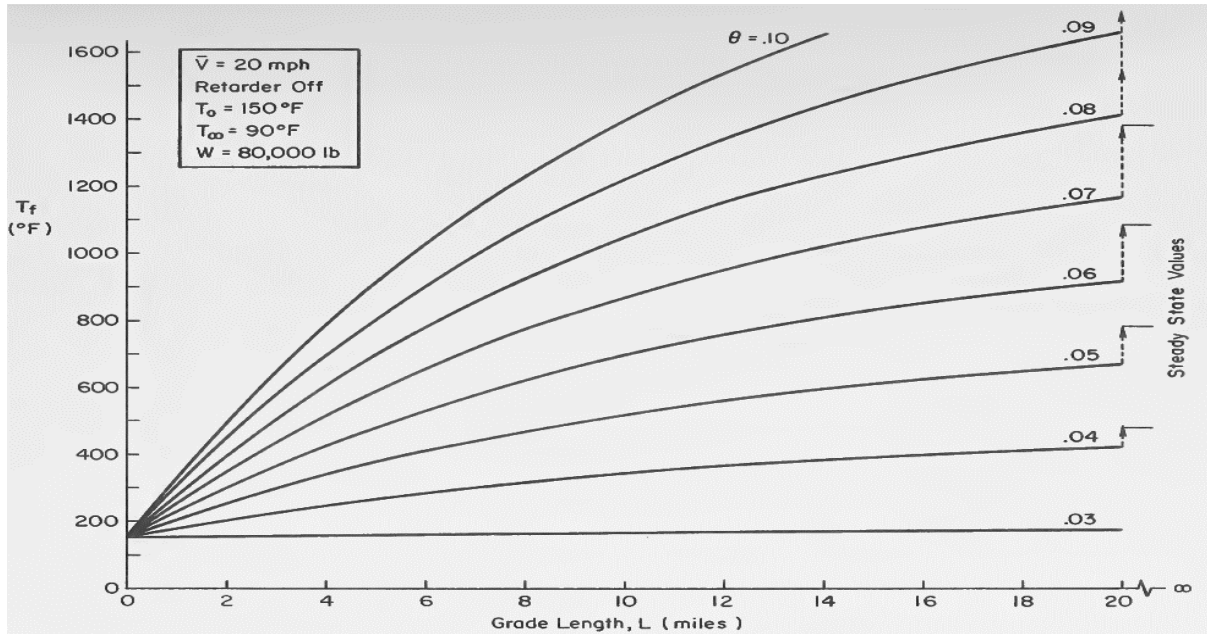
Table 2. Summary of FHWA GSRS Model Parameters.

Expression	Units
$T_f = T_o + [T_\infty - T_o + K_2 HP_B][1 - e^{K_1 L/V}]$	°F
$HP_B = (W\theta - F_{drag}) \frac{V}{375} - HP_{eng}$	hp
$K_1 = 1.23 + 0.0256V$	1/hr
$K_2 = (0.100 + 0.00208V)^{-1}$	°F/hp
$F_{drag} = 450 + 17.25V$	lb
$HP_{eng} = 73$	hp
$T_\infty = 90$	°F
$T_o = 150$	°F

The use of the GSRS model requires an understanding of how the brake temperature interacts with different variables. Insights into these interactions may be achieved by plotting brake temperature as a function of the independent variables.

© 1981 FHWA.

Figure 33 is a plot of the variation of grade in the brake temperature-grade length plane. The graph shows an initial rapid rise in temperature that eventually becomes asymptotic as the brake temperature approaches a steady-state value.



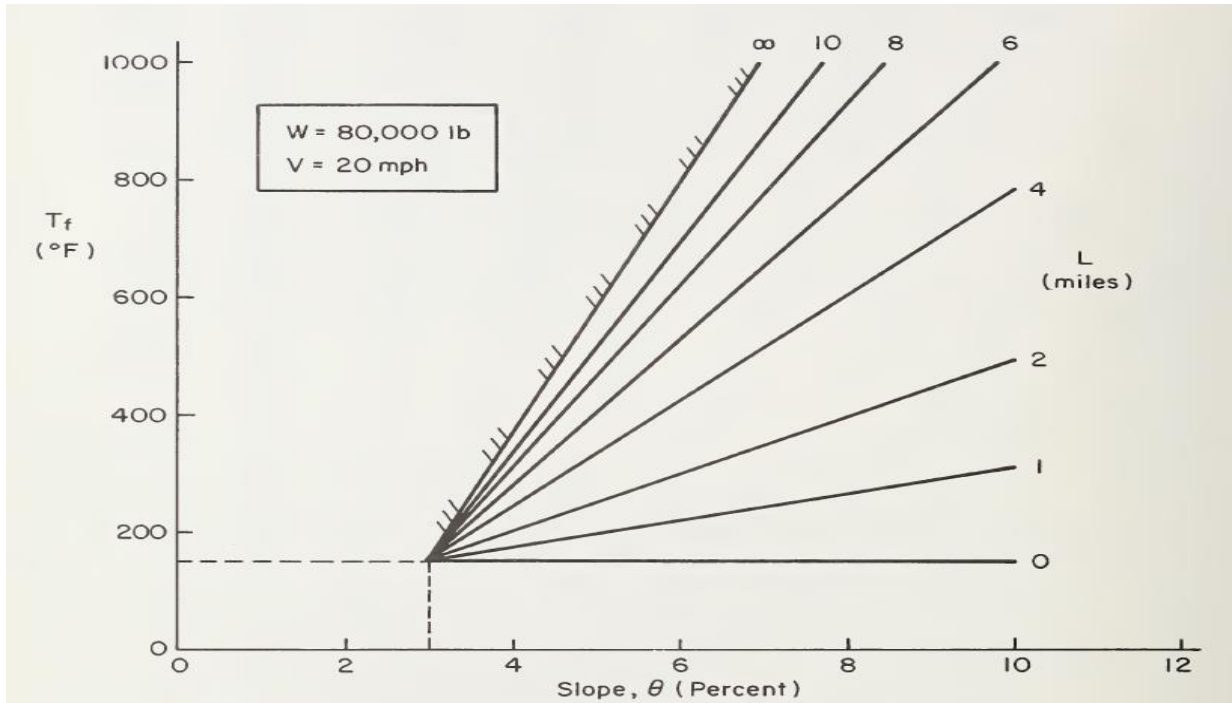
© 1981 FHWA.

Figure 33. Graph. Variation of Length with Temperature. (Myers et al., 1981).

© 1981 FHWA.

Figure 34. Graph. Variation of Grade with Temperature. (Myers et al., 1981).

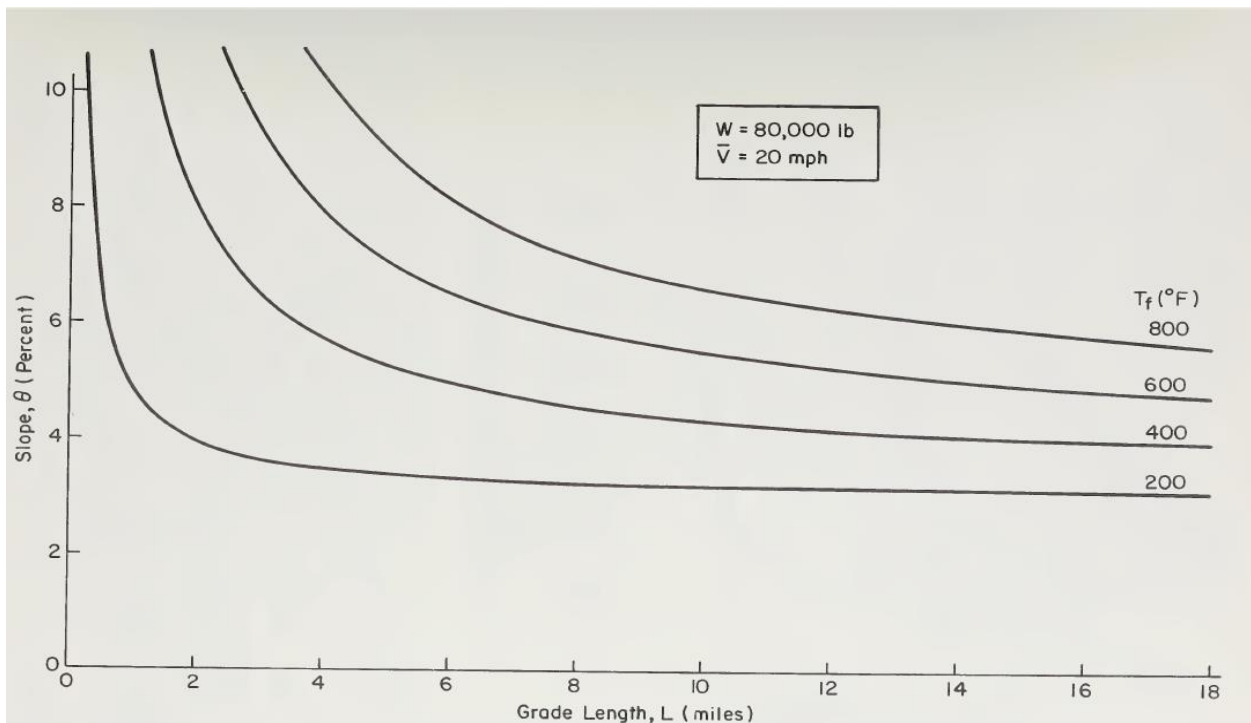
shows a plot of brake temperature with grade. It may be observed that for a given grade length, the final brake temperature varies linearly with slope. This increase corresponds with an increase in grade length and increases asymptotically for an infinitely long grade as it approaches a steady-state value.



© 1981 FHWA.

Figure 34. Graph. Variation of Grade with Temperature. (Myers et al., 1981).

Error! Reference source not found. shows a plot of final temperature contours in the grade and length parameter plane. The shape is hyperbolic and shows that for a given final brake temperature, a steep hill is always shorter than a shallower hill. (Myers et al., 1981).



© 1981 FHWA.

Figure 35. Graph. Isotherms as a Function of Grade and Length. (Myers et al., 1981).

© 1981 FHWA.

Figure 36, © 1981 FHWA.

Figure 37 and © 1981 FHWA.

Figure 38 show the variation of brake temperature with weight (W) and speed (V). © 1981 FHWA.

Figure 36 shows a linear relationship between truck weight and speed. This linear relationship is similar to the relationship between temperature and slope (© 1981 FHWA).

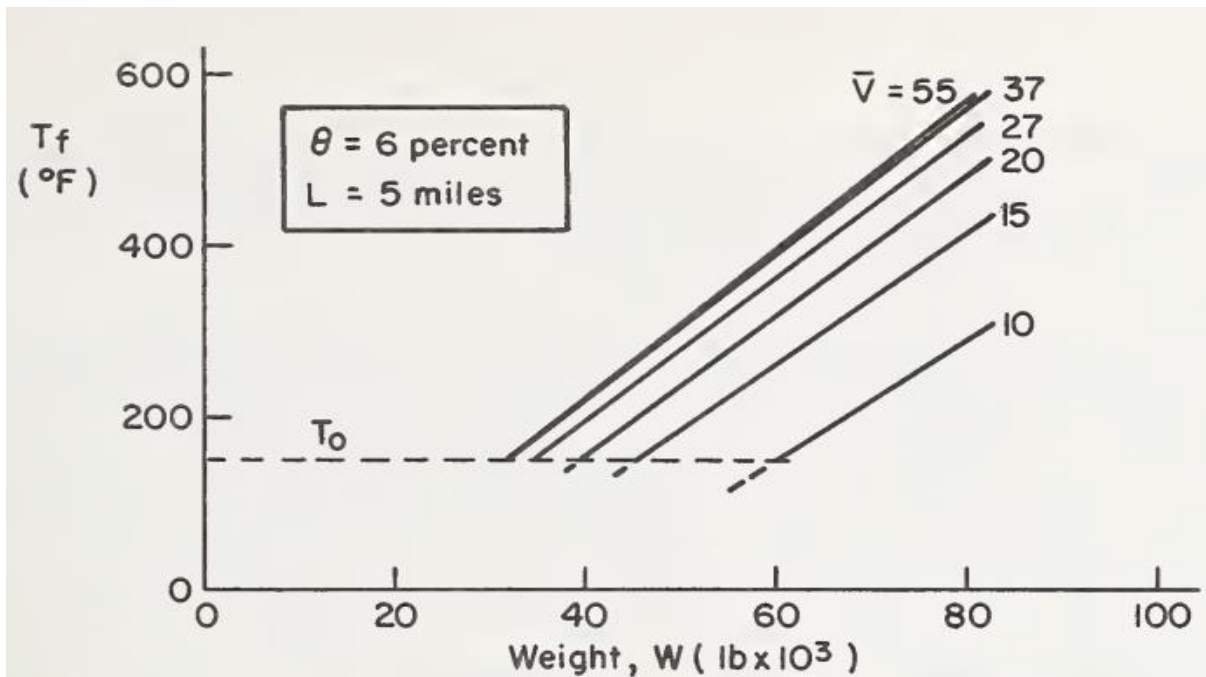
Figure 34. Graph. Variation of Grade with Temperature. (Myers et al., 1981).

). This similarity is because weight and slope appear as a product ($W\theta$) in the GSRS equation and represents the downgrade component of weight. (Myers et al., 1981).

© 1981 FHWA.

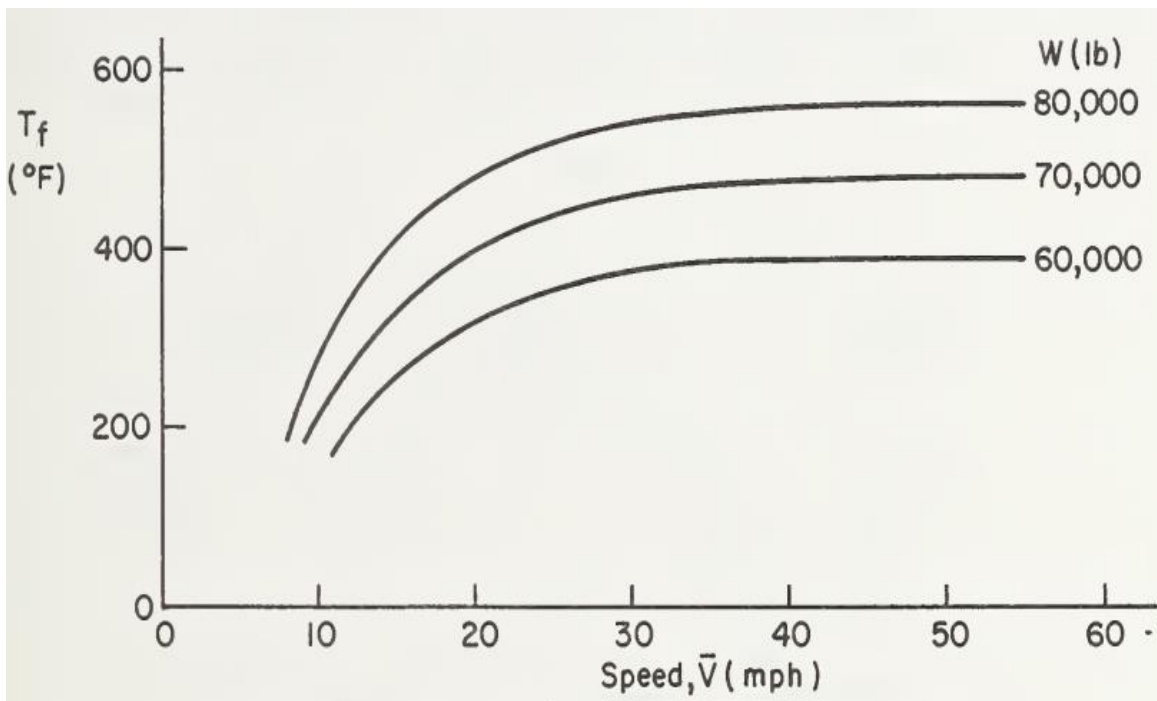
Figure 37 indicates that as weight increases with increasing speed, brake temperature will also increase. © 1981 FHWA.

Figure 38 shows a plot of temperature in the weight and speed plane. The plot is roughly hyperbolic with an increase in weight requiring a decrease in speed to maintain a constant brake temperature



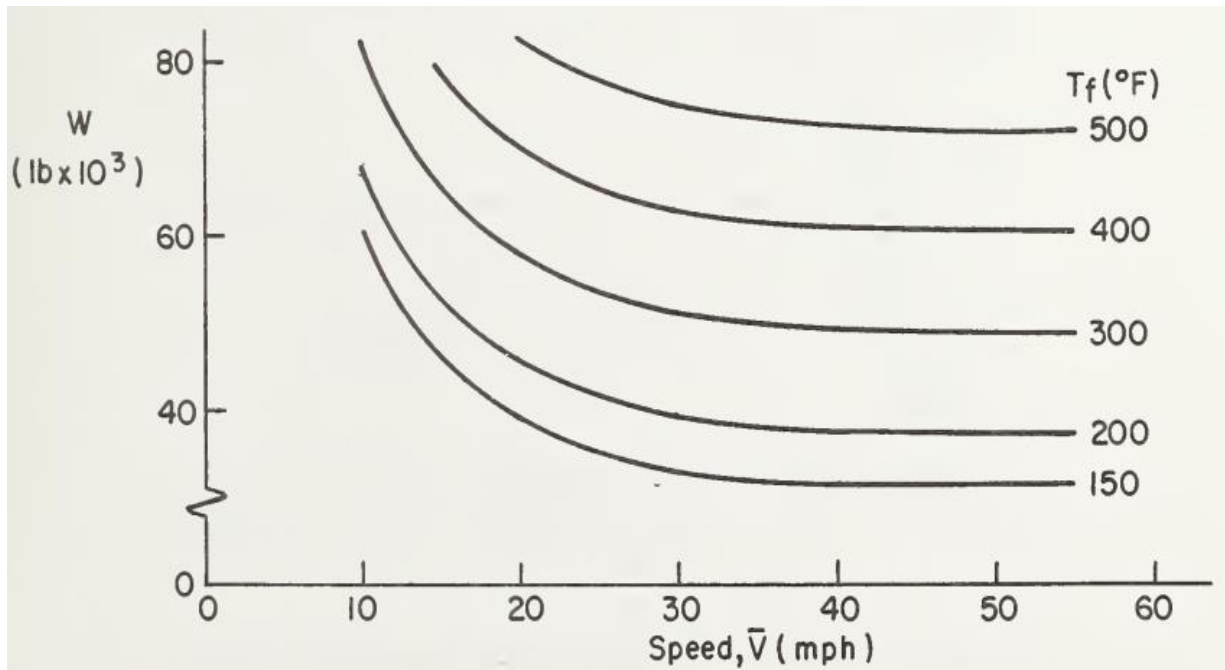
© 1981 FHWA.

Figure 36. Graph. Variation of Weight and Temperature with Speed as a Parameter. (Myers et al., 1981).



© 1981 FHWA.

Figure 37. Graph. Weight as a Function of Temperature and Speed. (Myers et al., 1981).



© 1981 FHWA.

Figure 38. Graph. Isotherms as a Function of Weight and Speed. (Myers et al., 1981).

In terms of the variation of temperature with regards to speed and distance, it can be observed, from © 1981 FHWA.

Figure 39, that for a grade of given length, the final brake temperature increases rapidly with descent speed in the low speed region. At higher speeds ($V > 30$ mph), the final temperature is found to be constant or decreases with increasing speed over a wide speed range. The plot trend shows an expected scenario and is related primarily to the speed variation of the heat transfer coefficient. To examine this concept in more detail, it is worth examining the variation of the final brake temperature (T_f) with speed from the basic factors in the brake temperature equation (Figure 29).

© 1981 FHWA.

Figure 40 shows the power absorption for various levels of the downgrade component of weight, $W\theta$. It may be observed that an increase in either the weight of the truck or slope of the grade will lead to an increase in the power absorbed by the brakes given any descent speed. Also, the power absorption increases almost linearly with speed (apart from the lowest level of $W\theta$). However, there is a limit beyond which the temperature will no longer increase (steady-state) as shown in © 1981 FHWA.

Figure 41. This limitation is due to the variation of the total effective heat transfer parameter, with velocity. The increasing heat transfer rate with increasing speed despite the increased power absorption results in the brake temperature flattening out at high speeds. This is manifested in the greater curvature of the $W\theta$ lines (shown in © 1981 FHWA.

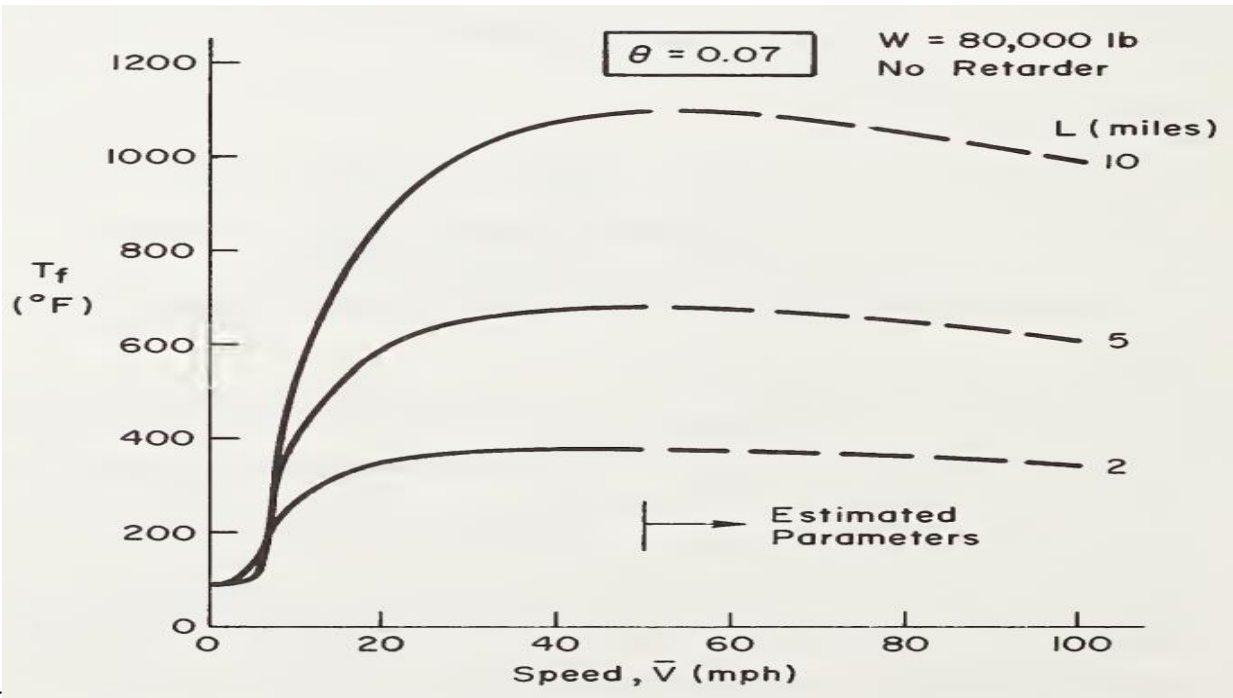
Figure 42) compared to © 1981 FHWA.

Figure 40. A further look at the plot of the inverse thermal distant constant K_1/V shown on © 1981 FHWA.

Figure 43 indicates it has an additional flattening effect shown by the shape of the exponential, finite length factor. Multiplying the exponential factors by the steady-state temperature curves (from © 1981 FHWA.

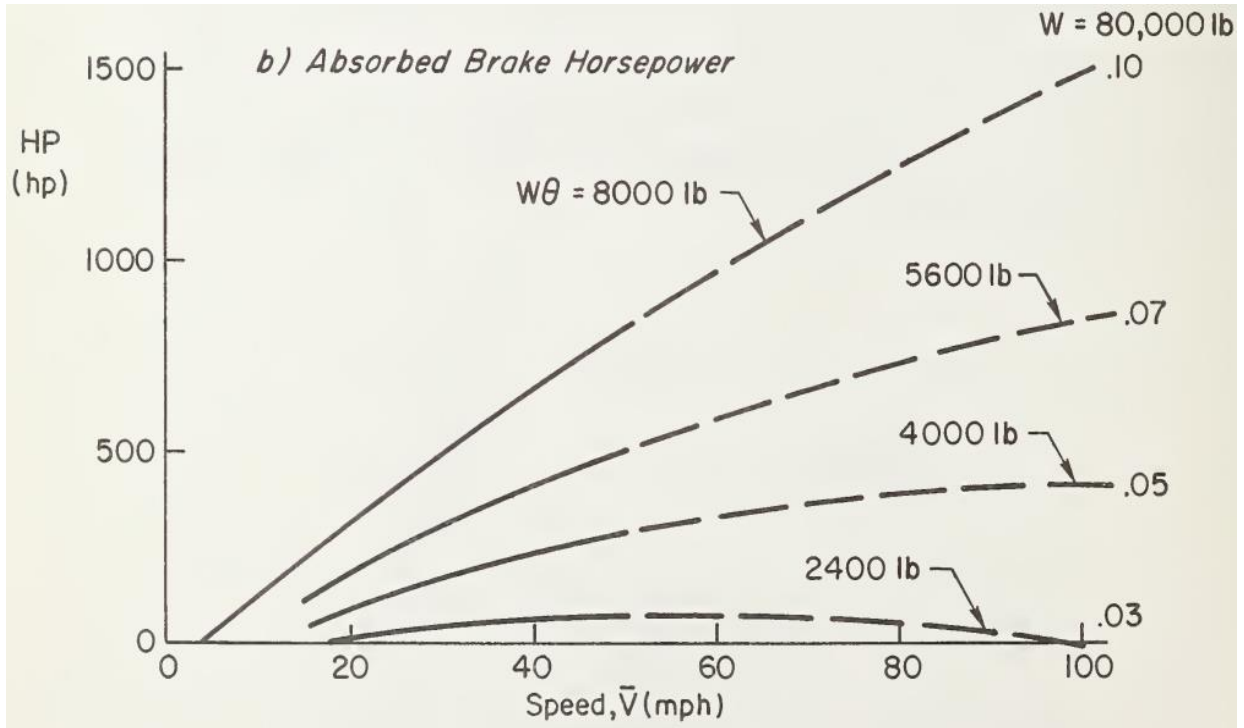
Figure 42) for $\theta = 0.07$ results in the T_f curves of © 1981 FHWA.

Figure 39.



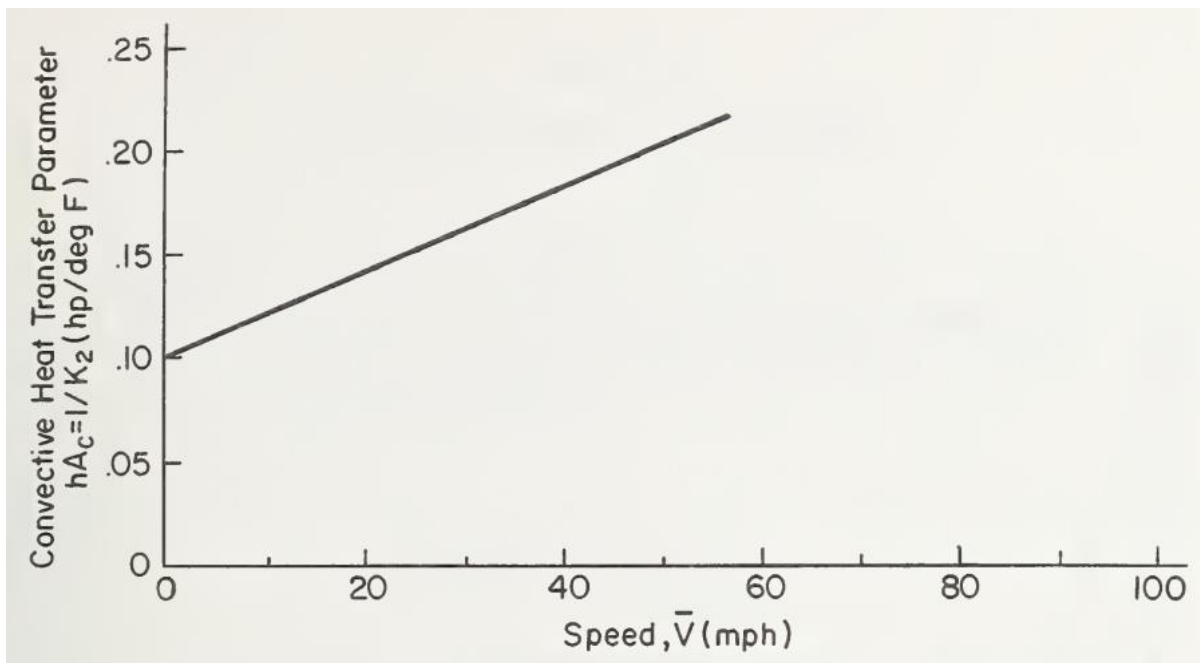
© 1981 FHWA.

Figure 39. Graph. Variation of Brake Temperature with Speed. (Myers et al., 1981).



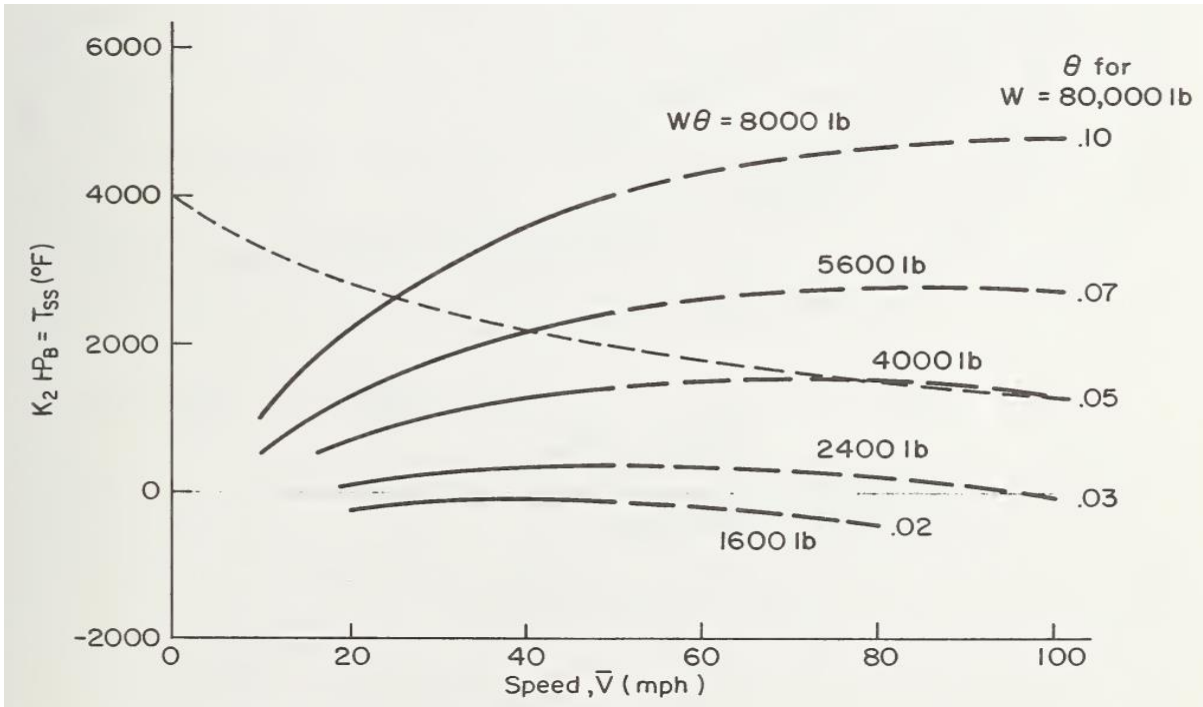
© 1981 FHWA.

Figure 40. Graph. Variation of Brake Horsepower Absorption with Speed. (Myers et al., 1981).



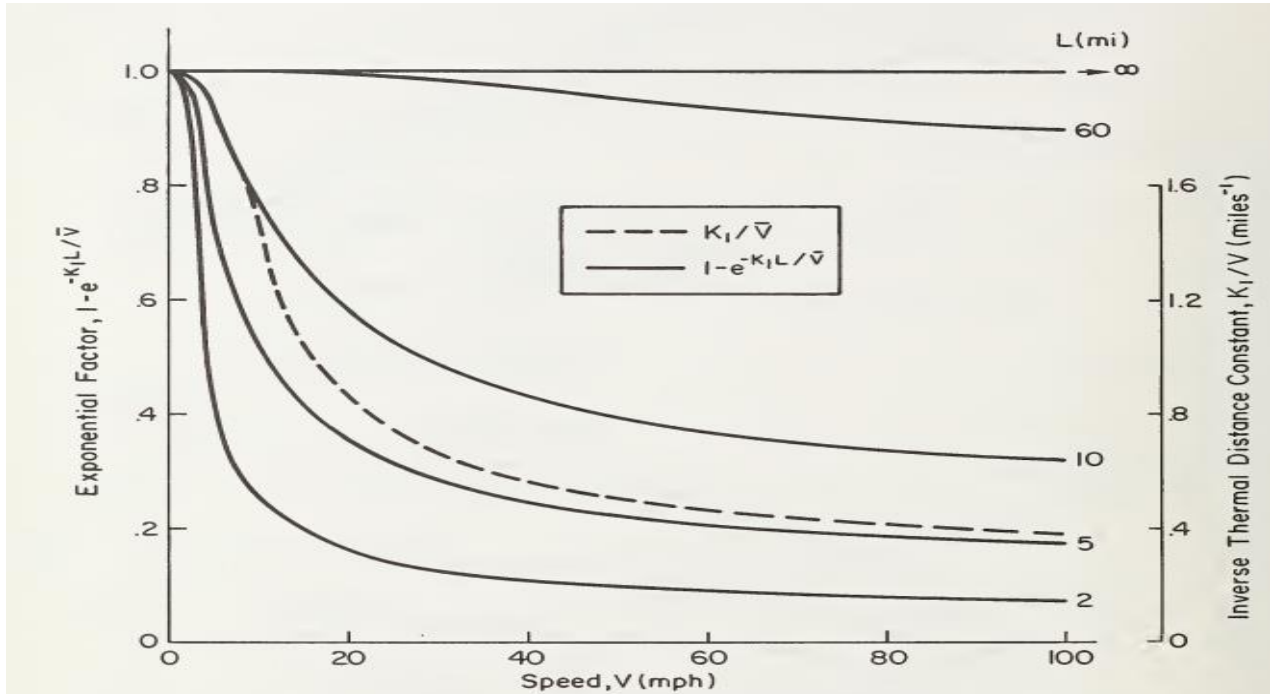
© 1981 FHWA.

Figure 41. Graph. Variation of Convective Heat Transfer Parameter with Speed. (Myers et al., 1981).



© 1981 FHWA.

Figure 42. Graph. Steady-State Brake Temperature. (Myers et al., 1981).



© 1981 FHWA.

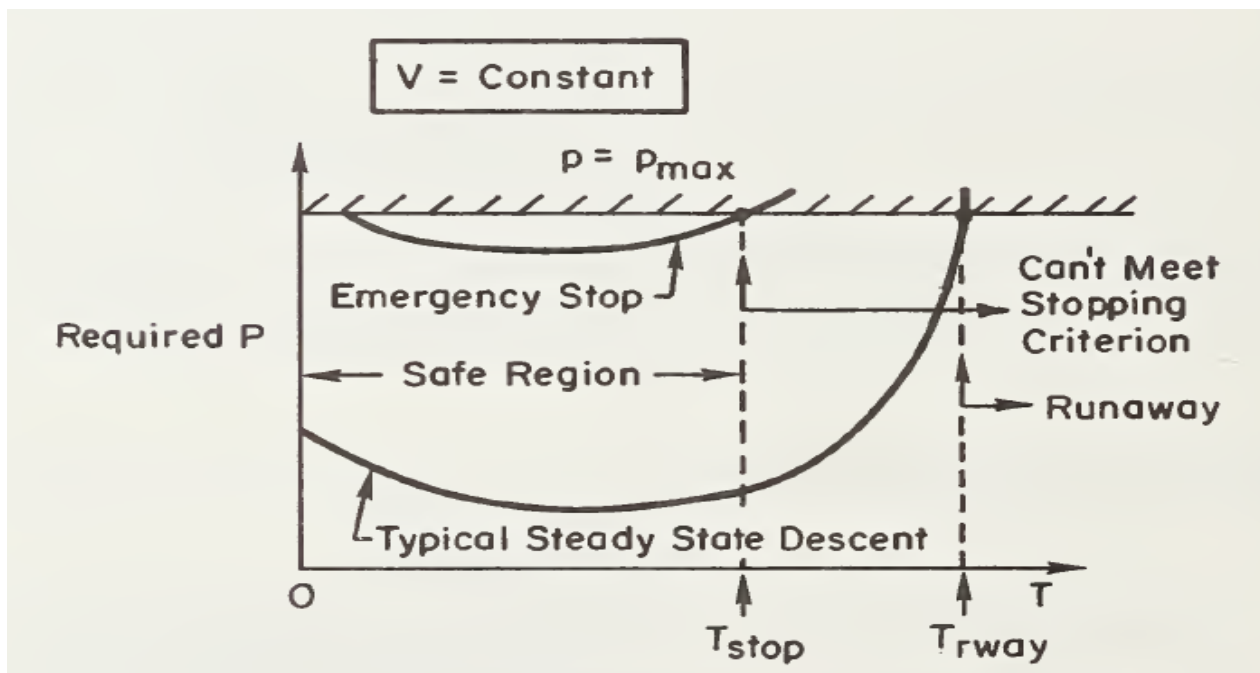
Figure 43. Graph. Exponential Variation of Steady-State Temperature. (Myers et al., 1981).

Brake Temperature Limit and Maximum Descent Speed

A workable GSRS requires an analysis of brake fade with increasing brake temperature. For a given grade descent, the available braking force must be equal to the force required. As the brake temperature increases during the grade descent, the pressure required to generate the brake force increases. With brake fade developing, the pressure required to achieve the required braking force also increases. However, there is a maximum pressure limit that the brake system can produce. This means that there is a maximum temperature limit beyond which safe braking can no longer be accomplished. © 1981 FHWA.

Figure 44 shows a plot of brake temperature with pressure variation. The limiting temperature is lowest for the emergency stopping requirement. An increase in temperature to T_{stop} will result in an inability of the brake system to make an emergency stop. However, a runaway will not occur at this temperature. An additional increase in temperature is required to T_{rway} before a runaway incident can occur. (Myers et al., 1981).

The preceding discussion shows that for a given constant speed and a brake pressure limit; emergency stop, and runaway situations can be specified in terms of temperature. This concept is completely equivalent to the use of a stopping distance criteria or deceleration. (Myers et al., 1981).



© 1981 FHWA.

Figure 44. Graph. Brake Pressure Variation with Temperature. (Myers et al., 1981).

Though the effects of speed fade are not clearly defined, it is known that the greatest loss of brake efficiency occurs at high speed. Consequently, lower values of T_{stop} and T_{rway} occur at high speeds. Therefore, for a driver to have sufficient braking force during grade descent, it is necessary to maintain a brake temperature at or below some temperature limit, T_{lim} , which is less

than or equal to T_{stop} . This logic is the temperature limit concept on which the GSRS is based. GSRS aids drivers in maintaining downgrade temperatures at or below T_{lim} ; and a single value of T_{lim} is used for all truck loads and speeds.

The use of a single value of T_{lim} may be deemed conservative. However, the range of variations of the temperature limit with speed among trucks is comparable to the uncertainty with which the limit can be determined for any specific truck and speed. (Myers et al., 1981). The temperature limit concept is akin to what is commonly practiced by truck drivers in the field. Truck drivers frequently watch their mirrors for signs of smoking brakes which is an indication that the brakes are about to fade. Going by the temperature limit concept, the task of a driver on a downgrade is therefore to control brake temperature, by selecting an appropriate gear and speed for the downgrade in question. This implies that a temperature constraint is imposed on the brake system which must be satisfied during the grade descent. This can be written as (Figure 45):

$$T(x) = T_{lim}$$

Figure 45. Equation. Limiting Temperature Constraint.

The equation in Figure 45 simply implies that the brake temperature may never exceed the temperature limit at any point on the grade during descent. A possible strategy to satisfy this constraint will for a driver to pick a speed such that the steady-state temperature (T_{ss}) (which is only slope dependent) is less than or equal to the temperature limit (Figure 46) :

$$T_{ss} = T_{lim}$$

Figure 46. Equation. Steady-State at Limiting Temperature.

However, this has been found to be too conservative and would require drivers to descend a grade at a much lower speed than is necessary to keep the brake temperature below T_{lim} . (Johnson et al., 1982a). As an example, to descend a 5-mile-long, 6 percent grade in a 70,000 lb truck such that $T_{ss} = T_{lim}$, a speed less than 13 mph is required. But it is possible to descend this grade at 28 mph without exceeding the temperature limit. (Myers et al., 1981). It is therefore important to consider the length and slope of the grade in determining the maximum safe descent speed.

An issue of time arises in setting up maximum safe descent speeds for grades. A practical GSRS in addition to guiding drivers to maintain brake temperatures below the temperature limit must also allow drivers to descend the grade as quickly as possible, within the constraints of safety. A conservative system that advises unrealistically low descent speeds will likely be ignored by drivers. This means a workable GSRS must not only overcome the temperature control problem, but also an optimal control problem.

From © 1981 FHWA.

Figure 33, brake temperature increases monotonically along the grade for a constant speed descent. This means that for a single grade, brake temperature will always be highest at the bottom of the grade. Thus, if a descent speed is selected which ensures that the final brake

temperature at the bottom of the grade is just equal to the temperature limit, the maximum safe speed will have been selected for that downgrade that minimizes the descent time. This translates to (Figure 47):

$$T_f = T_{lim}$$

Figure 47. Equation. Limiting Temperature at Bottom of Grade.

This requirement is applicable to a constant descent speed. The use of the GSRS to safely descend grades requires drivers to control brake temperature below a limiting temperature, a process referred to as “open-loop”. This means that drivers must select the speed and corresponding gear before beginning descent and maintaining it all the way down the grade. Downshifting on downgrades is very dangerous as it may be impossible to get the gears engaged once the truck is in neutral on a grade. (Bowman, 1989). The primary main disadvantage of open-loop is that it does not automatically compensate for variations in grade geometry or truck weight. What this means is that drivers and highway designers are confronted with the task of determining the correct speed for many grades, trucks and loads.

Myers et al., 1981 defines the maximum safe descent speed (V_{max}) as:

“The (constant) descent speed, less than or equal to the speed limit which produces a maximum brake temperature equal to the temperature limit when maximum engine retardation is used”. (Myers et al., 1981).

In other words, V_{max} is the speed which satisfies the optimal control requirement. This implies that $T_f = T_{lim}$ as shown in Figure 48.

$$T_f = T_o + [T_\infty - T_o + K_2 HP_B][1 - e^{K_1 L/V}] = T_{lim}$$

Figure 48. Equation. Relationship between Final and Limiting Brake Temperature.

where, HP_B is based on maximum engine retardation (selection of the right gear to produce maximum engine retardation). V_{max} could be solved explicitly by rearranging the equation in Figure 48 . However, the complexity of the functional relationships between V, K_1 , K_2 and HP_B prohibit that from being done. Instead, an indirect approach can be adopted by rearranging the equation in Figure 48 to solve explicitly for L (Figure 49). (Myers et al., 1981).

$$L = -\frac{V_{max}}{K_1} \ln \left[1 - \frac{T_f - T_o}{T_\infty - T_o + K_2 HP_B} \right]$$

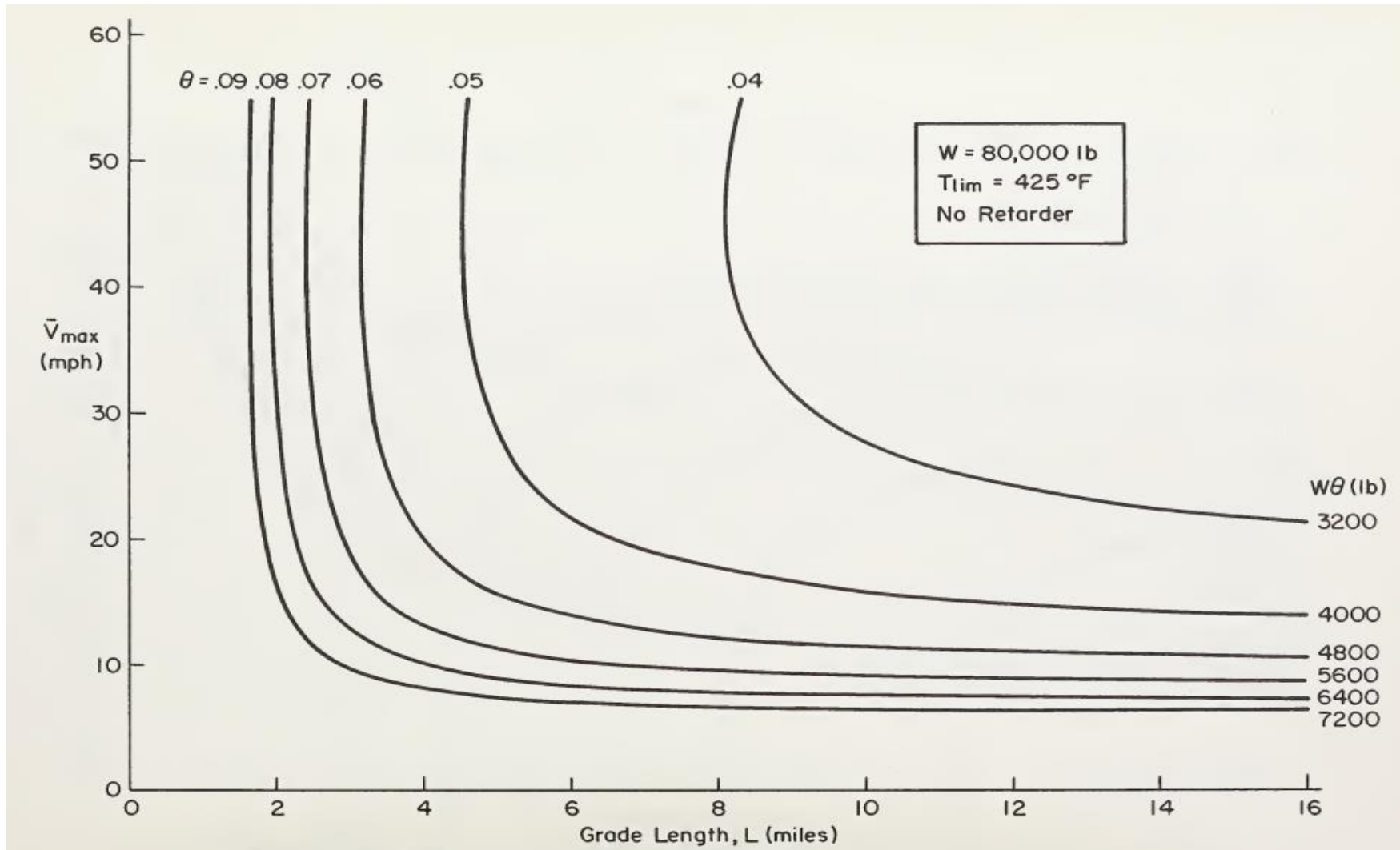
Figure 49. Equation. Relation for Plotting Maximum Descent Speed Curves.

A value of V_{max} can now be substituted into the equation in Figure 49 from which L is computed. This exercise can be performed for several slopes (θ s) to define V_{max} contours (© 1981 FHWA).

Figure 50). These V_{max} contours form the basis for the application of GSRS. Maximum descent speeds can be easily estimated from the contours.

Weight Specific Speed (WSS) Signs from the GSRS

To effectively have a workable GSRS, the optimal control and the human factor problems must be solved. The optimum control problem as discussed previously refers to the establishment of safe descent speeds that maintain brake temperatures below the temperature limit but also allow drivers to descend the grade quickly. The human factor requires that the GSRS be easy and convenient to use for a driver. These two issues present a challenge in the application of the GSRS because there are too many variables (θ , W and L) for the driver to assess. This complication can be managed by presenting a simplified GSRS while sacrificing some accuracy. (Myers et al., 1981).



© 1981 FHWA.

Figure 50. Graph. Maximum slopes for V_{max} and grade length. (Myers et al., 1981).

An effective GSRS must be relative. This means it must be dependent on the grade parameters only, and must not measure grade severity of a truck for a specific grade. This was achieved in this study by using a representative truck. The representative truck is defined by a reference weight used as a basis for all other weights. The reference weight used in the test program was 80,000 lb.

The use of a representative truck and weight in defining the GSRS parameters implies V_{max} may still be truck dependent. However, a partitioning of the V_{max} axis into simple discrete severity intervals may lessen the effects the test truck introduced into the model. Myers et al., 1981 suggest that formulating a relative grade severity rating (GSR) for a reference weight will have speed uniqueness when used for a truck at the reference weight. (Myers et al., 1981). It was also demonstrated that some conservative errors arise when the GSR is extended to other weights. However, these errors were found to be insignificant. (Myers et al., 1981).

The ultimate result of the GSRS is a sign intended to provide information about the grade severity and most importantly, recommend grade descent speeds. This system is aptly suited to provide a formal direction to inexperienced drivers on speed selection for downgrades. These signs are installed on the top of each hill and are presented in the form of weight categories with recommended speeds corresponding to each weight. These are known as the WSS signs. (see Figure 7).

WSS signs are derived from the GSRS brake temperature model. The model is used to solve the “inverse problem.” That is, it is used to determine the speed that corresponds to a given final brake temperature at the bottom of a hill, at a given weight. (Johnson et al., 1982a). WSS signs consist of discrete weights corresponding to values of V_{max} . Because each WSS sign is unique for each grade, speed values on the grade could be easily calculated directly from the GSRS equation. This makes the system easy to use because the resultant WSS sign is presented in a one-dimensional format of a single column of weights and speeds.

Several considerations should be noted in the partitioning and rating of grades. The WSS signs should have numerical GSR values in the form of integers that increase sequentially with grade severity, and should be distinguishable from speed limit numbers. Secondly, the number of categories on each WSS sign should not exceed five. WSS signs with intervals exceeding five result in too much information being presented on the sign for truck drivers to read, process and respond to while accomplishing the necessary driving tasks. (Bowman, 1989). While this process will lead to the loss of some accuracy, the information loss will not be excessive, and the accuracy of the system will not be overly compromised. The maximum number of intervals can be maintained by varying weight increments between each interval. Also, ease of reading of the signs can be achieved by using round numbers for weight, specifically multiples of 5,000 lb.

The maximum weight category on each sign should be the maximum weight permitted for the highway on which the sign will be installed. The weights should then decrease in equal increments from the maximum to the lowest weight. The selection of the weight increment to be used for each sign is based on practical considerations and unworkable recommendations should be avoided. For instance, it is pointless to specify speed changes of 1 or 2 mph between weight categories (for example using 5000 lb increments) since most speedometers do not read to such

accuracy. In this instance, weight categories of 10,000 lb would be more appropriate. (Bowman, 1989). Details about the formulation of WSS signs are presented in chapter five.

Multi-grade Hills

Multi-grade hills, for the purposes of developing the GSRS are those hills that contain significant sections of upgrade or downgrade shallow that braking is not required. (Johnson et al., 1982a). These sections break up a multi-grade into an alternating set of braking intervals (locations where braking is required) and non-braking intervals (locations where no braking is required). Braking intervals may be represented by an equivalent constant slope, θ_{equiv} for purposes of analysis even though slope variations may exist within the interval. Non-braking intervals are locations where speeds and corresponding gears may be changed for descent in the next braking interval. WSS signs can be placed at these points with GSR information for the next braking interval. The non-braking intervals also provide an opportunity to choose a preselected temperature profile that will be maintained during the hill descent.

In analyzing multi-grades for the placement of WSS signs, Bowman, 1989 considered multi-grades as a series of separate downgrades on which trucks have high initial brake temperatures. (Bowman, 1989). That means the end of a non-braking interval at the beginning of the next downgrade can be considered as the starting point whose initial temperature will be the final temperature at the end of the preceding non-braking interval.

CHAPTER SUMMARY

Formulation of the GSRS and brake temperature model requires an understanding of the grade descent problem, brake systems and brake overheating. Severe downgrades generate large amounts of heating that must be absorbed by brake systems. Insufficient braking capacity on downgrades leads to brake fade and truck runaways. Different types of fade exist. These include friction fade, fluid fade, domino and mechanical fade.

Brake systems have the responsibility of slowing down trucks on downgrades. Brake systems on trucks are of two types; service and auxiliary brakes. Service brakes provide the main retarding forces to slow trucks while auxiliary brakes assist in this function. Service brakes on trucks are drums and disc brakes. Drum brakes are predominantly installed on most trucks but are more susceptible to brake fade. The retarders installed on trucks include compression brakes, exhaust retarders, hydraulic and electric retarders.

Formulation of the brake temperature model involves accounting for all braking and non-braking forces retarding motion. The balance of energy in the brake system must also be considered before a comprehensive integration of the brake temperature equation can be done. From the initial differential equation of the energy balance equation, standard integration techniques are employed to arrive at the final brake temperature equation.

The integrated temperature equation helps in defining maximum safe descent speeds on downgrades. This forms the basis of the GSRS. A limiting temperature is defined that should not be exceeded for a loaded truck descending a downgrade with specific characteristics. From the brake temperature model, WSS signs can be developed for different weight categories. WSS

signs are installed at the start downgrades and provide advisory descent speeds to inexperienced or drivers unfamiliar with the downgrade

CHAPTER 4: METHODOLOGY

This chapter discusses the methodology adopted for this study. An overview of the methodology is first discussed. A description of the representative truck used to conduct the tests is followed by a discussion of the tests undertaken. Overall, the chapter aims to discuss all the processes and steps taken to obtain safe advisory speeds on downgrades.

TEST METHODOLOGY

The truck tests form one part of updating and implementing the GSRS. The flow chart of the methodology for the whole study is shown on Figure 51.

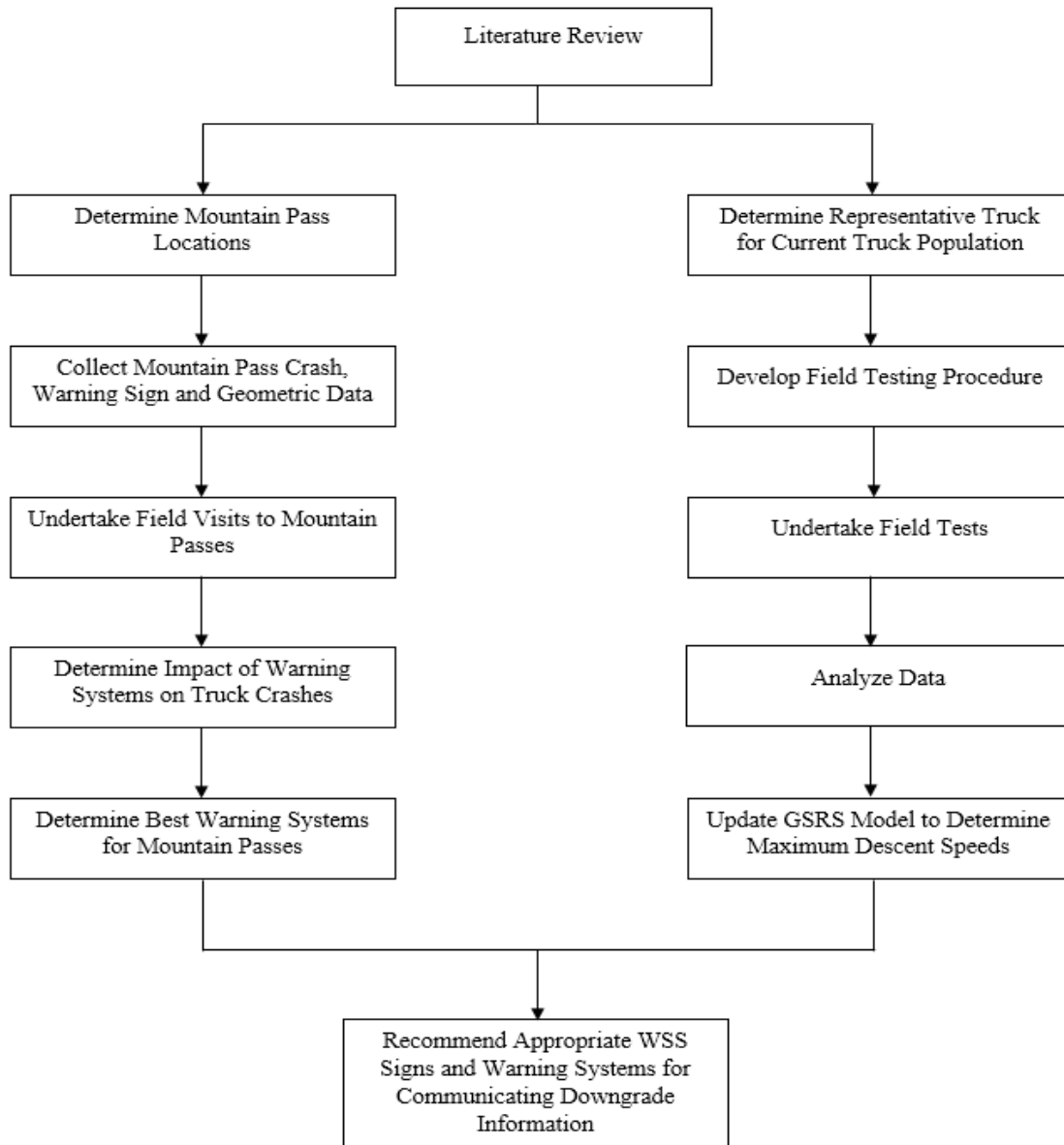


Figure 51. Flowchart. GSRS Methodology.

TEST PROGRAM OVERVIEW

The full-scale truck tests were conducted to obtain data necessary to update the truck braking model on which the maximum descent speeds will be based. Field tests conducted were chosen based on previous tests conducted by Myers et al., 1981. Factors such as economy, simplicity, time constraints, accuracy requirements and compliance with current published standards were also considered.

Three main tests were conducted to derive the important truck parameters. These were coast-down, cool-down and hill descent tests. The coast-down and cool-down tests were run on level ground while the hill descent tests were conducted on slopes of constant grade. A validation test was undertaken as well to test the accuracy of the updated model. Table 3 gives a summary of the tests, conditions under which they were done and the reasons they were conducted. Due to time, and other constraints, simulation was employed to augment the data collected for some of the tests. These are discussed in chapter 5.

Table 3. Test Types and Purpose of Tests.

Type of Test	Test Condition	Purpose of Test
Coast-down	On flat ground. Coast to a stop (no braking)	To determine non-brake forces as a function of speed
Cool-down	Constant speed, no braking	To define the diffusivity constant (K_1) for brakes.
Hill Descent	On constant grade. Braking is used to maintain constant speed.	To determine temperature characteristics of and thermal constant (K_2), of brakes during steady braking.
Validation	On constant grade. Braking is used to maintain constant speed.	To test robustness of updated model.

The complete tests carried out including the test vehicle preparation are shown on the flowchart in Figure .

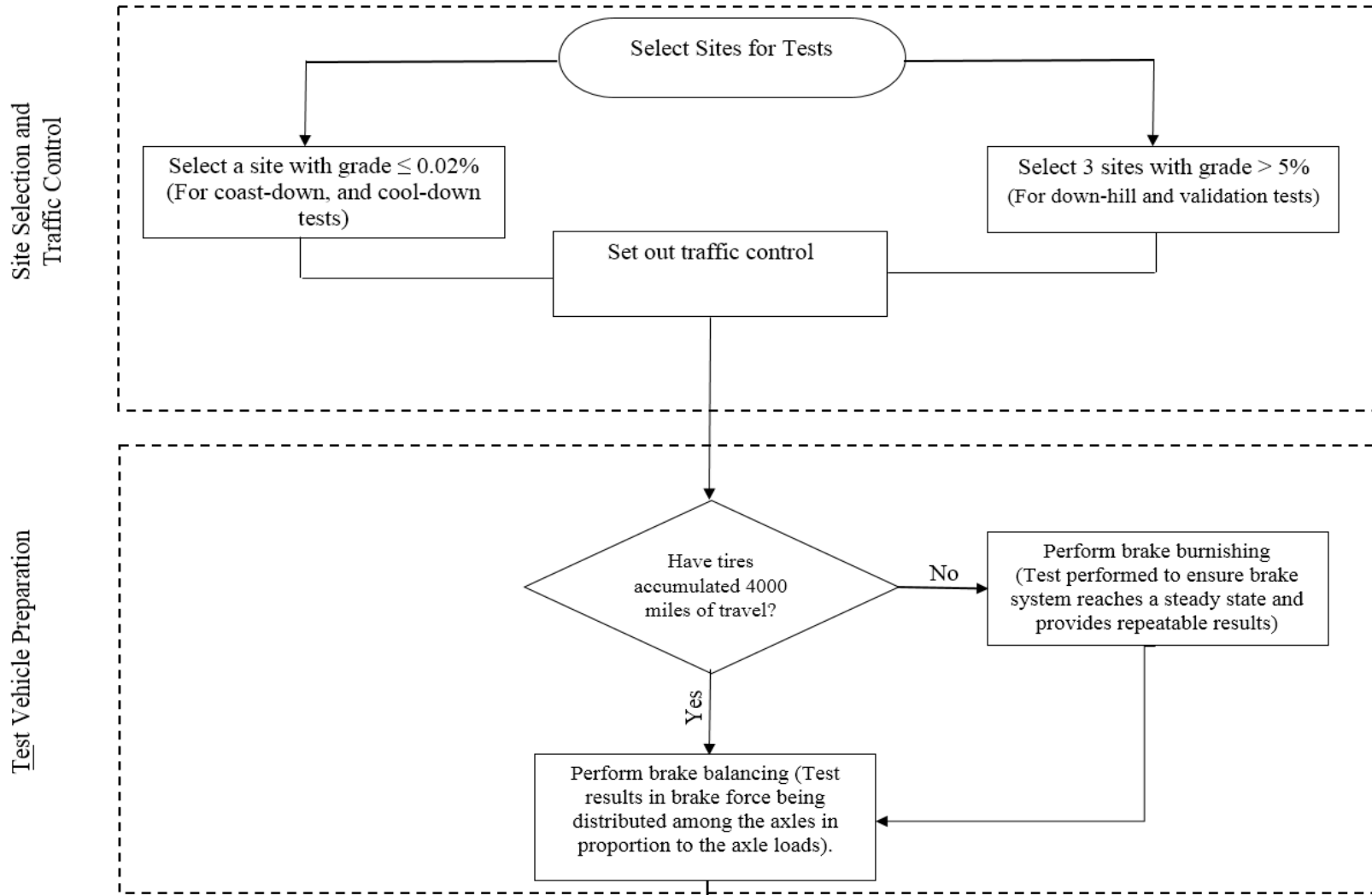


Figure 52. Flowchart. GSRs Test Flowchart.

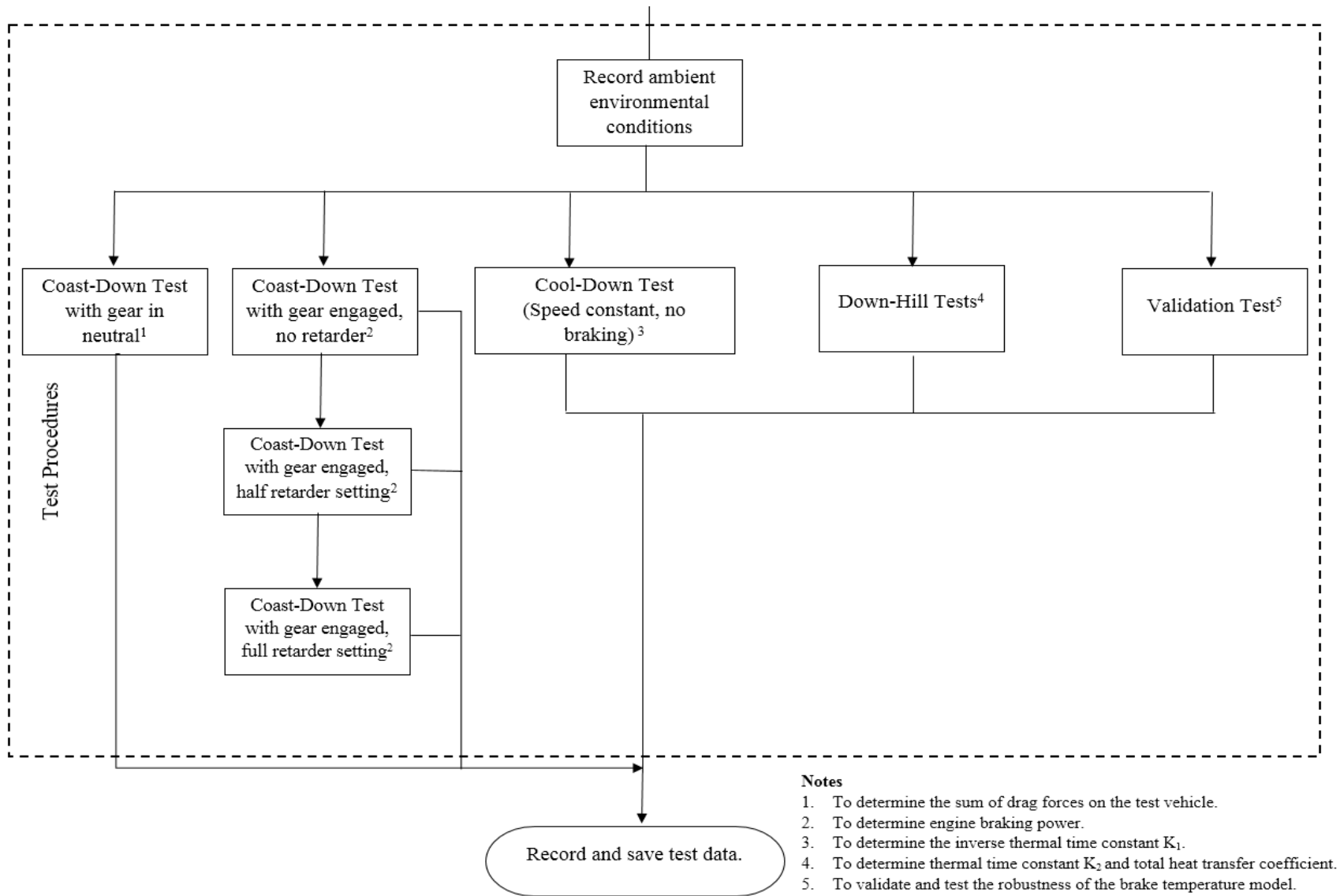


Figure 52 Continued. Flowchart. GSRs Test Flowchart.

TEST VEHICLE PREPARATION

The truck chosen for the tests was a typical class 8 sleeper-cab truck combination. This represents the heavy-duty class of tractor-semitrailer combinations. A description and picture of the representative truck and its specification are as shown in Table 4 and Figure 53.

Table 4. Test Truck Specification.

Specification	Description
Make/Model	Kenworth T680 Series (2016)
Cab Style	Sleeper
Trailer Model	Hyundai (2007)
Trailer Type	Van
Gross Vehicle Weight Rating	36287 kg (80,000 lb)
Number of Axles	5
Front Axle	Meritor MFS13
Rear Axles	Dana Spicer DSH-40 Dual
Trailer Length	53 ft
Tires	Bridgestone 295/75R22.5
Engine	Cummins ISX-15 Engine (2013)
Service Brakes (Steer Axle)	Bendix Air Disc Brakes ADB22X
Service Brakes (Drive and Trailer Axle)	Castlite S-Cam Dual Brakes (16.5 inch x 7 inch)
Retarder	Jacobs Engine Brake (Intebrake) - 2010
Transmission	Eaton Fuller 13-Speed Manual

The test truck was instrumented to measure several atmospheric, brake and truck parameters including brake temperature, vehicle speed, deceleration, engine speed, GPS coordinates, brake application pressure, atmospheric pressure, ambient humidity, and number of snubs. The parameters and instruments used to measure them are shown in Table 5.

A schematic of the instrumentation is shown on Figure 54. Infrared sensors were installed on all ten brakes of the truck. A brake pressure transducer was also connected to the main brake line from the tractor. These were then connected to signal conditioning and power distribution boxes on the tractor and trailer. A connection was made from the signal conditioning and power distribution boxes to a controller box in the cab. Power for the whole setup was provided from the truck routed through the controller box to the power distribution boxes and sensors. Communication with the truck engine was achieved using the Controller Area Network (CANbus). Data from sensors and the truck engine was collected by the Compact Data Acquisition (cDAQ) chassis. The cDAQ is designed to control the timing, synchronization, and data transfers between the different modules of the instrumentation set up. Figure 55, Figure 56 and

Figure 57 show components of the instrumentation set up.



Figure 53. Photo. Test Truck.

Table 5. Truck Instrumentation and Measured Parameters

Measured Parameter	Instrument or Sensor
Brake Temperature	Infrared sensor
Vehicle Speed	Controller Area Network (CAN bus)
Deceleration	CAN bus
Vehicle Gross Weight	Weigh Station
Engine Speed	CAN bus
Coordinates	GPS
Brake Application Pressure	Pressure Transducer
Ambient Temperature	Thermocouple
Wind speed and Direction	Weather Station
Atmospheric Pressure	Weather Station
Ambient Humidity	Weather Station
Number of Snubs	CAN bus

The data acquired from the instruments and sensors were then transferred onto a laptop computer running a proprietary software (MICAS-X®) through an Ethernet cable (© 2017 OCC.

Figure 58 and © 2017 OCC.

Figure 59). MICAS-X® enabled real-time monitoring and display of the data. This meant that changes to test procedures in reaction to changing test conditions could be undertaken quickly. Errors in data collection which arose during testing were also identified and corrected in time. The software run continuously during the test procedures and saved the data as Excel.csv files onto the laptop computer. Loading for testing was done by packing the truck with water bottles was used as the load for testing

Figure 60).

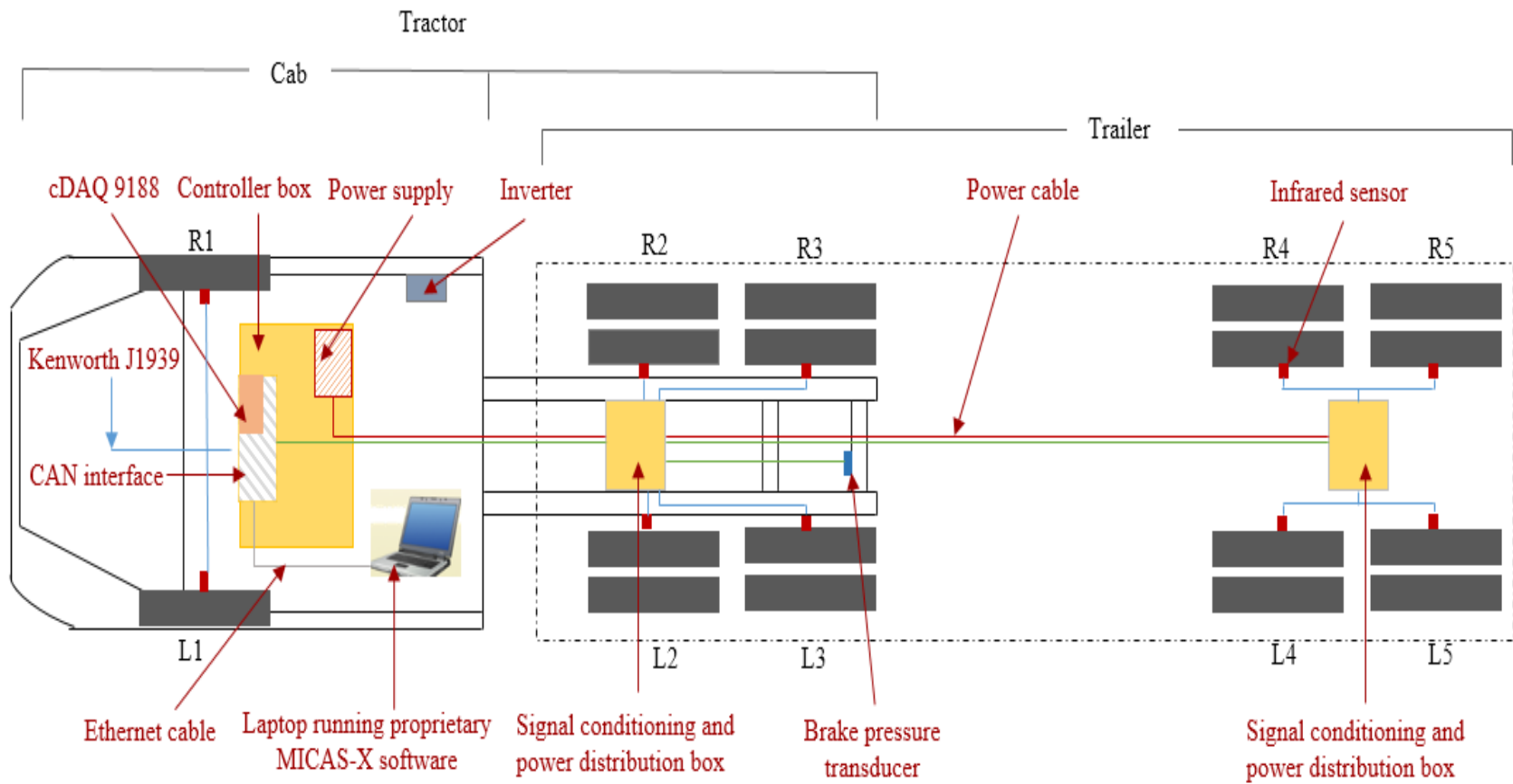


Figure 54. Diagram. Instrumentation Layout.

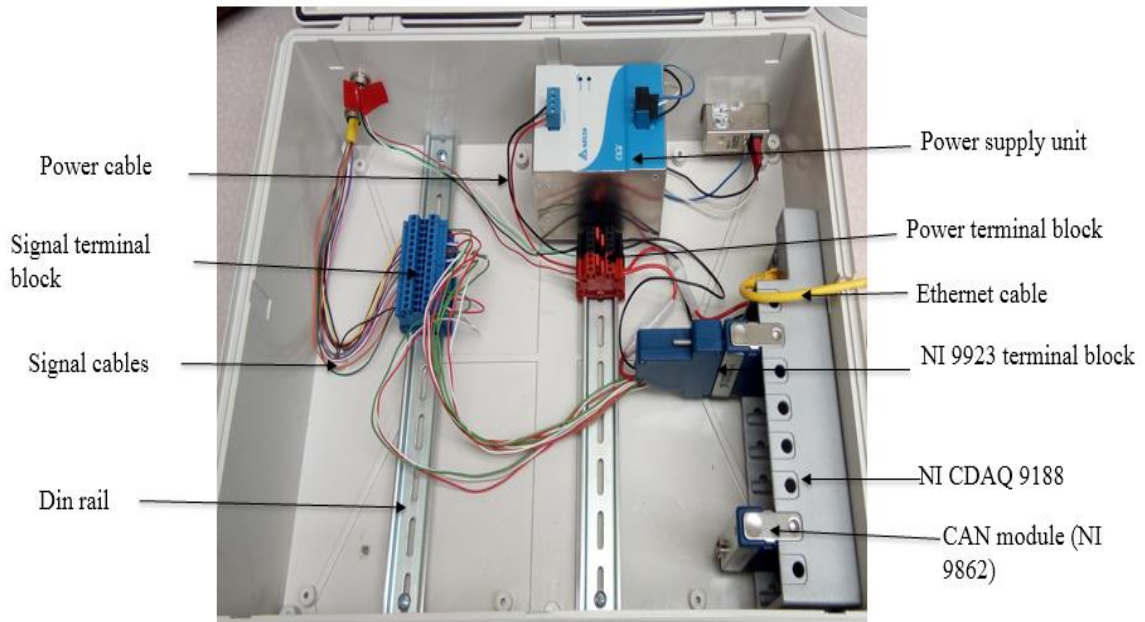


Figure 55. Photo. Cab Controller Box.

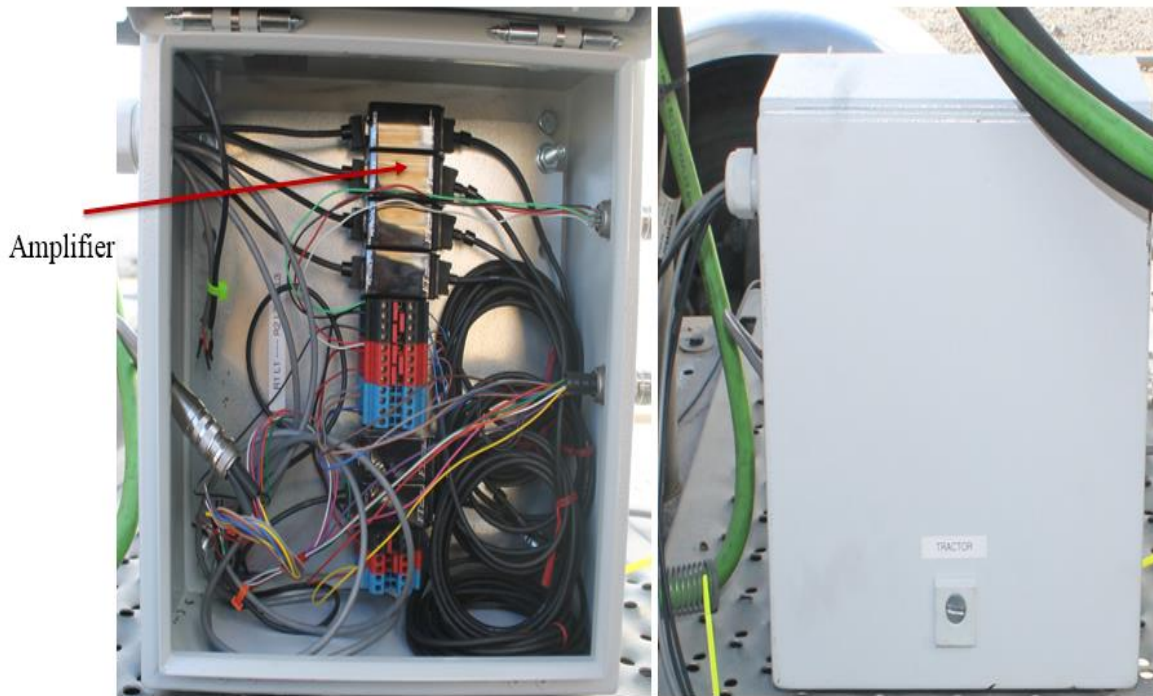


Figure 56. Photo. Signal Conditioning and Power Distribution Box.



a. Infrared Sensor.



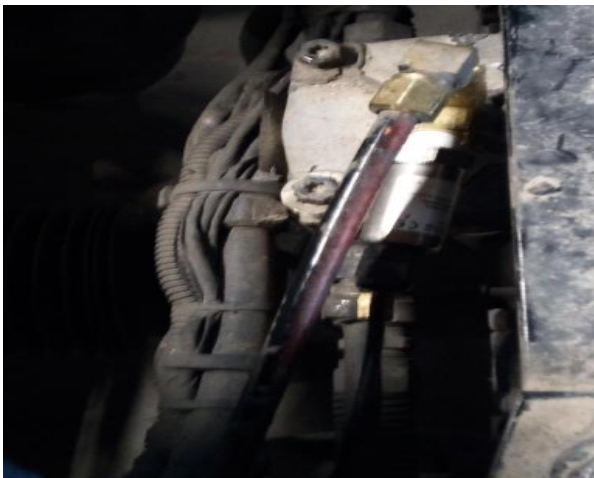
b. Infrared Sensor Installed on Drum.



c. Hand-Held Infrared Sensor.



d. Infrared Sensor Installed on Disc Brake

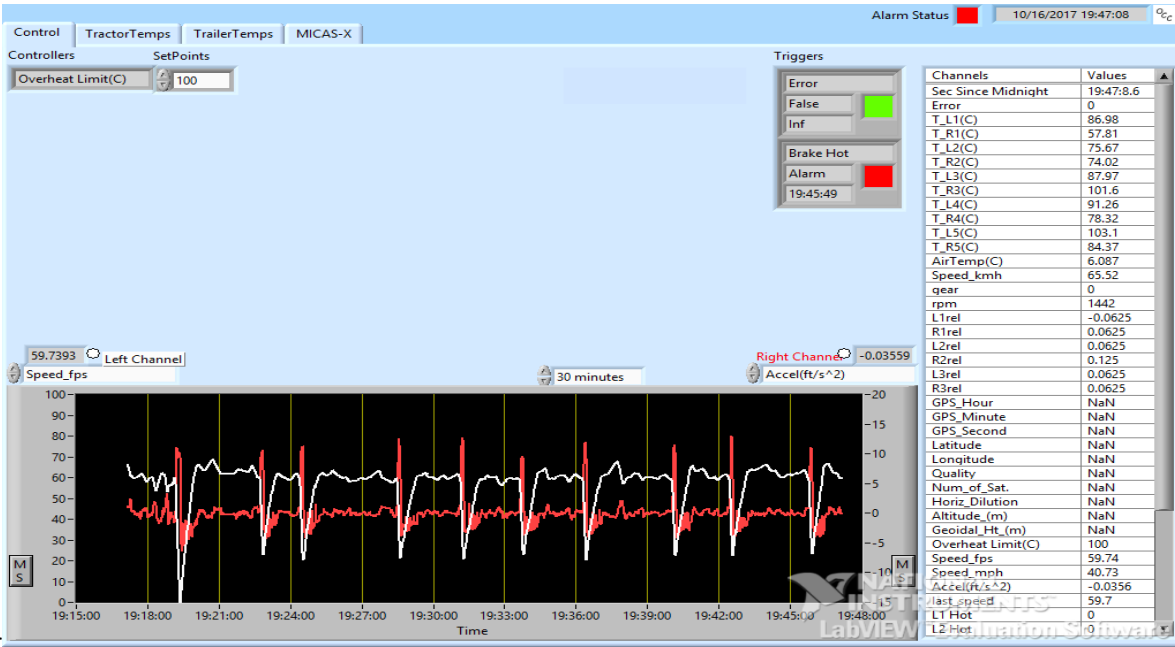


e. Pressure Transducer.



f. Signal Conditioning/Power Distribution Box on Trailer.

Figure 57. Photos. Truck Instrumentation and Sensors.



© 2017 OCC.

Figure 58. Photo. MICAS-X® Display. (Original Code Consulting, 2017).



© 2017 OCC.

Figure 59. Photo. MICAS-X® Plots. (Original Code Consulting, 2017).



Figure 60. Photo. Loading for Tests.

TEST DESCRIPTION

The field tests were conducted in two phases. The first series of tests were done to assess the instrumentation and prepare the test vehicle. The main tests were conducted afterwards. The sequence of testing is as follows:

- Site selection and traffic control,
- Test vehicle preparation,
- Coast-down tests,
- Cool-down tests, and
- Down-hill tests.

Site Selection and Traffic Control

Sites were first selected for the tests to be conducted. The site selected for the coast-down testing was required to be straight with a grade of less than 0.02 percent. (EPA, 2011). This requirement was difficult to meet and so a straight section with a 0.40 percent grade was selected with slope corrections made during data analysis. Locations for hill descent and validation tests were chosen to have grades greater than 5 percent. Table 6 shows the locations tests were conducted on.

Traffic control was provided by WYDOT. Radio broadcasts were made to inform residents within the vicinity of the test locations of the field tests. WYDOT vehicles with warning signs were driven ahead and behind the test vehicle at all times during the field testing.

Figure 61 shows traffic control WYDOT vehicles during testing.

Table 6. Test Locations.

Test	Section	From (MP)	To (MP)	Length (Miles)	Average Grade (percent)
Coast-down	WY 789 (ML 34B)	171.5	180.0	8.5	0.4
Cool-down	WY 789 (ML 34B)	163.0	144.0	19.0	0.4
Hill descent	US 16 (ML 36B)	70.0	73.9	3.9	4.3
	US 16 (ML 36B)	82.0	87.5	5.5	6.1
	US 16 (ML 36B)	38.3	34.0	4.3	7.0
Validation	US 16 (ML 36B)	67.4	73.9	6.5	Variable



Figure 61. Photo. WYDOT Traffic Vehicles.

Test Vehicle Preparation Tests

To ensure that accurate and repeatable data would be obtained in the tests, two procedures were conducted. These were:

- Brake burnishing tests
- Brake balancing tests

Brake Burnish Test

Burnishing involves applying many braking cycles to new brakes which will result in wear and tear and lead to a steady-state in which a given application pressure and brake temperature result

in a unique repeatable braking force. The brake burnish tests were required because the trailer brakes were new. New brakes are required to undergo many brake application cycles so that wear and heating effects cause the brake systems to reach a steady-state such that braking forces are repeatable. This should take at least 200 runs. Ambient temperature for test is between 32°F and 100°F. The brake burnish tests were conducted as specified by SAE J992. (Tuegel, 1968).

Burnish Procedure

1. Hottest brake should be under 200°F.
2. Pre-burnish by performing 10 stops from 20 mph to 0 mph at a minimum deceleration of 14 ft/s² and 1.0 mile intervals.
3. Perform the brake burnish procedure by making 200 snubs from 40-20 mph at a deceleration rate of 10 ft/s² in normal gear range.
4. Accelerate to 40 mph at moderate acceleration and drive at 40 mph between snub applications.
5. The application interval is 1.5 miles for each snub from 40 to 20 mph.
6. Bring vehicle to a full stop on every 25th burnish application. Measure brake temperatures and application pressures. Allow brakes to cool to ambient temperature before continuing.
7. Check the drum temperatures after burnishing.
8. Check brake adjustment for proper settings according to the manufacturer specifications.

Brake Balance Test

This test is done to ensure that brake force is properly distributed among the brakes in proportion to the axle loads. The balancing procedure was conducted indirectly by measuring the brake temperature and adjusting air pressure to brakes until temperature differences were minimal. Brake temperatures checked after burnishing which are cooler by approximately 50°F side-to-side, and 100°F front-to-rear, than the others indicate a possible lack of braking effort on those wheels and may be an indication of brake imbalance. Also, the air system setup for the truck was checked to ensure proper balance of the brakes.

Main Field Tests

Three main field tests were conducted to validate the brake temperature model. These were:

1. Coast-down tests
2. Cool-down tests
3. Hill descent tests

The tests and procedures are described below.

Coast-down Tests

The purpose of the coast-down tests is to determine the sum of the “drag” forces on the test vehicle, as well as engine braking force as a function of weight and velocity. Coast-down tests were also conducted with the gear engaged to determine engine braking force. The test for determining drag forces consists of launching a motor vehicle from a certain speed with the engine disengaged and ascertaining the current speed and distance covered during the free rolling, till the vehicle stops. The test is modified to determine engine braking force by coasting-down the vehicle engaged in gear. The test is conducted on a level road. Vehicle speed, engine

speed, ambient temperature and relative wind velocity, relative wind direction, and maximum observed wind speed (gust) were measured. The tests were conducted under loaded and unloaded conditions according to the modified Environmental Protection Agency (EPA) procedure for Society of Automotive Engineers (SAE) J1265/J2265.

Test conditions as per SAE J2263 require dry level road with grade no more than 0.5 percent, ambient temperature between 41 to 95°F, average wind speed not exceeding 21.7mph, average cross winds not exceeding 9.3 mph, and no precipitation. (SAE Recommended Practice J2263, 2008). Due to time and environmental constraints, the field coast-down testing was supported with simulation. Details of the simulation procedure are discussed in chapter 5.

Coast-down Test Procedure

1. Prepare test vehicle.
 - a. Weigh vehicle.
 - b. Measure frontal area of vehicle.
 - c. Perform a precondition procedure by driving vehicle for 30 minutes at an average speed of 50 mph.
 - d. Vehicle windows and vents must be closed during test with headlights turned on.
2. Record initial environmental data:
 - a. The following variables should be recorded during the test: ambient temperature, atmospheric pressure, wind velocity and direction, and the maximum observed wind speed.
 - b. If any of the above variables are out of bounds of the SAE constraints, the test should not be pursued.
 - c. The test should commence immediately following preconditioning.
3. Execute Coast-Down Test.
 - a. With the data acquisition system in standby mode and occupants ready to record, accelerate vehicle to 75 mph which is 5 mph above the test speed of 70 mph. Note the time coast-down was started.
 - b. Start the recording equipment, shift to neutral and let the engine idle. Vehicle regenerative braking shall be disabled during coast-down testing to minimize changes to the mechanical system.
 - c. Keep vehicle straight on path in neutral while performing coast-down.
 - d. Once vehicle velocity has decreased below 15 mph, stop data acquisition system, return vehicle to gear, bring vehicle to a stop in a safe location, and save data file.
4. Repeat
 - a. Repeat step 4, pairing coast-down runs in opposite directions. A total of at least 10 valid runs should be executed making a complete set per each load tested.
 - b. All valid coast-down run times in each direction must be within 2 standard deviations of the mean of the valid coast-down runtimes in that direction.
5. A plot of velocity versus time during a coast-down is required for data analysis.

Coast-down Test to Determine Engine Braking

1. Repeat the coast-down test with the transmission in drive i.e. clutch engaged (full, half and off engine brake setting).
2. Use different gears to ensure the engine operating range is covered.

3. Plot velocity versus time during coast-down for data analysis.

Cool-Down Tests

To calibrate the brake temperature model to update the GSRS model, it was necessary to determine the brake heat transfer properties. Cool-down tests were done to determine the effective total heat transfer coefficient as a function of speed. The tests are conducted on a level road. Vehicle speed, application pressure, brake temperature, ambient temperature, and wind velocity were measured.

Cool-down test Procedure

1. Measure the ambient brake temperatures (T_{∞}).
2. Perform a series of snubs to heat brakes to a temperature above 500°F (T_o).
3. Accelerate vehicle, release brakes and drive at a steady test speed.
4. Record decrease in temperature until the temperature of the brakes is equal to the ambient temperature (T_{∞}).
5. There should be no braking during the data acquisition.
6. The experiment is conducted for three nominal speeds corresponding to typical vehicle operating speeds (20 mph, 30 mph, and 45 mph) and 0 mph to determine cooling rates at zero velocity.

Hill Descent Test

The purpose of the test is to find the variation of brake pressure and temperature during a steady hill descent as a function of weight, grade percent, grade length, engine braking and descent speed. The test is to also determine the total convective heat transfer parameter, and the brake force as a function of pressure, speed and temperature. Parameters measured are application pressure, vehicle speed, and brake temperature on each axle.

Hill Descent Test Procedure

1. Measure brake temperature before commencing tests.
2. Ensure that brakes are cool ($T \leq 200^{\circ}\text{F}$ on hottest brake). This can be achieved by driving the vehicle for some time to allow convection to cool the brakes.
3. Set engine brake to appropriate setting (full brake, half brake or no brake).
4. Accelerate vehicle to a speed 5 mph above the test speed.
5. Descend hill maintaining speed constant by modulating brake pressure.
6. Conduct the tests on different selected downgrades.
7. Allow brakes to cool ($T \leq 200^{\circ}\text{F}$ on hottest brake) before each hill descent.
8. Conduct tests at different typical truck operating speeds on downgrades.

Validation Test

The validation hill descent tests was conducted to validate and test the robustness of the temperature model developed. Parameters measured were application pressure, vehicle speed, and brake temperature on each axle.

Validation Test Procedure

1. Repeat the hill descent tests with a lower loading (74,000 lb).
2. Conduct constant speed grade descent tests on selected downgrades.
3. Conduct tests with no retarder.

CHAPTER SUMMARY

This chapter presented the test methodology adopted for this study. The instrumentation, test vehicle preparation, and main tests are discussed. Three main tests were conducted to update the parameters of the GSRS model. A validation test was performed to test the robustness of the updated model.

The vehicle chosen for the test was a five axle, class 8 sleeper-cab truck combination. The vehicle used for the tests has disc brakes on the steer axle, and drum brakes for all other axles. The test truck was instrumented to measure several parameters including vehicle speed, brake temperature, engine speed, GPS coordinates, deceleration, ambient temperature and number of snubs. Weather parameters such as wind speed and direction, atmospheric pressure and ambient humidity were obtained from a nearby weather station.

The preparatory tests conducted for the study were brake burnishing and balancing. Brake burnishing tests are done for new brakes to allow wear and heating effects to cause the brake system to reach a steady state. The burnish test involves many cycles of brake applications with cooling on every 25th application. Brake balance tests were conducted to ensure there was adequate brake force distribution between all the axles. The tests were conducted indirectly by measuring the brake temperature and adjusting air pressure to brakes until the differences in the temperatures were minimized.

The three main tests conducted to update the GSRS model parameters were coast-down, cool-down, and hill descent tests. Coast-down tests were undertaken to determine the sum of the drag forces on the test vehicle. The tests involved driving the test vehicle to a predetermined speed on a flat ground, disengaging the transmission, and allowing the vehicle to coast while measuring speed and time of the coasting. Cool-down tests determined the cooling characteristics of the brake system. The tests were conducted by heating up the brakes through snubbing, and driving at a constant speed until the brakes cooled to ambient temperature. The duration of the tests and speeds were measured. Hill descent tests determined the heating characteristics of the brakes. The hill descent tests were conducted by driving the test vehicle on a grade at a constant speed while measuring brake temperature, time of descent and application pressure. A validation test was then undertaken to assess the robustness and accuracy of the updated temperature model. The test was conducted at a lower loading and on a multi-grade.

CHAPTER 5: RESULTS

This chapter presents the results of the field tests and the updated GSRs brake temperature model. The use of simulation in some of the tests are also discussed.

VEHICLE PREPARATORY TESTS

The main vehicle preparatory tests required to be undertaken were the brake burnish and balance tests. These tests were done to ensure the repeatability and accuracy of the test results.

Brake Burnish Tests

Brake burnish tests are carried out on new brakes. The brakes on the trailer were new and so a burnish test was required. Accordingly, it was considered mandatory to conduct the burnish tests due to the state of the trailer brakes. The brake effectiveness was assessed by monitoring the ratio of lateral acceleration (a_x) to application pressure (P). Figure 62 shows the results of the burnish tests. The results show that the ratio of a_x/P becomes largely steady after 75 burnish snubs.

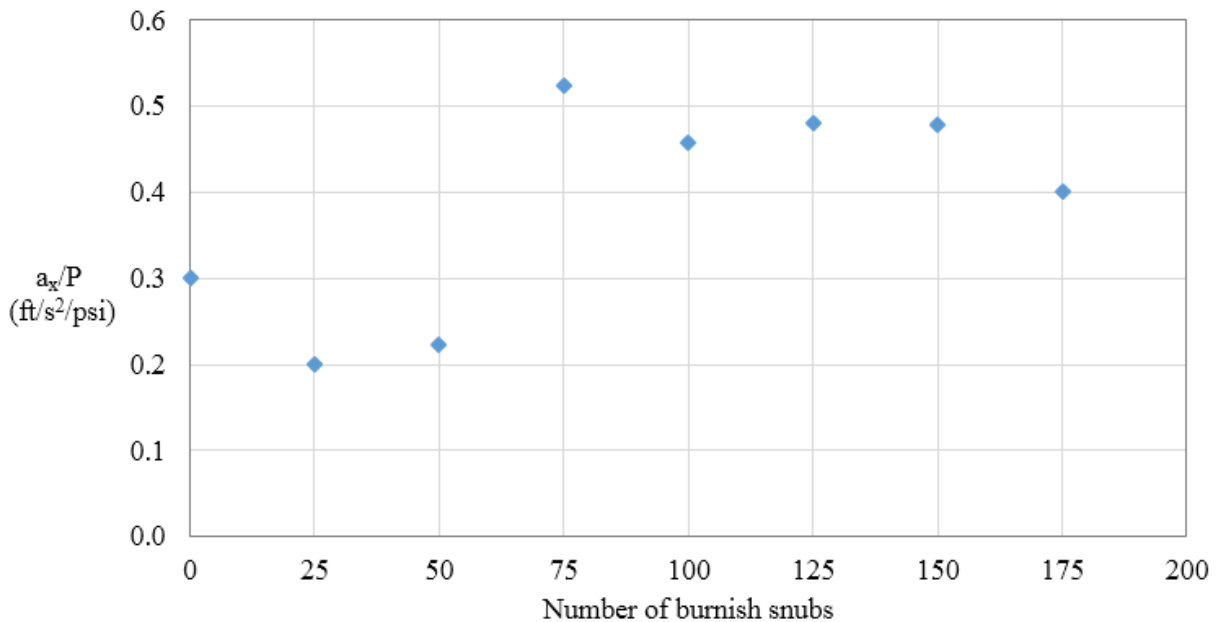


Figure 62. Plot. Brake Effectiveness during Burnish Tests.

Brake Balance Tests

It was not possible to conduct the brake balance tests according to specifications of SAE J225 due to the design of the test truck. The test procedure SAE J225 requires air pressure to be disconnected to individual axles during the test, (SAE Recommended Practice J2263, 2008). This could not be done because of the design of the air system of the test truck. Instead, the differences in brake temperatures between axles were monitored by adjusting air pressure for each individual axle to ensure the brake temperature difference were minimal, and each axle was

supplying the required braking force. A degree of imbalance was found to be present among the brakes. Nevertheless, the tests were continued.

FIELD TESTS TO UPDATE THE GSRS

Coast-down Tests (No Engine Braking)

Coast-down analysis is used to infer the road load acting on a vehicle when it is unpowered. The test vehicle is driven to a maximum speed of interest, shifted into neutral and allowed to decelerate freely while velocity and time of deceleration are measured. For a vehicle in free motion, the forces that resist forward motion are:

1. Aerodynamic drag (F_{aero}) = resistance to motion due to air,
2. Rolling resistance (F_{rr}) = resistance to motion due to frictional force between the tires and road surface, and
3. Grade drag (F_{grade}) = resistance to motion due to grade effects.

These forces contribute together to the total road load on a vehicle. Taking into account that drag forces always act in a direction opposite to vehicle speed and using Newton's second law for a vehicle traveling in a straight line, a drag force equation may be written as (Figure 62):

$$-M_e \frac{dv}{dt} = F_{aero} + F_{rr} \pm F_{grade}$$

Figure 63. Equation. Sum of Drag Forces Acting on a Truck.

where,

M_e = effective mass of the vehicle (lb),

V = vehicle speed (mph), and

t = deceleration time (s).

The effective mass accounts for the rotational inertia of the wheels and other rotating components and is different from the static mass of the vehicle. For coast-down analysis, the effective mass of the drivetrain components may be ignored. (SAE Recommended Practice J1263, 2010). The rotational inertia of the wheels is a property that inhibits changes to the speed of the wheels, and acts in an equivalent manner as an extra mass to the vehicle that inhibits changes to the vehicle speed. (McAuliffe and Chuang, 2017). The effective mass may be estimated as 3 percent of the total mass of the test vehicle. (SAE Recommended Practice J1263, 2010). This is expressed in Figure 64 as:

$$M_e = 1.03M$$

Figure 64. Equation. Effective Mass.

The coast-down equation, Figure 62 is simplified to the equation in Figure 65:

$$F = A + Cv^2$$

Figure 65. Equation. Drag Force Equation.

where, A and C are coefficients to be determined by regression analyses. This is the form recommended by SAE J1263 and the J1263 modified EPA Phase 1 protocol. (EPA, 2011; SAE Recommended Practice J1263, 2010). The intercept A , is analogous to the rolling resistance while C , is the aerodynamic drag term. This form was adopted for the coast-down data analysis.

The test track selected for coast-down runs was on Wyoming highway 789 outside Worland, Wyoming. The actual test track (excluding length required for acceleration) is straight and approximately 2.5 miles long with a gentle grade of 0.14 percent in the northbound direction. The test track is shown in

Original Photo: © 2018 Google ® (see Acknowledgements section).

Figure 66.



Original Photo: © 2018 Google ® (see Acknowledgements section).

Figure 66. Photo. © 2018 Google. Coast-down Test Track. (Google, 2018).

The coast-down test procedure requires measurement of vehicle position, vehicle speed, time, engine speed, ambient conditions (temperature and barometric pressure), and wind conditions. Vehicle location was measured by an on-board GPS. The speed, time, engine rpm, and some other variables of interest were measured using a J1939 data link. Communication with the truck's computer system to extract and log data was achieved by using the MICAS-X® software. The air temperature was measured by a thermocouple temperature probe that was installed on a trailer axle of the vehicle. Data was logged every half second. Data was collected within the speed range of 70 mph to 15 mph, as specified by SAE J1263. (SAE Recommended Practice J1263, 2010).

Twelve valid tests runs were conducted for the coast-down without engine braking. The truck was tested in both loaded (80,000 lb) and unloaded (40,000 lb) conditions. Figure 67 shows a plot of the velocity-time trace for coast-down runs in the north- and southbound directions. Plots for other coast-down runs can be found in Appendix 1. The run time for the northbound direction is higher because it is in the direction of the downgrade. Due to the short length of the test track,

the coast-down runs were split into low and high-speed runs. The high-speed runs were from 70–45 mph, while the low speed runs were from 44–15 mph. These runs were later combined for the analysis. Regression analysis was then conducted to determine the coefficients A and B for each direction separately, after which they were paired for an average value.

Table 7 shows the results of the coast-down analyses. The results were corrected for grade and wind effects.

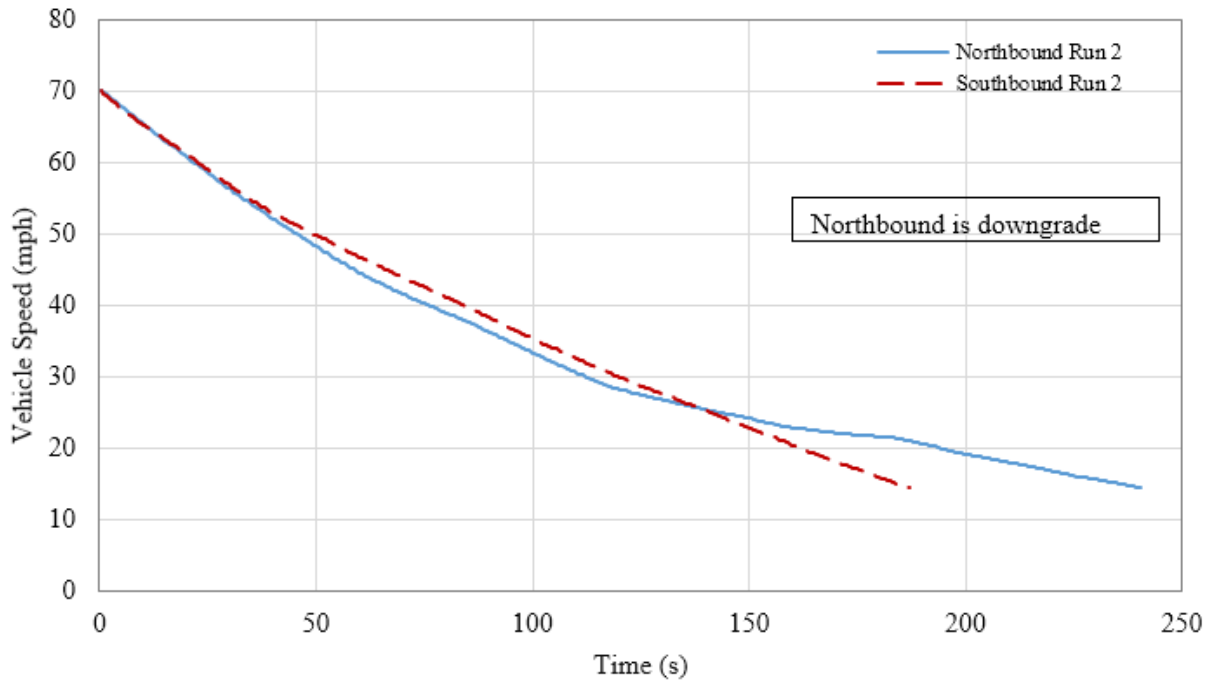


Figure 67. Velocity-Time Trace for Coast-down Run. (Truck Loaded – No Jake Brake).

Simulation analysis was used to simulate additional coast-down runs for different truck weights. This enabled more truck weights to be analyzed than was possible on the field due to time constraints and the need to speed up the testing process. The simulation scenarios were run using the TruckSim® software, an easy to use software. The software has a standard interface to MATLAB® /Simulink® and provides the ability to test different scenarios including different test vehicles, road, wind and loading conditions. TruckSim® provides an interactive 3D visualizer along with engineering charts and plots that make it possible to analyze the simulation outputs. These outputs were downloaded as an excel csv file for further analysis. © 2018 TruckSim®

Figure 68 and © 2018 TruckSim®

Figure 69 show a screenshot and velocity-time plot of a simulation run on the TruckSim® software respectively. The truck chosen to run the simulation runs had a similar aerodynamic design to the truck used for the field tests. The condition of zero-wind and grade from the simulation was chosen for the analysis because the coast-down procedure assumes very minimal to no wind conditions and a level track. (Yasin, 1979).

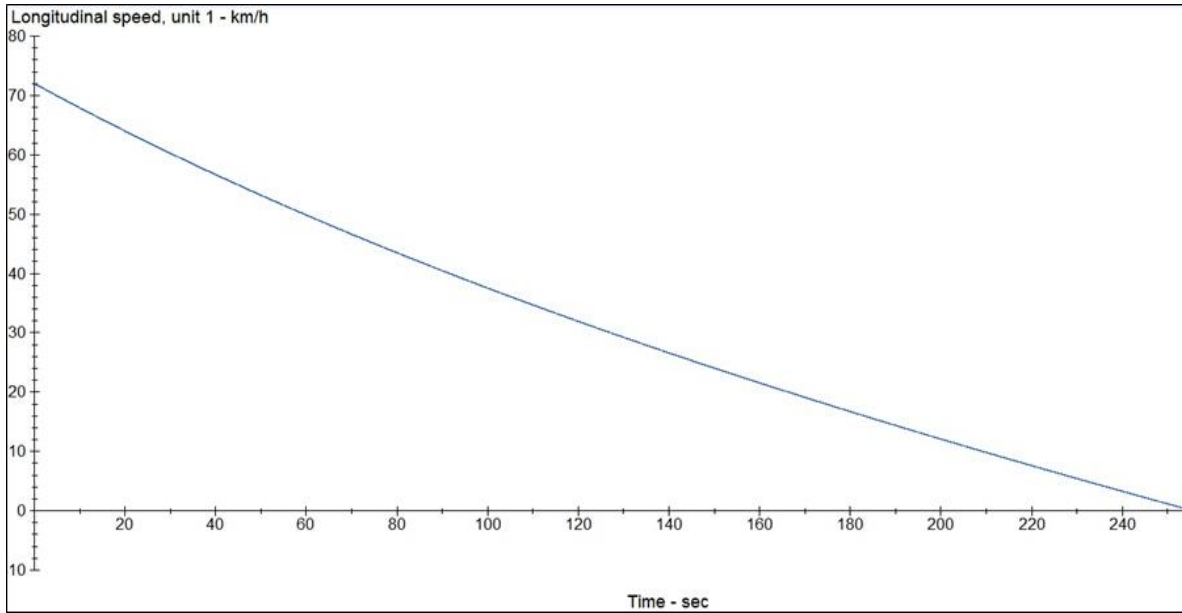
Table 7. Drag Terms from Field Coast-down Analysis

Direction/Run	A (lb)	C (lb/mph ²)
Loaded (80,000 lb)		
NB1	445.84	0.128
SB1	846.35	0.126
Average run 1	646.10	0.127
NB2	473.32	0.123
SB2	798.65	0.130
Average run 2	635.99	0.127
NB3	434.35	0.130
SB3	844.70	0.116
Average run 3	639.53	0.123
NB4	439.53	0.126
SB4	848.84	0.113
Average run 4	644.19	0.120
Overall field average coefficients (loaded)	641.45	0.124
Unloaded (40,000 lb)		
NB5	104.72	0.185
SB5	446.03	0.098
Average run 5	275.38	0.142
NB6	101.68	0.184
SB6	415.82	0.104
Average run 6	258.75	0.144
Overall field average coefficients (unloaded)	267.06	0.140



© 2018 TruckSim®

Figure 68. Photo. TruckSim 3D Visualization of a Coast-down Run. (Mechanical Simulation Corp., 2018).



© 2018 TruckSim®

Figure 69. Photo. Velocity-Time Trace Plot of a Coast-down Run from TruckSim. (Mechanical Simulation Corp., 2018).

Table 8 shows results from the simulation test for 80,000 lb and 40,000 lb. Drag force equations from both the field and simulation coast-down runs for the two test weights were used to develop a calibration curve. The calibration curve (Figure 70) was then used to correct drag forces from the simulation software for weights which were not tested in the field. The next step involved averaging the corrected drag coefficients over all the weights used in the analysis. The coefficients from the loaded and unloaded test runs derived from the field tests were also used in arriving at the final coefficients used in the analysis (Table 9).

Figure 71 shows the flow chart of the process.

Table 8. Simulation Results for Loaded and Unloaded Test Weights.

Weight (lb)	A (lb)	C (lb/mph ²)
80,000	574.18	0.192
40,000	277.39	0.146

The calibration curve equation was derived as (Figure 70):

$$F_{corr} = 47.313 + 0.768F_{sim} + 0.001433W$$

Figure 70. Equation. Coast-down Calibration Curve.

where,

F_{corr} = corrected drag force from calibration curve (lb),

F_{sim} = drag force from simulation (lb), and

W = weight (lb).



Figure 71. Flowchart for Calibration Curve and Validation.

Table 9. Average Drag Coefficients from Field and Simulation Tests.

Weight (lb)	Source	A (lb)	C (lb/mph ²)
80,000	Field	643.46	0.124
75,000	Simulation	567.75	0.144
70,000	Simulation	531.96	0.140
65,000	Simulation	496.18	0.136
60,000	Simulation	460.42	0.132
55,000	Simulation	424.74	0.128
50,000	Simulation	389.10	0.123
45,000	Simulation	353.51	0.118
40,000	Field	267.07	0.143
Average drag coefficients		459.35	0.132

The final coast-down equation used for the analysis was (Figure 72):

$$F_{drag} = 459.35 + 0.132V^2$$

Figure 72. Equation. Calibrated Drag Force.

Coast-down Testing to Determine Engine Braking

Coast-down tests were conducted with the gear engaged to derive the engine brake force. This test was performed with the engine brake at full, half and, off settings. The settings are activated by selecting the number of cylinders (up to six) to provide retarding effort when the engine brake is activated. Three activated cylinders imply half of the engine's braking effort will be engaged while activating all six will result in maximum engine retardation. The runs covered relatively small distances, and so slope effects were not considered. The effects of rotating components of the engine, clutch parts, and wheel assembly are considered in computing the engine braking force. The following relation (Figure 73) was used to analyze the engine braking force. (Myers et al., 1981):

$$F_{eng} = -F_{drag} + \left[\frac{W}{g} + \frac{nI_w}{R^2} + I_{eng} \left(\frac{G_i}{R} \right)^2 \right] a_x$$

Figure 73. Equation. Determination of Engine Brake Force.

where,

F_{eng} = engine braking force (lb),

F_{drag} = drag force (lb),

W = weight of truck (lb)

g = acceleration due to gravity (ft/s²),

n = number of wheels,

R = tire rolling radius (ft)

I_{eng} = engine inertia (lb.ft.s²),

G_i = transmission gear ratio in ith gear,

a_x = longitudinal acceleration (ft/s²).

The rotating components of the engine and wheel assembly add on additional weight during testing. Due to unavailability of the engine inertia of the test truck because of its proprietary nature, the equation in Figure 73 could not be used as defined above. Instead, an approximation to the equation was made. Biggs, 1988, suggests that the engine, clutch, and wheel contribute 10 percent to the vehicle weight. (Biggs, 1988). Other researchers have estimated the effective mass from 5 percent to 2.5 times the mass of the vehicle. (Bennett, 1988; Bester, 1981; Watanada et al., 1987). An effective mass of 1.1 times the mass of the test vehicle was used for this study. Thus, engine brake force equation was rewritten as (Figure 74):

$$F_{eng} = -F_{drag} + 1.1M_e$$

Figure 74. Equation. Engine Brake Force Determination.

where, M_e = effective mass of rotating components of engine, clutch parts and wheel assembly. The engine brake force was converted to the convenient power absorption form (Figure 75) in the analysis:

$$HP_{eng} = \frac{F_{eng}V}{550}$$

Figure 75. Equation. Determining Horsepower into the Brakes.

where, V = velocity (ft/s). The engine brake force was analyzed within the engine operating range of 1400 to 2000 rpm. A plot of horsepower absorbed from the engine at three settings of the engine brake is shown in Figure 76.

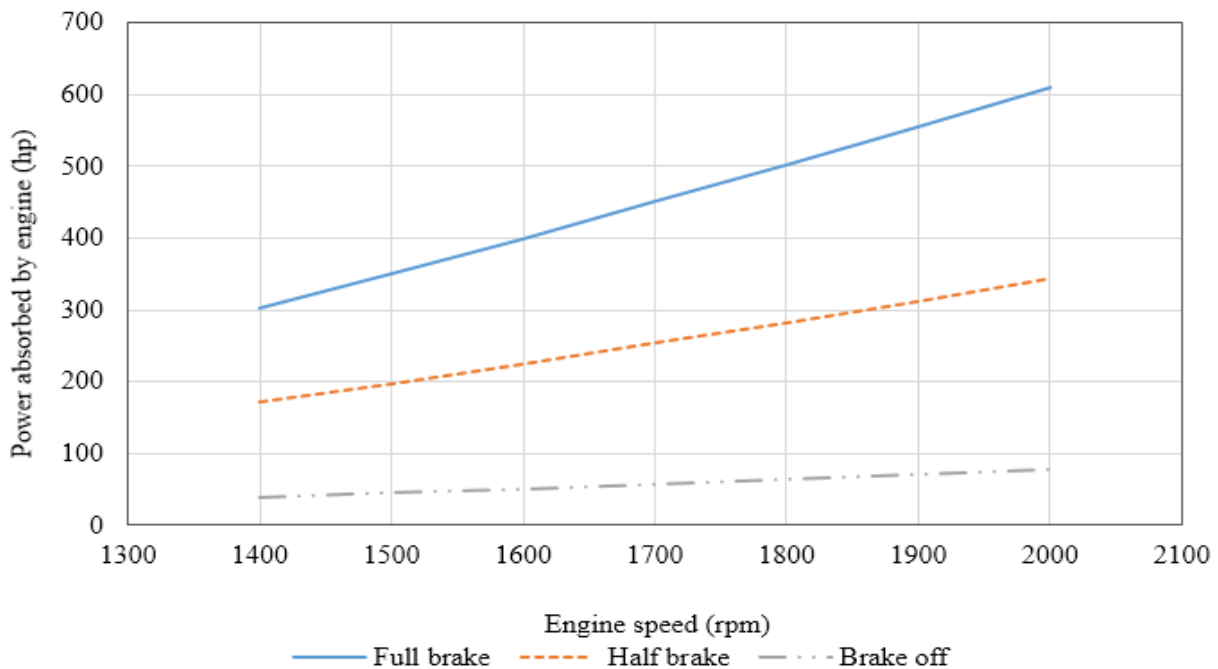


Figure 76. Graph. Estimation of Brake Force.

The retarding horsepower from the engine was measured at 1800 rpm which is the rated engine speed of the test truck. The results show that the retarding horsepower when the engine brake is off, at half and full setting are 63.3 hp, 238.0 hp and 502.0 hp respectively. At maximum retarding power, the results compare well with data published by Cummins limited for a horsepower of 1800 rpm. (Jacobs Vehicle Systems, 2010). The retarding force when the engine brake was off was also computed using data from the test truck manufacturer and the equation from Tetard et al., 1993, (Figure 20) as a check. The calculated brake horsepower was found to be 58 hp and 60 hp, respectively, using the two methods. The value of 63.3 hp for engine retardation (engine brake off) was thus considered satisfactory for the analysis.

Cool-down Tests

The cool-down results were analyzed using the Newton cooling equation. To extract the diffusivity constant (K_1), the Newton equation is rewritten as (Figure 77) :

$$\frac{T - T_{\infty}}{T_o - T_{\infty}} = e^{-K_1 t}$$

Figure 77. Equation. Newton Cooling.

which gives (Figure 78):

$$\ln\left(\frac{T - T_{\infty}}{T_o - T_{\infty}}\right) = -K_1 t$$

Figure 78. Equation. Modified Newton Cooling.

From the equation in Figure 78 above, a plot of $\ln\left(\frac{T - T_{\infty}}{T_o - T_{\infty}}\right)$ against time (t) should result in a straight line through the origin with a slope of $-K_1$. The extraction of K_1 was done at different speeds. Plots were made separately for left and right side brakes. However, a cable connecting sensors from the right side of the truck on brake 4 (R4) to the controller box was damaged during the test runs. This meant that temperature readings could only be collected from nine brake sensors instead of ten. However, it is important to note that a majority of the brake readings were available for the data analysis and the loss of a single reading should not adversely affect the outcome of the analysis. An example of a plot for the left side brakes is shown in Figure 80. Plots of other speeds are shown in appendix 2. Variations of K_1 with speed were plotted for left and right hand brakes (Figure 81 and Figure 82). Data points from the analysis were fitted with best fitting lines. The plots indicate that generally, the rate of cooling increases with increasing speed. This is the outcome expected as an increase in speed leads to more air flow over the brakes resulting in cooling. A model was then fitted to all the cool-down test observations to approximate K_1 as a function of speed (Figure 83). K_1 was expressed as (Figure 79):

$$K_1 = 1.1852 + 0.0331V$$

Figure 79. Equation. Relationship between K_1 and Truck Speed.

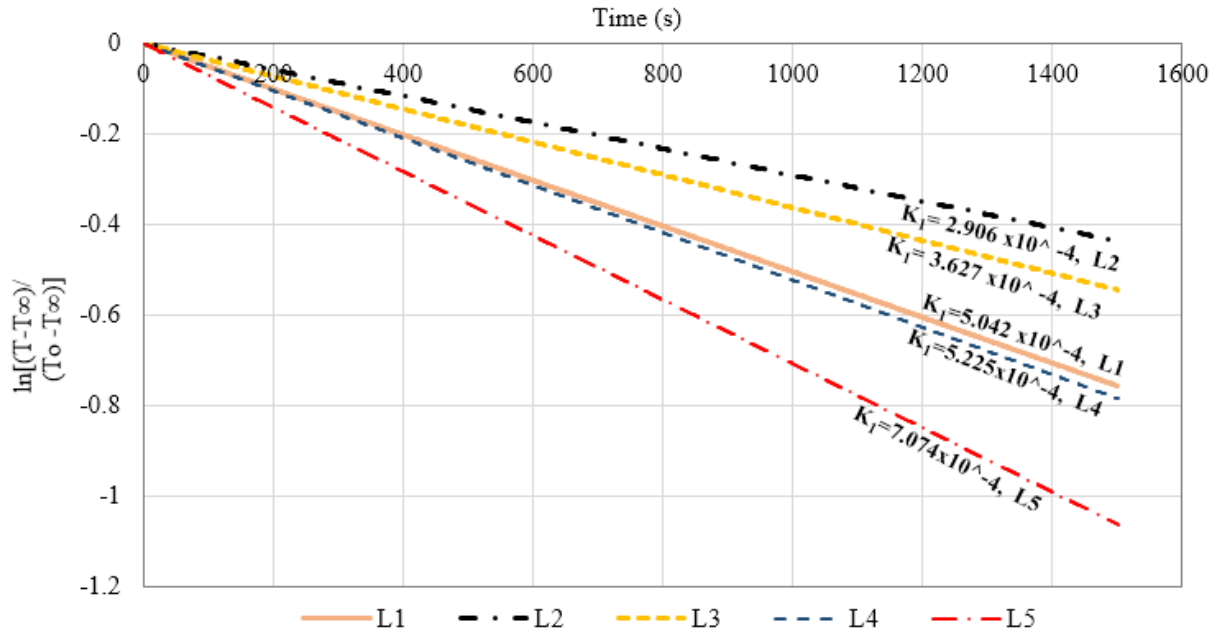


Figure 80. Graph. K_1 Extraction for $V = 0$ mph (Left Brakes).

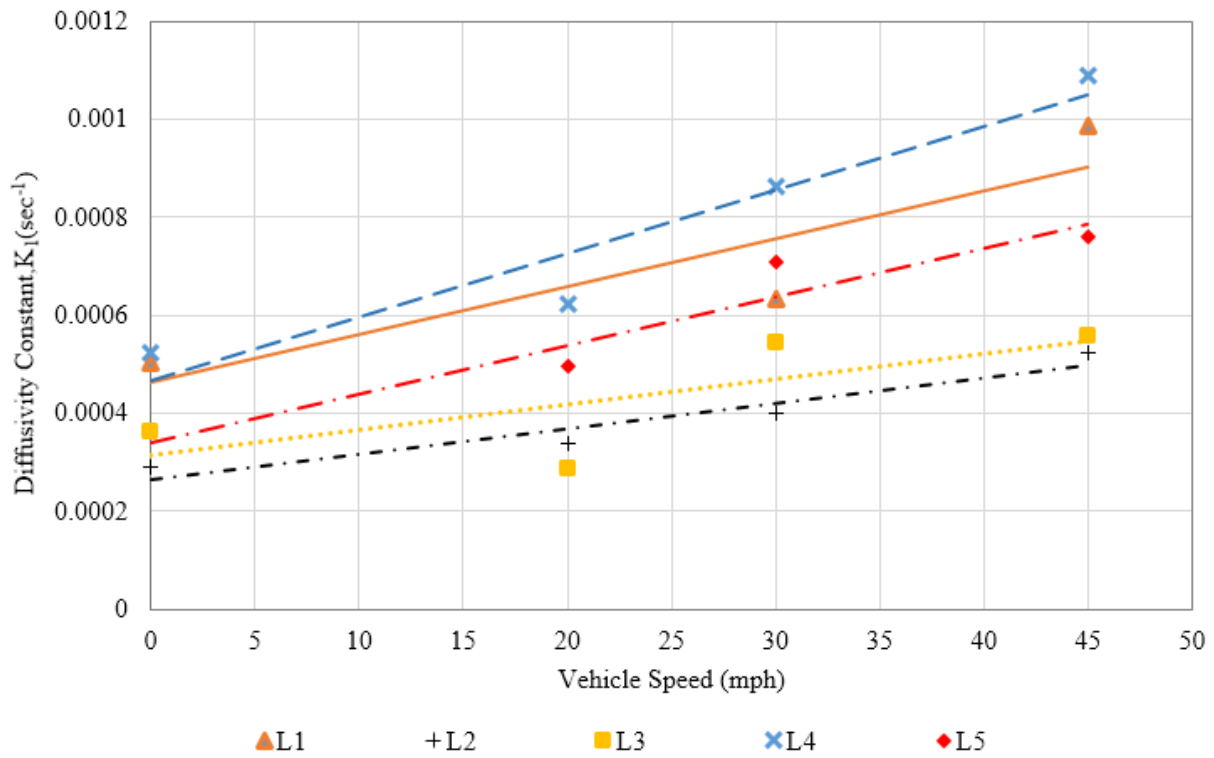


Figure 81. Graph. Variation of K_1 with Speed (Left Brakes).

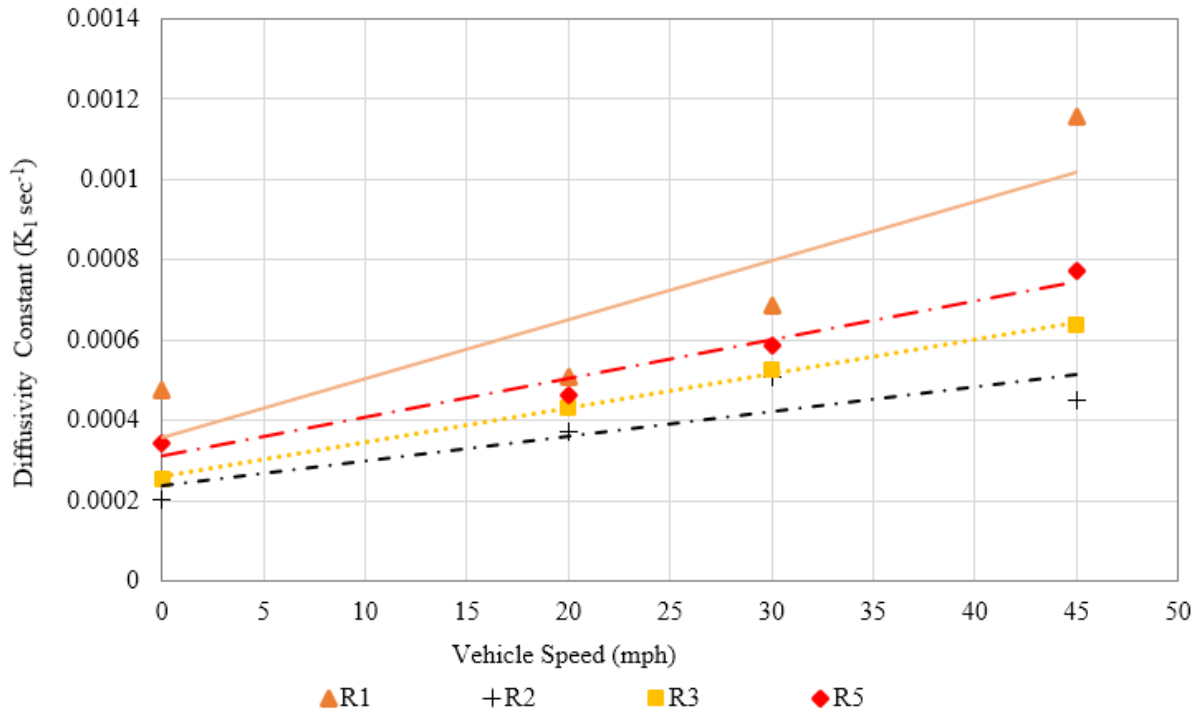


Figure 82. Graph. Variation of K_1 with Speed (Right Brakes).

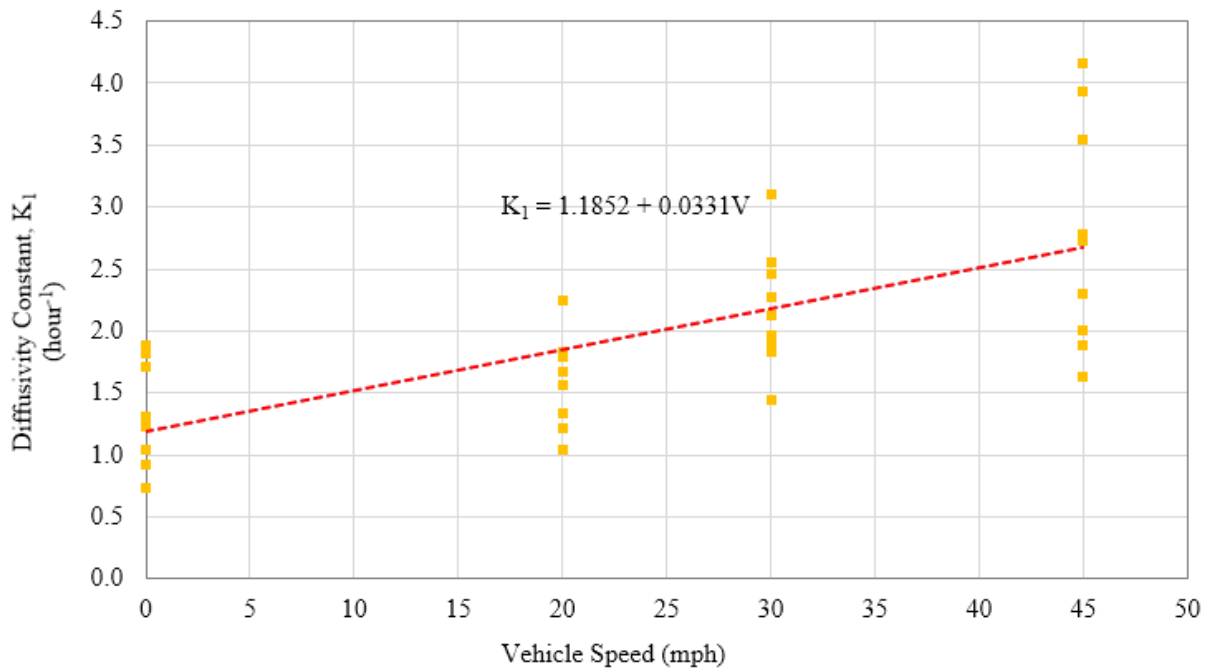


Figure 83. Graph. Expression of K_1 for Brake System in Terms of Speed.

Hill Descent Tests

The hill descent tests were adapted from Myers et al., 1981. This test aims at correlating brake temperature with the power absorbed during a grade descent. The procedure to correlate the observed brake temperature with power into the brakes was done by averaging the brake temperatures after each test run. It has been argued that even though there may be variation among the brake temperatures due to imbalance, this effect is of secondary importance. (Myers et al., 1981).

The correlation of brake temperature with power into the brakes was achieved by rearranging the brake temperature equation (Figure 29). The rearrangement was done to put the brake power absorption function $F_B V$, on one side of the equation and all other variables including the thermodynamic variables, collectively named T^* on the other side. This is expressed as (Figure 84):

$$T^* = \frac{T - T_o}{1 - e^{\frac{-k_1 L}{V}}} + (T_o - T_\infty) = K_2 F_B V$$

Figure 84. Equation. Correlation between Brake Temperature and Power into Brakes

This relation can be simplified as (Figure 85):

$$T^* = K_2 H P_B$$

Figure 85. Equation. Simplified Relation to Extract Brake Heating Constant (K_2).

From the equation in Figure 85, if a plot is made of T^* computed for each hill descent against $H P_B$, K_2 will be the slope of the graph. Separate plots were made for each hill descent. Test runs were made with different settings of the retarder. This was to simulate a change in truck weight. This approach was adopted to speed up the hill descent tests since actual loading and unloading takes a long time while a change of the retarder is achieved by just flicking a switch. The tests were conducted on three downgrades on United States (US) 16 at speeds of 21, 31, and 36 mph. Due to time constraints and inability to perform some tests on the field due to safety and time concerns, additional observations for the hill descent tests were obtained by simulation. The simulation was done using the TruckSim software. TruckSim has features which enable brake temperatures to be simulated for different loading and speed conditions. The software required the input of brake weight and specific heat capacity for accurate results. A weight of 102 lb was used as the default weight representing a Castlite brake drum with a specific heat capacity of 0.11 Btu/(lb-°F). Additional simulation runs were done to assess how comparable the field results were to simulation. Table 10 shows the results of the comparison. Hill descent runs at 10 and 50 mph were obtained from simulation

The simulation runs for comparisons were conducted for only 7 tests corresponding to field runs undertaken without a retarder (it is difficult to accurately estimate the weight of the truck loading with a retarder in use). It can be observed from

Table 11 that the absolute difference in brake temperatures between the field tests and simulation were less than 5 percent in five out of the seven tests.

Table 10. Comparison Simulation and Field Brake Temperatures.

Test No.	Weight (lb)	Grade (%)	Length (miles)	Speed (mph)	Av. Initial Brake Temp (°F)	Av. brake Temperature (°F) Field	Av. brake Temperature (°F) Simulation	Absolute Difference (%)
1	79400	7.0	4.30	21	133.05	302	288	4.6
2	79400	4.3	3.98	31	161.34	267	262	2.0
3	74000	7.0	4.30	31	127.36	244	253	3.7
4	74000	6.1	5.50	36	180.13	314	288	8.3
5	60,000	6.1	5.50	21	150.4	239	244	2.0
6	55000	7.0	4.30	31	115.75	197	206	4.5
7	60,000	6.1	5.50	31	153.82	189	203	7.2

All the test runs had an absolute difference of less than 10 percent with an average value of 4.6 percent. The use of the simulation software was therefore found to be suitable for simulating the hill descent tests. The hill descent test results at speeds of 10 mph and 50 mph were obtained solely from simulation. A plot of the downhill test is shown in Figure 86. The other plots for the hill descent tests can be found in Appendix 3.

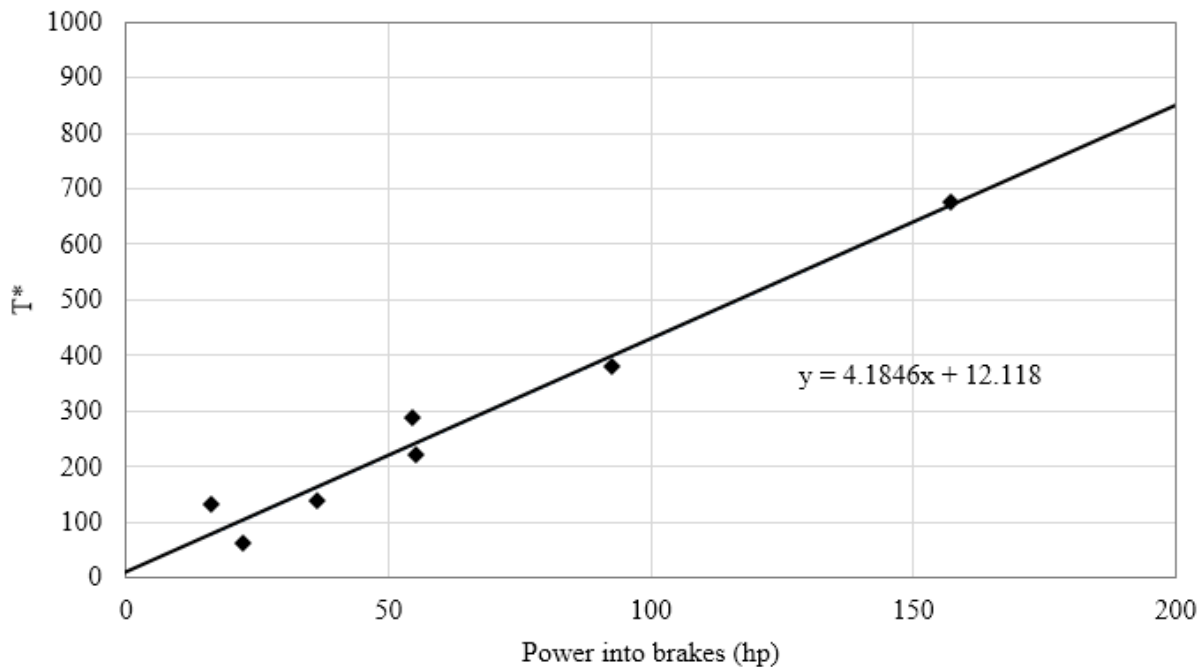


Figure 86. Graph. Plot of Temperature Parameters versus Power into Brakes at 10 mph.

From the equation in Figure 85, a plot of T^* against HP_B should result in a straight line through the origin. However, a look at the downhill plots shows this is not the case. The differences in the theoretical framework and the output from the field tests are likely due to instrumentation errors, assumptions to simplify the brake temperature model, measurement errors, and non-

linearity between observations for computed T^* and HP_B . However, the authors deemed these errors and issues not to be significant enough to affect predictions made by the resulting brake temperature model.

After extracting K_2 at different speeds, a straight line was fitted to a plot of the inverse slopes ($1/K_2$). An equation of $1/K_2$ was then derived in terms of V for use in the brake temperature equation. The equation relating $1/K_2$ to V was expressed as (Figure 87):

$$\frac{1}{K_2} = \frac{1}{hA_c} = 0.1602 + 0.0078V$$

Figure 87. Equation. Relation Between (K_2) and Speed.

The plot relating $1/K_2$ to V is shown in Figure 88.

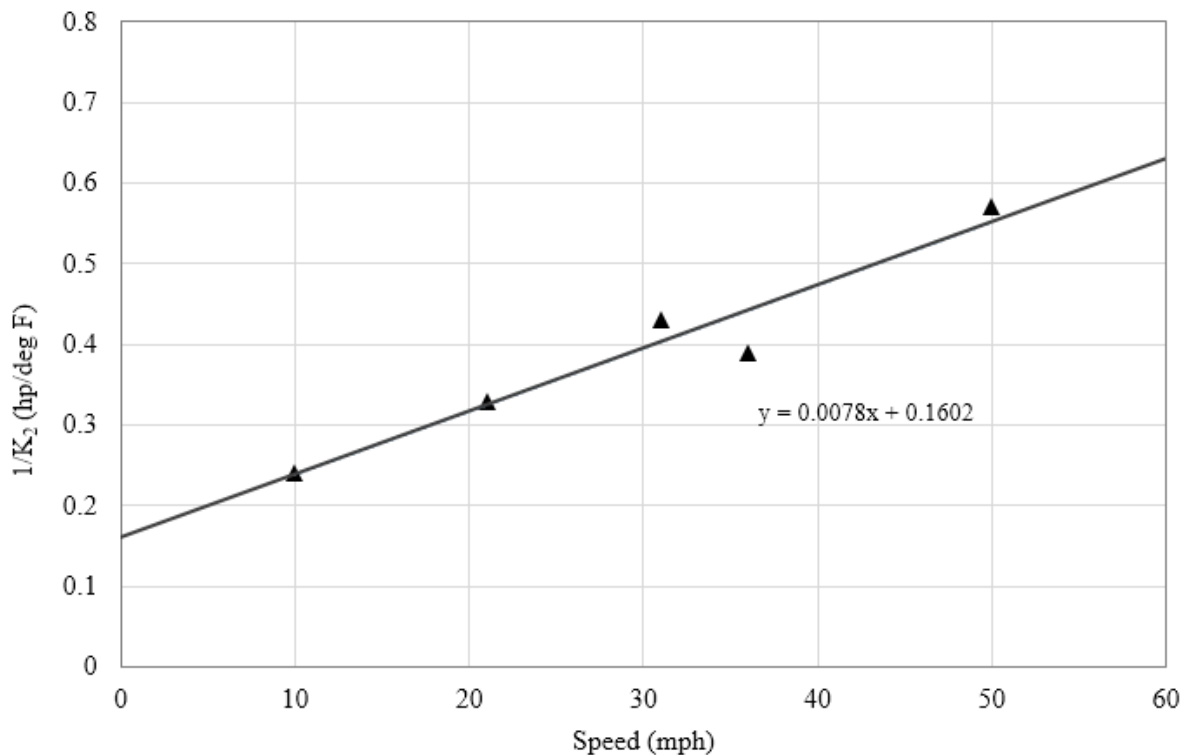


Figure 88. Graph. Variation of Heat Transfer Parameter ($1/K_2$) with Speed.

Use of the Updated Brake Temperature Model

With the parameters of the updated temperature model defined, it is now possible to predict maximum safe speeds on downgrades.

Table **11** is a summary of the updated model parameters.

Table 11. Summary of Updated Temperature Model Parameters.

Parameter	Expression/Value	Units
Brake temperature equation	$T_f = T_o + [T_\infty - T_o + K_2 HP_B][1 - e^{-K_1 L/V}]$	°F
Horsepower into brakes (HP_B)	$HP_B = (W\theta - F_{drag}) \frac{V}{375} - HP_{eng}$	hp
Drag forces (F_{drag})	$F_{drag} = 459.35 + 0.132V^2$	lb
Diffusivity constant (K_1)	$K_1 = 1.5x(1.1852 + 0.0331V)$	1/hr
Heat transfer parameter (K_2)	$K_2 = \frac{1}{hA_c} = (0.1602 + 0.0078V)^{-1}$	°F/hp
Engine brake force (HP_{eng})	$HP_{eng} = 63.3$	hp
Temperature from emergency stopping (T_E)	$T_E = 3.11 \times 10^{-7} WV^2$	°F
Ambient temperature (T_∞)	$T_\infty = 90$	°F
Initial brake temperature (T_o)	$T_o = 150$	°F

The updated brake temperature model allows for predicting final brake temperatures on downgrades and thus maximum downgrade speeds. The parameters defined in

Table 11 are used to plot maximum safe descent speeds (V_{max}), as a function of truck weight, grade steepness and truck braking length. Rearranging the brake temperature equation (Figure 29), and accounting for the temperature rise from emergency stopping (Figure 9), L can be express as (Figure 89):

$$L = -\frac{V}{K_1} \ln \left[\frac{T_{lim} - 90 - K_2 HP_B}{60 - K_2 HP_B} \right]$$

Figure 89. Equation. Determination of Maximum Descent Speed Plots.

Accurate plots are only possible with a precise definition of the limiting temperature T_{lim} . T_{lim} should be chosen to reflect the fade temperature of brake lining and drums, and the general brake imbalance characteristic of most trucks. Studies have suggested that brake drums and lining start to fade at about 500°F to 600°F (Bowman, 1989; J. C. Glennon, 2018; Marathon Brake Systems, 2013; The Brake Report, 2016). A conservative temperature of 500°F was chosen as the limiting temperature for this study; the same used by Johnson et al., 1982a. If this temperature is subsequently found to result in conservative speeds, the value may be reviewed upwards.

A final modification of the FHWA GSRS model was to multiply K_1 by a factor of 1.5. This is to account for nonlinear temperature gradients in the brakes during rapid stops. (Johnson et al., 1982a). Using the parameters of the updated temperature model, plots were made for L at V_{max} values for given grade steepness, truck speeds and weights. The parameters T_o and T_∞ were held at constant values to be representative of downgrade situations for isolated single-grade hills. For multi-grade hills, T_o is variable and is equivalent to the final temperature at the end of a non-braking section. An example of a maximum descent speed plot for an 80,000 lb truck is shown in Figure 90.

VALIDATION OF THE UPDATED BRAKE TEMPERATURE MODEL

The brake temperature model was validated by driving the test truck at a lower loading of 74,000 lb over a 6.5-mile multi-grade hill on the eastern face of United States (US) 16 highway (milepost 67.4 - 73.9). Validating the model on a multi-grade hill was challenging due to the large variability inherent in accurately predicting the grade and braking length of each section. Eight individual grades were identified over the section. Averaging of the grades was done due to the continuously changing slope characteristics of the sections identified, as required by the GSRS model. Downgrades ranged from 2 percent to 8 percent, with upgrades ranging from 4 percent to 5 percent. Figure 91 shows the grade profile of the route used for validating the temperature model. Multi-grades are characterized by heating and cooling sections. Downgrades represent sections where braking has to be done to control speed while no braking is required for level sections and upgrades. Downgrades are thus heating sections while upgrade/level sections are cooling sections. The test truck was driven at an approximate speed of 45 mph over the route with the brake temperatures being continuously measured. The updated GSRS temperature model was used to predict the temperatures at the end of each of the separate grades identified. The final brake temperature of the preceding grade was the initial temperature of the succeeding grade or cooling interval. This is the recommended procedure to generate the temperature profile of the multi-grade hill. (Bowman, 1989). The field temperature was then compared to the predicted temperature. Table 12 shows the results of the analysis while Figure 92 shows the comparison of these two temperatures.

The validation test showed a close match between the field and predicted temperatures. This indicates a close match between the field and the predicted temperatures using the updated GSRS model. The results show that the updated GSRS model can accurately approximate operational truck brake temperatures.

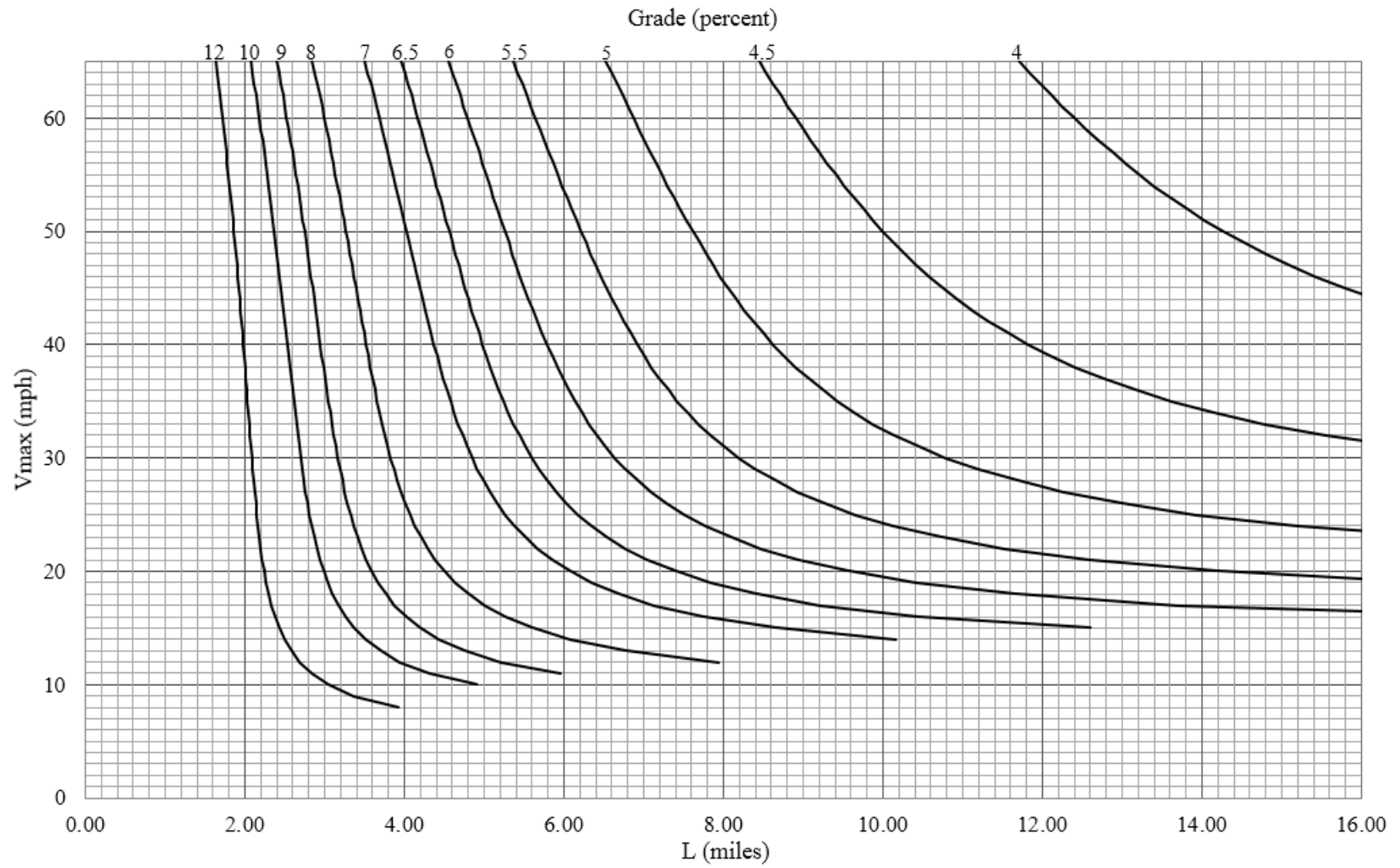


Figure 90. Graph. Maximum Safe Speed as a Function of Grade Length and Steepness for Truck Weight 80,000 lb.

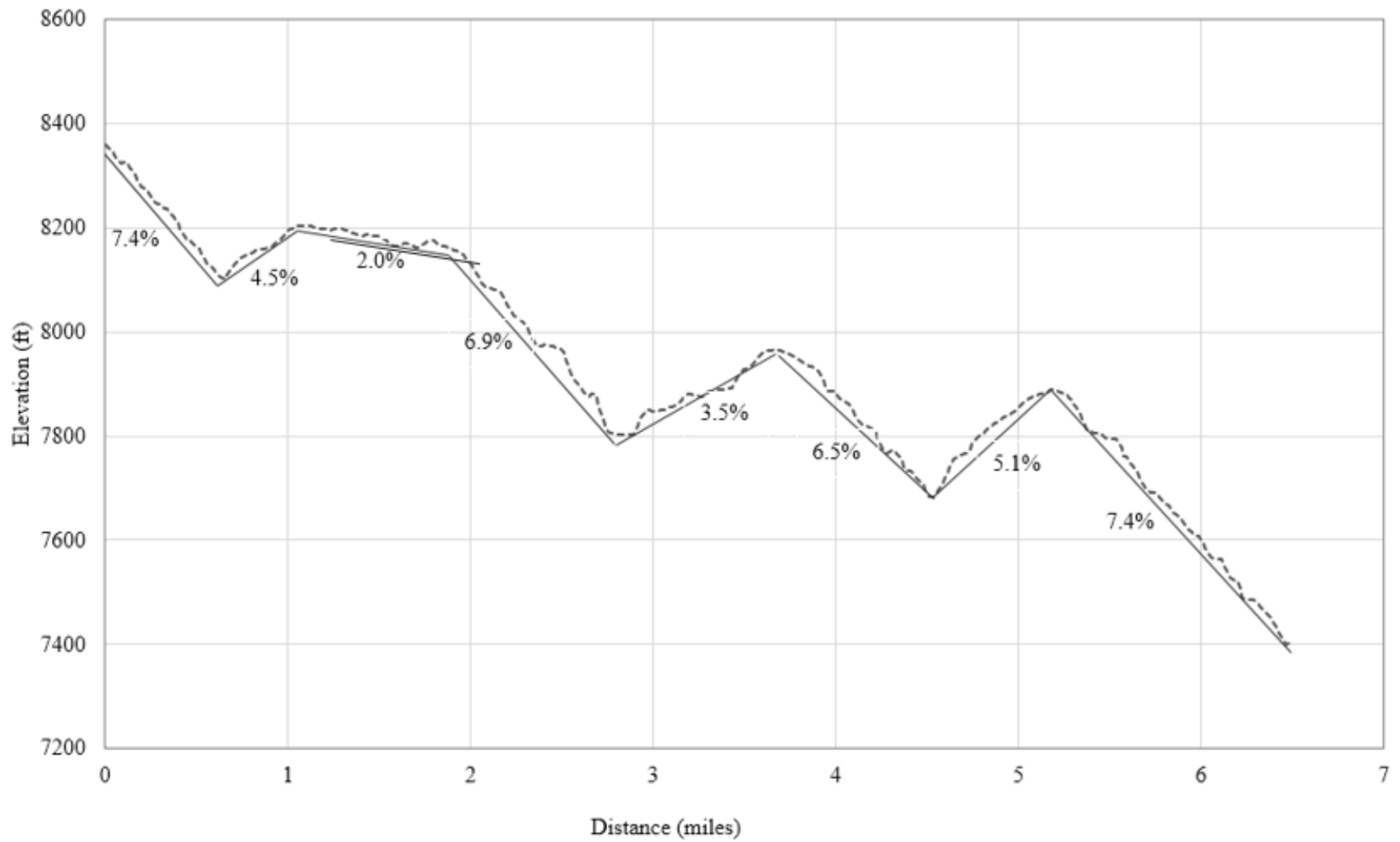


Figure 91. Graph. Grade Profile for Validation Test.

Table 12. Summary of Validation Test and Results.

Section No.	Upgrade/Downgrade	Distance (miles)	Grade (%)	Initial Brake Temp (°F)	Ambient Temp (°F)	Field Brake Temp (After Descent) (°F)	Predicted Brake Temp (°F)	Absolute Difference (%)
1	Downgrade	0.66	7.4	145.6	49.9	184.8	189.8	2.7
2	Upgrade	0.43	4.5	189.8	51.0	180.5	181.3	0.5
3	Downgrade	0.71	2.0	181.3	50.9	180.2	184.2	2.2
4	Downgrade	1.03	6.9	184.2	50.9	270.5	279.6	3.4
5	Upgrade	0.85	3.5	279.6	52.39	251.8	256.7	2.0
6	Downgrade	0.81	6.5	256.7	52.15	328.5	321.0	2.3
7	Upgrade	0.72	5.1	321.0	52.45	314.8	298.5	5.2
8	Downgrade	1.22	7.4	298.5	54.76	423.5	399.2	5.7

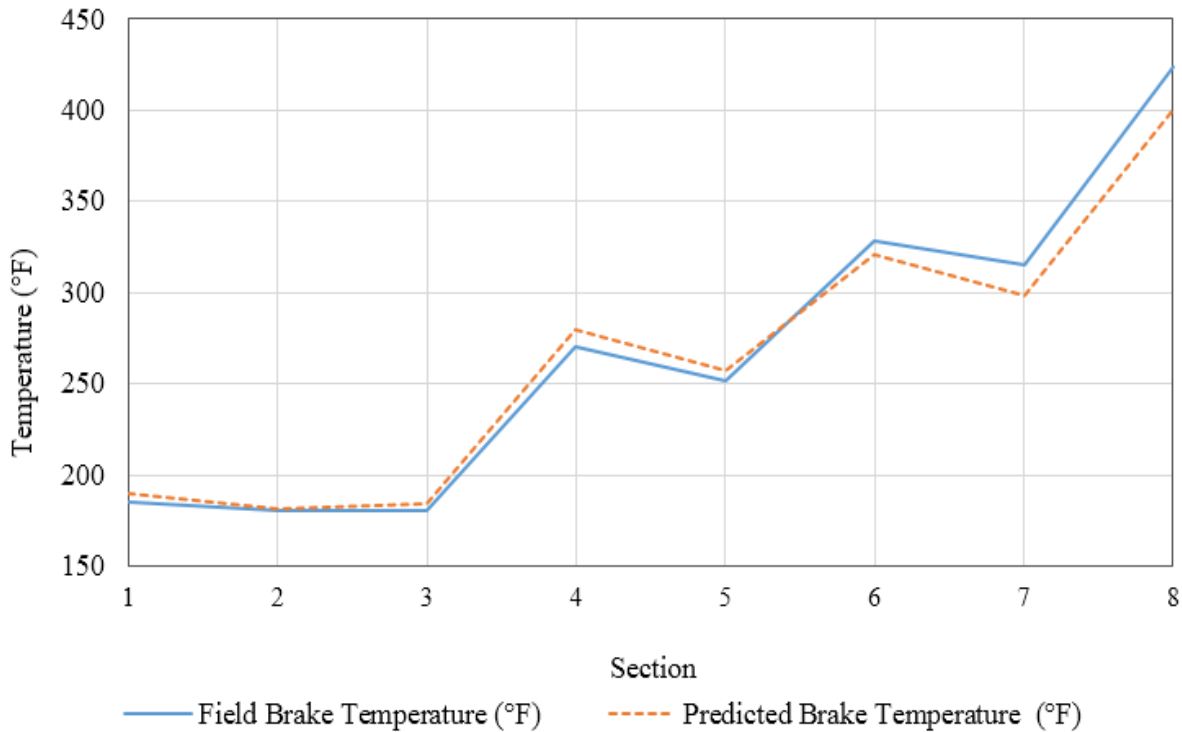


Figure 92. Graph. Comparison of Field and Predicted Brake Temperature from Validation Test.

WEIGHT SPECIFIC SPEED (WSS) SIGNS

The outcome of the GSRS is a sign posted before the downgrade with advisory speeds for different truck weights. The formulation, implementation, issues and some case studies regarding WSS signs have been discussed in detail by Bowman. (Bowman, 1989). Some highlights from the study are discussed below.

- The WSS sign by intent provides maximum safe descent speeds for trucks not equipped with retarders. Trucks equipped with retarders will be able to descend downgrades at higher safe speeds than recommended by the GSRS temperature model. However, the WSS signs have the potential for increasing downgrade safety for retarder equipped trucks. Retarder equipped trucks lose control on downgrades due to the same reason as trucks not equipped with retarders. Chosen descent speeds, which are much higher than the equipment being operated will result in brake overheating even with retarders installed on the truck.
- The use of exact speeds is not required on the WSS signs. Rounding speeds to 5 mph or 10 mph increments have been found to be effective in conveying information to truck drivers of the presence of a severe downgrade necessitating a speed reduction.
- The speeds presented on the WSS sign are the maximum safe speeds for the heaviest weight in each category. The weights shown on the sign should decrease in equal increments from the load limit of the highway. The weight increments should be in multiples of 5,000 or 10,000 lb. Practical considerations should be taken into account in recommending maximum descent speeds especially on higher severity grades where the recommended maximum safe speeds are under 20 mph. Changes in 5,000 lb increments will only result in changes of only a few mph. In such instances, it may be necessary to increase the weight increments to 10,000 lb. This is to avoid unworkable recommendations and to minimize sign complexity as it is pointless to specify speed changes of 1 or 2 mph.
- To engender confidence in the speeds displayed by the WSS signs, it is necessary to accurately estimate the percent decline and truck braking length. Truck braking length refers to the length of the downgrade section actually used for braking. This is obtained by observing at least five trucks as they descend and brake on the downgrade. (Bowman, 1989). Also, if the higher truck weight categories result in maximum safe speeds less than 10 mph, then the braking length should be obtained from field observations. However, the physical length of the grade can be used, if the truck braking length cannot be determined. Accurate measurement of the downgrade characteristics is to prevent estimated descent speeds being artificially low. Overly conservative speeds will lead to drivers disregarding the recommended speeds and travelling at higher speeds. Realistic speeds and driver confidence in the WSS signs will ensure voluntary compliance. Conversely, high unsafe speeds due to errors in estimating the percent decline and truck braking length will greatly endanger safety on downgrades.
- Determination of maximum safe descent speeds are analyzed by two methods based on the characteristic of the downgrade. Downgrades, which do not have enough cooling intervals and areas of safe downshifting, are considered as single slopes. They are analyzed by the continuous slope method. The maximum safe speeds which do not permit brake temperatures to exceed the limiting temperature are displayed on the WSS signs for the single grade. This is installed before the downgrade.

- Downgrades that have intervals of enough distance to permit safe downshifting, and where braking is not necessary, may be regarded as multi-grades hills. A separate downgrade method is used to determine the maximum safe descent speeds on multi-grades. Travel time is optimized by analyzing the multi-grade slope as a series of constant-speed braking intervals separated by non-braking intervals, on which the driver may downshift. The GSRS aids the driver in the selection of speeds on each braking interval. This is done by placing WSS signs at the end of each non-braking sections, in the same manner as for a single grade decline. Speed limits may be recommended only on the non-braking intervals to optimize the travel time. Speeds are progressively lowered on the first downgrade segments, thereby, causing corresponding changes in the truck brake temperatures. Varying the speed on the first group of downgrades allows the total travel time to be minimized. The dissipation of brake energy on non-braking intervals should be calculated with the resulting new temperature being the initial temperature of the next braking interval. Brake system temperatures of less than 90°F should not be used in the calculations.
- An optimization criterion is introduced in the calculation of safe speeds for multi-grade hills. This criterion, however, can result in successive decrements of weight having the same descent speeds followed by a relatively large speed increase for the next weight category. When this occurs, calculations should be done with the maximum temperature limit set to less than or equal to 530°F. The 30°F increment in the threshold temperature (i.e., from 500 to 530°F) accounts for brake temperature variability determined from field measurements. (Bowman, 1989). Descent speeds which result in brake temperatures exceeding 530°F should never be placed on the WSS signs.

Formulation of WSS Signs

The procedure to define weights and speeds for WSS signs are, (Bowman, 1989; Johnson et al., 1982a):

- Determine the grade percent (θ) and truck braking length (L) in miles, maximum load limit and maximum speed limit on the downgrade.
- Using the plots of V_{max} versus L for various values of θ , determine the heaviest weight, W_L , that is an integral multiple of 5,000 lb, and for which V_{max} is greater than or equal to the speed limit.
- Compute the number of 5,000 lb weight interval (N) between W_L and the maximum speed limit, W_M from (Figure 93):

$$N = \frac{W_M - W_L}{5,000}$$

Figure 93. Equation. Determining Number of Weight Intervals to be placed on WSS Sign.

- If N is less than or equal to 5, the column of weights will begin with W_L and increase in 5,000 lb increments to the load limit, W_M .
- If N is greater than 5, the column of weights for placement on the WSS sign will begin with the lower weight, (W_L) and increase in 10,000 lb to the load limit, W_M .

- The speed associated with each weight interval for the WSS sign (defined by the two adjacent weights in the weight column) will be the safe downgrade speed for the heaviest weight of the interval. The maximum speeds are then placed in columns for each weight category.

Example of Weight and Speed Determination, and Comparison of Maximum Speeds from the Modified GSRs (Old GSRs) and the Updated GSRs

Two case studies are presented to demonstrate the derivation of maximum safe descent speeds for different weight categories. Also, a comparison was made between the recommended speeds of the modified GSRs, by Johnson et al., 1982a (referred to as the ‘Old GSRs’), and the updated GSRs. Case study 1 is presented below while case study 2 can be found in Appendix 5.

Case Study 1

Case study 1 is a theoretical downgrade with parameters as follows:

- Downgrade = 7.00 percent
- Braking length = 6.00 miles
- Maximum weight = 80,000 lb
- Speed limit = 65 mph

Maximum Safe Speeds from Old GSRs Model

Plots used for this case study for the old GSRs model were derived from the modified GSRs model by Johnson et al., 1982a.

1. From the V_{max} versus L plot, the highest integral multiple of 5,000 lb for which V_{max} is greater than 65 mph is 60,000 lb.
2.
$$N = \frac{80,000 - 60,000}{5,000}$$

$$N = 3. N < 5$$
, so the column of weights will begin with 60,000 lb and increase in 5,000 lb increments to 80,000 lb.
3. From the V_{max} versus L plots, the maximum truck weights and corresponding speeds are (Table 13):

Table 13. Maximum Truck Weights and Estimated Safe Speeds (Case Study 1 - Old GSRs).

Maximum Truck Weight (lb)	Maximum Safe Speed (mph)
80,000	22
75,000	27
70,000	30
65,000	43
60,000	65

The four increments of truck weights and speeds to the nearest 5 mph are as shown below on (Table 14).

Table 14. Maximum Truck Weights and Approximate Safe Speeds (Case Study 1 - Old GSRs).

Weight Increments (lb)	Maximum Safe Speed (mph)
61,000 - 65,000	45
66,000 - 70,000	30
71,000 - 75,000	25
76,000 - 80,000	20

Maximum Safe Speeds from Updated GSRs Model

Plots used for deriving the maximum safe speeds were obtained from the updated GSRs model and are found in appendix 4.

1. From the V_{max} versus L plot, the highest integral multiple of 5,000 lb for which V_{max} is greater than 65 mph is 65,000 lb.
2.
$$N = \frac{80,000 - 70,000}{5,000}$$

$$N = 2.$$
 The column of weights will begin with 70,000 lb and increase in 5,000 lb increments to 80,000 lb.
3. From the V_{max} versus L plots, the maximum truck weights and corresponding speeds are (Table 15):

Table 15. Maximum Truck Weights and Estimated Safe Speeds (Case Study 1 - Updated GSRs).

Maximum Truck Weight (lb)	Maximum Safe Speed (mph)
80,000	20
75,000	26
70,000	35
65,000	53
60,000	65

The three increments of truck weights and speeds to the nearest 5 mph are as shown below on Table 16.

Table 16. Maximum Truck Weights and Approximate Safe Speeds (Case Study 1 - Updated GSRs).

Weight Increments (lb)	Maximum Safe Speed (mph)
61,000 - 65,000	55
66,000 - 70,000	35
71,000 - 75,000	25
76,000 - 80,000	20

The results from the case studies indicate maximum safe speeds derived from the updated model are higher compared to similar weight categories for the old GSRs model. This speed difference

may be a reflection of the improved truck designs resulting in less drag, better braking systems, and an update to the general design of systems of the current truck population. Though the maximum descent speed differences are apparent between the two models, the difference is not extreme and only reflects changes in the current and truck designs of the 1980s. The recommended speeds derived from the updated GSRS model based on the case studies are not hazardous and will not lead to excessive speeding on downgrades and mountain passes.

USE OF RETARDERS

The GSRS was developed mainly for trucks without retarders. However, a significant portion of the truck population have retarders that assist the service brakes in slowing down loaded trucks on downgrades. The use of a retarder is equivalent to a weight reduction for a loaded truck. Johnson et al., 1982a, proposed a method for computing this equivalent weight reduction. This equivalent weight decrease (ΔW) can be found using the equation in Figure 94. (Johnson et al., 1982a):

$$\Delta W = \frac{\Delta HP_R \times 375}{\theta V}$$

Figure 94. Equation. Determination of Equivalent Weight Reduction Due to Retarder Use.

where,

ΔHP_R = the increase in horsepower absorbed by the engine (over that for the same engine without a retarder),

θ = grade slope (radians)

V = truck speed (mph).

As an example, consider a truck loaded to 90,000 lb descending a 5 percent grade 8 miles long. From the maximum speed plots for a 90,000 lb vehicle (appendix 4), the maximum safe descent speed is 28 mph. For a truck whose retarder absorbs 200 hp, the equivalent weight decrease is found from the equation, in Figure 94, to be 53,571 lb. Rounding this off (in the conservation direction) to 50,000 lb, the driver looks for a speed corresponding to a 50,000 lb lighter truck regardless of his current weight.

Some arbitrary scenarios have been created to demonstrate the weight reduction effect of a retarder and its impact on maximum safe descent speeds.

Table **17** below shows these scenarios for a truck loaded at 80,000 lb at full and half engine brake settings. The maximum speed limit for this scenario is 65 mph.

Table 17. Effect of Retarder on Truck Weight.

Full Engine Brake Engaged (502 hp @ 1800 rpm)				
	7%, 5 miles	6%, 6 miles	5%, 7 miles	4%, 12 miles
Speed from updated GSRS (mph)	28	37	61	61
Increase in hp absorbed ($\Delta H P_R$) (hp)	438.7	438.7	438.7	438.7
Equivalent weight decrease (ΔW) (lb)	83,934.9	74,104.7	53,938.5	65,282.7
New weight (80,000 lb - ΔW) (lb)	-3,934.9	5,895.3	26,061.5	14,717.3
Round up weight (lb)	0	60,000	25,000	15,000
New speed from updated GSRS (mph)	65	65	65	65
Half Engine Brake Engaged (238 hp @ 1800 rpm)				
	7%, 5 miles	6%, 6 miles	5%, 7 miles	4%, 12 miles
Speed from updated GSRS (mph)	28	37	61	63
Increase in hp absorbed ($\Delta H P_R$) (hp)	174.7	174.7	174.7	174.7
Equivalent weight decrease (ΔW) (lb)	33,424.7	29,510.1	21,479.5	25,997.0
New weight (80,000 lb - ΔW) (lb)	46,575.3	50,489.9	58,520.5	54,003.0
Round up weight (lb)	45,000	50,000	60,000	55,000
New speed from updated GSRS (mph)	65	65	65	65

It may be observed from the analysis in

Table 17, that the retarder produced a weight reduction effect such that an 80,000 lb truck is capable of traveling at the speed limit. The weight decrease depends mainly on the power absorption of the retarder. This implies that it is necessary to rate each retarder type in terms of equivalent weight decrease. However, with different retarder types, ratings and settings available, this process is cumbersome and requires additional calculation by the driver to estimate a safe descent speed. This will defeat the goal of making WSS signs simple and easy to read and apply. Current driver license manuals for commercial and heavy vehicles recommend that vehicles equipped with retarders should be engaged to obtain maximum engine brake retardation on severe downgrades (maximum retarder settings should be used). Several analyses were conducted for different loading conditions and slopes using the test truck maximum engine brake retardation horsepower of 502 hp. In most of the scenarios considered, the equivalent weight reduction, due to the use of the retarder, resulted in weights that enabled the truck to travel at the designated speed limit of the highway in question. Due to inadequate information on the maximum retarding horsepower of retarders on the market and the need to simplify the WSS signs, it is recommended that the maximum safe descent speed for a retarder-engaged truck on a downgrade should be the highest recommended speed on the WSS sign. Such speeds may be deemed conservative under some situations but will be generally appropriate considering the differences in retarding horsepower available to different trucks.

CHAPTER SUMMARY

This chapter discussed the results of the field tests and their use in updating the GSRS model. Results of the truck preparatory tests, coast-down, cool-down, hill descent, and validation tests were discussed. The use of simulation to provide additional data for the main tests due to time and other constraints were also discussed. Next, the use of the updated temperature model for deriving maximum speed limits on downgrades was demonstrated. The final part of the chapter presented the formulation of WSS signs. Issues with the preparation and use of WSS signs as discussed by Johnson et al., 1982a were highlighted. Two case studies allowed for an illustration of how to derive maximum descent speeds for the WSS signs and a comparison of the recommended speeds from the old GSRS and the updated temperature model.

Coast-down, cool-down and hill descent tests were undertaken to update the GSRS model. A temperature of 500°F was used as the limiting temperature of the model as was the case in the previous GSRS model by Johnson et al., 1982a. The updated model was modified based on recommendations from previous studies. The new model accounted for the temperature rise due to an emergency stopping in deriving maximum safe descent speeds. Also, the diffusivity constant K_1 , was multiplied by a factor of 1.5 to account for non-linear temperature gradients arising from rapid stops. Additionally, the brake temperature equation was modified to account for the cooling that occurs on non-braking sections. The brake heating term K_2HP_B should be set to zero on upgrades and non-braking sections of sufficient length.

The updated temperature model was compared to field data by driving the test truck loaded at an approximate weight of 74,000 lb over a multi-grade section at about 45 mph. The updated model was used to predict the brake temperatures at the end of the downgrades and non-braking sections and compared with the field data. The results showed a close match, which indicated that the updated model accurately predicts field brake temperatures.

The formulation of WSS signs from the GSRS is the ultimate output from the GSRS. WSS signs are installed before downgrades with advisory speeds based on truck weights. The speeds on the WSS signs are not exact but have been found to be effective in conveying information of truck severity to drivers. Formulating the WSS signs requires accurate estimation of the percent decline and truck braking length. Artificially low estimated speeds resulting from inaccurate measurement of the grade characteristics will lead to drivers disregarding the recommended speeds. Higher unsafe speeds derived from incorrectly measured downgrade characteristics will endanger safety on the downgrades.

A comparison between recommended speeds from the GSRS model, by Johnson et al., 1982a, and the updated model showed the speeds from the new model were higher. The updated speeds may lead to an increase in driver confidence in the WSS signs and compliance to the recommended speeds.

CHAPTER 6: CONCLUSIONS AND RECOMMENDATIONS

This chapter is a summary of the study and implementation of the GSRS. Recommendations from the study are also provided in this chapter.

CONCLUSIONS

Summary

Mountainous downgrades present significant challenges to truck drivers. The high amount of heat generated during downgrade descents causes brake heating and truck runaways. Truck crashes on downgrades, due to brake fade and runaways have devastating consequences on lives and property. In an attempt to guide truck drivers to safely descend downgrades, different studies have proposed various grade severity rating systems. These have included the BPR in the 1950s, Hykes and Lill's grade rating systems. However, these previous grade rating systems were beset by challenges such as oversimplification, exclusion of truck parameters in deriving the severity rating and an inability to safely predict safe speeds. Also, most of the previous rating systems did not consider the heat characteristics of the brake system and its interaction with the environment. Drivers still had to rely on their experience to select safe descent speeds despite the use of the rating systems.

In the 1980s, the FHWA sponsored a program to develop a grade severity rating system to accurately predict maximum downgrade descent speeds for trucks. A mathematical model, derived from the principles of thermodynamics was used to predict brake temperatures at the bottom of the grade during descents. This model developed by Myers et al., 1981 through field tests with a five axle truck predicted truck system temperature based on grade length and steepness, and on total truck weight and speed. (Myers et al., 1981). The brake temperature model also considered truck factors, brake characteristics and environmental factors, such as, initial temperature of the truck weight, engine rpm, non-brake resistive forces, brake heat dissipation, initial brake, and ambient temperature. Subsequent validation tests proved the brake temperature model developed accurately predicted truck temperatures. (Hanscom, 1985).

Modifications were made to the brake temperature equation, by Johnson et al., 1982a. It was found that the determination of a maximum safe descent speed also required that there should be sufficient braking capacity available to make an emergency stop on, or at the bottom of a downgrade. The brake temperature model was therefore modified to account for the emergency stopping criteria. WSS signs were derived from the brake temperature model, and installed at the top of downgrades to recommend safe descent speeds based on truck weights. The concept of the GSRS and WSS signs presented a leap in downgrade safety. Drivers now had advisory speeds that told them exactly how to descend the downgrade, rather than giving them information that still requires evaluation under different loading conditions.

In the intervening years since the GSRS was developed, there has been a radical change in design of the typical truck. Fuel conservation measures have led to streamlined designs to lower drag forces on truck. Also, radial tires have been adopted in the industry that have resulted in faster rotation by virtue of their smaller diameters, and a change in loading characteristics as a consequence. Engine retardation and friction have also changed in the intervening years. Rules have been passed to reduce the stopping distance of trucks by up to 30 percent. This has had implications on the design of truck brake systems. Generally, brakes have been made larger to

comply with the stopping rule while other trucks have adopted disc brakes on some wheels. The result of these changes in truck characteristics have meant the speeds recommended by the GSRS are conservative. (Janson, 1999). Low advisory speeds increase the risk of truck drivers ignoring recommended speeds as unrealistic and disregarding the GSRS as a whole. This will lead to a reduced safety on downgrades.

Due to the reasons mentioned above, this study was commissioned to update the GSRS. The mathematical model developed by Myers et al., 1981, was maintained in its form. Field tests were conducted with a five axle truck to update the parameters of the GSRS.

Field Tests

Field tests were conducted with an instrumented five-axle truck. Different variables were measured during the tests including vehicle speed, deceleration, truck weight, GPS coordinates, ambient temperature, wind speed and direction, humidity, brake application pressure, etc. Data acquisition in real time during the test procedures, was achieved through the use of a proprietary software, MICAS-X®. Three main field tests were conducted to update the GSRS model. These were coast-down, cool-down, and hill descent tests.

Coast-down tests were conducted to determine the sum of drag and engine brake forces as a function of weight and velocity. The coast-down tests were conducted by launching the test vehicle with the engine disengaged to allow free rolling of the vehicle. The speeds and distances covered during the tests were recorded during the test procedure. To determine the engine brake force, the coast-down tests were done with the gear engaged. Simulation coast-down tests were done to augment data collected from the field and to shorten the test time.

Cool-down tests were undertaken to define the brake heat transfer properties. The brakes were heated by performing a series of snubs to raise the brake temperatures above 500°F. The truck was then driven at a constant speed with no braking to cool the brakes to ambient temperature. The test was conducted at several vehicle operating speeds, (20 mph, 30 mph, 45 mph), and 0 mph.

The purpose of the hill-descent tests was to determine the heating characteristics of the brake system as a function of weight, grade percent and length, and speed. While maintaining constant speed using modulated brake pressure, the test vehicle was driven down a grade. To define the heating properties of the brake system, the test was conducted on different downgrades. The engine brake was set to different configurations to mimic a reduction in weight to speed up the test process. To provide additional data for the analysis, hill descent tests were also conducted using software simulation.

A validation test was carried out to check the robustness of the updated model by driving over a series of downgrades and upgrades. Inclusion of downgrades and upgrades in the validation test was done deliberately to test the model performance in accurately predicting the brake system temperatures on heating and cooling sections. The validation test produced satisfactory results and suggested that the predicted temperatures were close to field temperature values.

Updated GSRS Model and Implementation

The updated temperature model parameters form the updated GSRS model. This updated model takes into account the current truck design and brake characteristics. The GSRS model assumes a constant speed of descent, and engine rpm maintained near the allowable maximum for the

engine (i.e. the appropriate gear is used). The model will be used to estimate maximum safe descent speeds for truck weights and grade characteristics. Implementation of the updated GSRS model will be accomplished through the use of WSS signs. The maximum safe descent speeds will be displayed as advisory signs for different truck weight categories. The updated GSRS model can also be used to generate accurate brake temperature profiles for downgrades to determine truck escape ramp locations.

Some main changes to the GSRS model and its implementation were proposed by Bowman and Coleman, 1989; Johnson et al., 1982a. Maximum descent speeds calculated should include an emergency stopping criteria. This modification of the Myers et al. GSRS model accounts for the additional heating which would occur during a stop at the end of the downgrade. (Johnson et al., 1982a). Another modification proposed was multiplying the diffusivity constant, K_1 , by a factor of 1.5 to account for nonlinear temperature gradients in the brakes during rapid deceleration. (Johnson et al., 1982a; Ruhl et al., 2006). With regards to the development of WSS signs, it was suggested that a temperature of 530°F may be considered as a limiting temperature in situations where succeeding weight categories produce similar descent speeds when a temperature of 500°F is used for the analysis. (Bowman, 1989). Bowman, 1989, suggested that for upgrades or non-braking sections, 0 percent grades should be used in the model. This was tested in the validation of the updated GSRS model and produced satisfactory results.

WSS signs were developed from two case studies using the updated and old GSRS models for comparison. The comparison showed that the updated model results in higher speeds compared to the old GSRS for the same weight categories. However, the speed differences were not extreme and should improve safety on downgrades, while retaining driver confidence and compliance.

For ease of implementation of the model, a software application will be developed. The initial brake temperature to be specified will be a default value of 150°F. Values below 90°F should not be input for the initial temperatures. The software will be an invaluable help in easily recommending safe speeds on multi-grade as manual speed determination on such sections could be cumbersome.

The previous GSRS model was used in downhill truck warning systems, such as those in Colorado, British Columbia and Oregon. The systems operated by weighing and classifying trucks as they approached long downhills. Safe descent speeds were then calculated and displayed for the trucks based on their weight and classification. The updated model can be used to upgrade the algorithm predicting descent speeds on these downhill warning systems to improve truck safety.

RECOMMENDATIONS

The findings of this study will be used to address the incidence of truck crashes on downgrades by providing maximum safe descent speeds on downgrades. The following are recommendations based on the analysis and conclusions drawn from the study. They are:

- Drivers should be educated on the use of the GSRS and WSS signs. The education should focus on mountain driving, and the need to modify driving behavior to adhere to advisory speeds recommended by WSS and other signs to promote safety on mountain passes. This education is even more important for inexperienced drivers new to driving on

mountainous highways, and drivers unfamiliar with the terrain. The use of WSS signs have been shown to promote safety and marks an improvement over other warning methods. WSS signs provide drivers with safe descent speeds instead of just giving them information requiring further evaluation.

- The trucking industry should be encouraged to adopt and install disc brakes, especially for fleets that frequently travel over mountain passes. Disc brakes are much more resistant to brake fade, and their adoption will reduce the incidence of runaway truck crashes on mountain passes. Also, truck fleets should install retarders to augment and reduce the braking burden on the service brakes. The use of retarders are known to reduce maintenance and prolong the life of service brakes.
- Brake systems have to be regularly checked and maintained. Previous studies have found that brake imbalance is a significant contributor to brake fade and truck runaway crashes. Reducing of brake imbalance among the truck fleet will go a long way to reduce the incidence of truck crashes on mountain passes. It is recommended that WYDOT intensifies inspection of brakes for maintenance and balance issues.
- An important modification to the GSRS model relates to its application on non-braking sections. Grade values on upgrades and other non-braking sections should be set to zero. This will account for the cooling which occurs on non-braking sections.
- A User's Manual has been written as a guide for the implementation of the GSRS and the use of WSS signs as part of the study. The manual underscores important steps to be taken in identifying hazardous downgrades, estimating downgrade percent and truck braking length, and installation of WSS signs. The guidelines in the manual form an important piece in the implementation of the GSRS. Much of the information from the manual relies on an earlier report on a GSRS user's manual. (Bowman, 1989).
- The GSRS was developed primarily for trucks not fitted with retarders or other auxiliary brakes. Analysis of different weights and downgrades for the representative truck used for the field tests indicates that it is possible to travel at the speed limits on downgrades, without the brakes heating beyond the limiting temperature of 500°F when the retarder is engaged. This study recommends that trucks fitted with retarders choose descent speeds corresponding to the lowest weight interval (highest speed) on the WSS sign.
- It is important for safety evaluation studies to be undertaken after implementation of the GSRS and WSS signs. Before-after study effects at high severity sites should be tested. Safety evaluation may also be accomplished by measuring the mean speeds of trucks at locations with grades of high severity before and after installation of WSS signs. The proportion of trucks with smoking brakes may also be evaluated after installation of WSS signs in comparison to when the signs were not installed.

FUTURE STUDIES

The test truck used to update the GSRS model had disc brakes on its steer axle. However the general truck population in the United States is mostly fitted with drum brakes on all axles, including steer axles. It is therefore important to assess the impact, if any, that the steer disc brakes will have on the estimation of accurate brake temperatures at the bottom of downgrades for trucks fitted with only drum brakes. If significant differences are found between predicted temperatures of the updated temperature models, and field brake temperatures from trucks with only drum brakes, the brake temperature model can be calibrated to reflect these changes.

The tests will involve measuring brake temperatures of several random volunteer trucks as they descend different downgrades. Drivers parked in brake inspection areas before downgrades will be asked if they would be willing to stop at the bottom of the downgrade to have their brake temperatures measured. No recommendations of descent speed or the use of retarders will be made, and the drivers will be encouraged to drive as they normally would. Drivers will be assured of their anonymity with only pertinent truck information, such as weight and number of axles being recorded. Brake temperatures before descent will be measured using hand-held sensors at the top of the downgrade. The truck will then be followed with its descent speed being recorded and verifying any speed changes. At the bottom of the downgrade, the brake temperatures will be measured again. This will be done until a sufficient sample size for the analysis is obtained.

Alternatively, a single truck fitted with only drum brakes can be used for the correlation tests. The test truck will be loaded to different weights and driven over different downgrades. Brake temperatures will be measured at the top of the downgrade before descent and again at the bottom of the grade. Changes in the truck weight may be simulated by engaging the retarder of the truck. This alternative may provide better flexibility and will serve as additional validation tests for the updated GSRS model.

If the correlation between the predicted brake temperatures from the updated model and brake temperatures from the field tests are high, this will be an indication that the updated GSRS model will predict accurate temperatures for trucks fitted with only drum brakes. For a low correlation, the updated GSRS model will be calibrated to reflect the brake characteristics of the general truck population.

Additionally, a software will be developed for ease of implementation of the GSRS and WSS signs. The software will allow engineers to easily formulate WSS signs and predict brake temperatures without a comprehensive understanding of the brake temperature model. The software will be simplified so that only basic inputs such as grade percent, braking length, initial brake temperature and ambient temperature will be required.

REFERENCES

- AASHTO, 2011. A Policy on Geometric Design of Highways and Streets, 6th Editions. Washington D.C.
- Abdelwahab, W., Morral, J.F., 1997. Determining Need for and Location of Truck Escape Ramps. *J. Transp. Eng.* 123, 350–356.
- American Truckers Associations, 2016. ATA Releases 2016 Edition of American Trucking Trends [WWW Document]. *Truck Trends*. URL <http://www.trucking.org/article/ATA-Releases-2016-Edition-of-American-Trucking-Trends> (accessed 8.17.16).
- Bendix Spicer Foundation Brake LLC, 2013. the Federal Reduced Stopping Distance Mandate: Impact and Solutions Updated August 2013. Elyria, Ohio.
- Bendix Spicer Foundation Brake LLC, 2011. The Compelling Case for Air Disc Brakes in Heavy Duty Braking: A White Paper. Elyria, Ohio.
- Bennett, C.R., 1988. The New Zealand Vehicle Operating Costs Model-Report to the National Roads Board. Wellington, New Zealand.
- Berg, T., 2014. Brake Trends: Drum vs Discs [WWW Document]. *Saf. Compliance*. URL <https://www.truckinginfo.com/155132/brake-trends-drums-vs-discs>
- Bester, C., 1981. Fuel Consumption of Highway Traffic. University of Pretoria.
- Biggs, D.C., 1988. Estimating Fuel Consumption of Light to Heavy Vehicles.
- Bowman, B.L., 1989. Grade Severity Rating System (GSRS) : Users Manual. Virginia.
- Bowman, B.L., Coleman, J.A., 1989. Impact of Fuel Conservation Measures on Safe Truck Downgrade Speeds. *J. Transp. Eng.* 115, 351–369.
- Burr, R., 2015. Fatal Crash West of Dayton [WWW Document]. URL <http://www.bighornmountainradio.com/pages/22298157.php?>
- Carr, J., 2015. Top 5 Heavy Duty Truck Manufacturers on the Market in 2015 [WWW Document]. *Equip. Watch*.
- Cummins, D.D., 1966. The Jacobs Engine Brake Application and Performance. *Soc. Automot. Eng.* 1–7. doi:doi:10.4271/660740
- Day, A.J., 1988. An Analysis of Speed , Temperature , and Performance Characteristics of Automotive Drum Brakes. *J. Tribol.* 110, 298–303.
- Eady, P., Chong, L., Gelston, P., 2015. Advanced Systems for Managing Heavy Vehicle Speed on Steep Descents. Sydney, Australia.
- EPA, 2011. Final Rulemaking to Establish the Greenhouse Gas Emission Standards and Fuel Efficiency Standards for Medium- and Heavy-Duty Engines and Vehicles: Regulatory Impact Analysis. Washington D.C.
- Fancher, P.S., Day, J., Bunch, H., 1981. Retarders for Heavy Vehicles: Evaluation of Performance Characteristics and In-Service Costs. Washington D.C.

Federal Motor Carrier Safety Administration, 2016. Large Truck and Bus Crash Facts 2014.

Federal Motor Carrier Safety Administration, 2014. Commercial Motor Vehicle Facts-March 2013 [WWW Document]. URL <https://www.fmcsa.dot.gov/safety/data-and-statistics/commercial-motor-vehicle-facts---march-2013> (accessed 5.23.18).

FHWA, 2015. Compilation of Existing State Truck Size and Weight Laws: Report to Congress. Washington D.C.

FHWA, 2009. Manual on Uniform Traffic Control Devices for Streets and Highways.

Fisher, P.D., 1961. The Why and How of Combination Vehicle Braking. Soc. Automot. Eng.

For Construction Pros, 2012. New Stopping Requirements Lead to the Development of More Capable Brakes [WWW Document]. Enhanc. Brakes Pull all Stops. URL <https://www.forconstructionpros.com/equipment/fleet-maintenance/other-components/article/10620394/tractor-brakes-enhance-safety>

Glennon, J., 2018. Crash Forensics.com [WWW Document]. URL <http://www.crashforensics.com/> (accessed 5.14.18).

Glennon, J., 1998. Runaway Truck Crashes [WWW Document]. Crash Forensics. URL <http://www.crashforensics.com/mountaingradecrashes.cfm>

Glennon, J.C., 2018. Crash Forensics.com [WWW Document]. Brake Fail. Anal. URL <http://www.crashforensics.com/brakefailure.cfm>

Goodyear Commercial Tire Systems, 2008. Factors Affecting Truck Fuel Economy.

Google, 2018. Google Earth.

Hanscom, F.R., 1985. Field Tests of the Grade Severity Rating System. Washington D.C.

Hykes, P.G., 1963. Truck Downhill Control Prediction Procedure. Soc. Automot. Eng. 630A.

Jacobs Vehicle Systems, 2010. Jacobs Engine Brake (Intebrake) for the Cummins ISX 15L Engine. Bloomfield, Cincinnati.

James, C.J., 2012. Analysis of Parasitic Losses in Heavy Duty Diesel Engines. Massachusetts Institute of Technology.

Janson, B.N., 1999. Evaluation of Downhill Truck Speed Warning System on I-70 West of Eisenhower Tunnel. Denver.

Johnson, W.A., DiMarco, R.J., Allen, R.W., 1982a. The Development and Evaluation of a Prototype Grade Severity Rating System. Washington D.C.

Johnson, W.A., Myers, T.T., DiMarco, R.J., Allen, W.R., 1982b. A Downhill Grade Severity Rating System. Soc. Automot. Eng. 811263.

Kenworth.com, 2018. Kenworth the World's Best [WWW Document]. Trucks. URL <https://www.kenworth.com/trucks/>

Larson, L.L., 1987. A Review of Truck Escape Ramps. Phoenix, Arizona.

- Lill, R.A., 1977. Review of BMCS Analysis and Summary of Accident Investigations, 1973-1976 With Respect to Downgrade Runaway Type Accidents.
- Lill, R.A., 1975. Development of Grade Severity Rating System.
- Limpert, R., 2011. Brake Design and Safety, Third. ed. SAE International.
- Limpert, R., 1975. Cooling Analysis of Disc Brake Rotors. SAE Int.
- Limpert, R., Andrews, D., 1987. Analysis of Truck Braking Accidents. Soc. Automot. Eng.
- Marathon Brake Systems, 2013. Brake Temperatures [WWW Document]. Know Your Brake Temp.
- Marsh, A., 2016. A Tipping Point for Disc Brakes in North American Trucking? [WWW Document]. Fleet Own. URL <http://www.fleetowner.com/equipment/tipping-point-disc-brakes-north-american-trucking>
- McAuliffe, B., Chuang, D., 2017. Coast-down and Constant-speed Testing of a Tractor-trailer Combination in Support of Regulatory Developments for Greenhouse Gas Emissions.
- Mechanical Simulation Corp., 2018. TruckSim Mechanical Simulation.
- Morgan, J., 2015. Investing in Aerodynamics to Improve Fuel Efficiency [WWW Document]. Fleet Equip. URL <http://www.fleetequipmentmag.com/truck-trailer-aerodynamics-fuel-efficiency/>
- Murphy, R., Limpert, R., Segel, L., 1971. Bus, Truck, Tractor/Trailer Braking Performance. Ann Arbor, Michigan.
- Myers, T.T., Irving, L.A., Walter, A.J., 1981. Feasibility of Grade Severity Rating System. Washington, DC.
- National Highway Traffic Safety Administration, 2009. Federal Motor Vehicle Standards; Air Brake Systems. Washington D.C.
- National Highway Traffic Safety Administration, 1991. Commercial Motor Vehicle Speed Control Devices. Washington D.C.
- National Research Council, 2010. Technologies and Approaches to Reducing the Fuel Consumption of Medium- and Heavy-Duty Vehicles. Washington D.C. doi:10.17226/12845
- Original Code Consulting, 2017. MICAS-X.
- Pandey, S.N., Khaliq, A., Zaka, Z., Saleem, M.S., 2015. Retarders Used As Braking System in Heavy Vehicles-A Review. Int. J. Mech. Eng. Robot. Res. 4, 1–5.
- Performance Review Institute, 2018. Performance Review Institute [WWW Document]. Brake Lining Qualif. Progr. URL <https://p-r-i.org/other-programs/automotive-qpl/brake-lining/>
- Roberts, J., 2014. The Bendix Guide to Air Disc Brake Friction Replacement [WWW Document]. Commer. Carr. J. URL <https://www.ccjdigital.com/the-bendix-guide-to-air-disc-brake-friction-replacement/>

- Robinson, M., McGowen, P., Habets, A., 2002. Safety Applications of ITS in Rural Areas. Washington D.C.
- Ruhl, R.L., Inendino, L.V., Southcombe, E.J., Ruhl, R.A., 2006. Usable Models for Free and Forced Cooling of Commercial Vehicle Drum Brakes. SAE Int. 14.
- SAE Recommended Practice J1263, 2010. Road Load Measurement and Dynamometer Simulation Using Coastdown Techniques.
- SAE Recommended Practice J2263, 2008. Road Load Measurement Using Onboard Anemometry and Coastdown Techniques.
- Sean, B., 2017. Medium/Heavy Duty Truck Engines, Fuel and Computerized Management Systems, Fifth Edit. ed. Cengage Learning, Boston, MA.
- Singh, S., 2017. The Tesla Truck: Is Elon Musk Pulling Wool Over Our Eyes? [WWW Document]. Autos. URL <https://www.forbes.com/sites/sarwantsingh/2017/11/20/analysts-take-on-tesla-semi-truck-is-elon-musk-pulling-wool-over-our-eyes/#f174b38a4146> (accessed 5.18.18).
- Statista.com, 2018. Class 8 Truck Manufacturers' Share in the U.S. as of December 2017 [WWW Document]. URL <https://www.statista.com/statistics/274937/market-share-of-truck-manufacturers-in-the-united-states/>
- Tetard, C., Roumegoux, J.P., Huet, R., Quincy, R., Vulin, D., 1993. Unsafe Practices of Truck Drivers on Long Grades: The Case of the Expressway in the Mont-Blanc-Le Fayet Tunnel. Int. J. Veh. Des. 1, 63–78.
- The Brake Report, 2016. There's More to Your Friction than a Temperature Rating [WWW Document]. Brake Rep. URL <https://thebrakereport.com/theres-friction-temperature-rating/>
- Trevorrow, N., Eady, P., 2010. Heavy Vehicle Brake Safety on Long and Very Steep Roads: Final Report. Sydney, Australia.
- Truckinginfo.com, 2018. PepsiCo Installs Stemco Products to Improve Fuel Efficiency of 1,600 Trailers [WWW Document]. Fuel Smarts. URL <https://www.truckinginfo.com/301057/pepsico-installs-stemco-products-to-improve-fuel-efficiency-of-1-600-trailers>
- Tuegel, R., 1968. Truck and Bus Brake System Performance Requirements.
- U.S.Department of Transportation, 2015. US Bureau of Transportation Statistics [WWW Document]. Freight Facts 2015. URL http://www.rita.dot.gov/bts/sites/rita.dot.gov/bts/files/data_and_statistics/by_subject/freight/freight_facts_2015/chapter5 (accessed 9.1.16).
- VanOstrand, M., 2014. Rush of Truck Rollovers Prompts WYDOT to Take Action [WWW Document]. URL <http://www.kotatv.com/news/wyoming-news/rash-of-truck-rollovers-prompts-wydot-to-take-action/27846600>
- Watanada, T., Dhareshwar, A.M., Lima, P.R.S., 1987. Vehicle Speeds and Operating Costs. Washington D.C.

- Wilson, M., 2000. FleetOwner [WWW Document]. Engine Retard. URL http://www.fleetowner.com/mag/fleet_engine_retarders (accessed 4.2.18).
- Woodrooffe, J., 2014. Reducing Truck Fuel Use and Emissions:Tires, Aerodynamics, Engine Efficiency, and Size and Weight Regulations. Ann Arbor, Michigan.
- YouTube, 2015. Learning TV for Kids: Drawing Cargo Ship, Van, Utility Truck, Semi-Trailer and Forklift [WWW Document]. URL <https://www.youtube.com/watch?v=eQx57GzC2Rs>
- WYDOT, 2016. WYDOT Quick Facts: Speed Limits. Cheyenne, Wyoming.
- Wyoming Highway Patrol, 2018. Size and Weight Permit Limits [WWW Document].
- Wyoming Highway Patrol, 2014. 80 mph Speed Limit Coming to More than Half of Wyoming's Interstate Mileage [WWW Document]. URL <http://www.whp.dot.state.wy.us/news/80-mph-speed-limit-coming-to-more-than-half-of-wyomings-interstate-mil>
- Yasin, T.P., 1979. The Analytical Basis of Automobile Coastdown Testing. Soc. Automot. Eng. 780334, 1596–1605.

APPENDIX 1: COAST-DOWN PLOTS

Coast-down Test Plots to Determine Drag Forces (Truck Loaded- No Jake Brake)

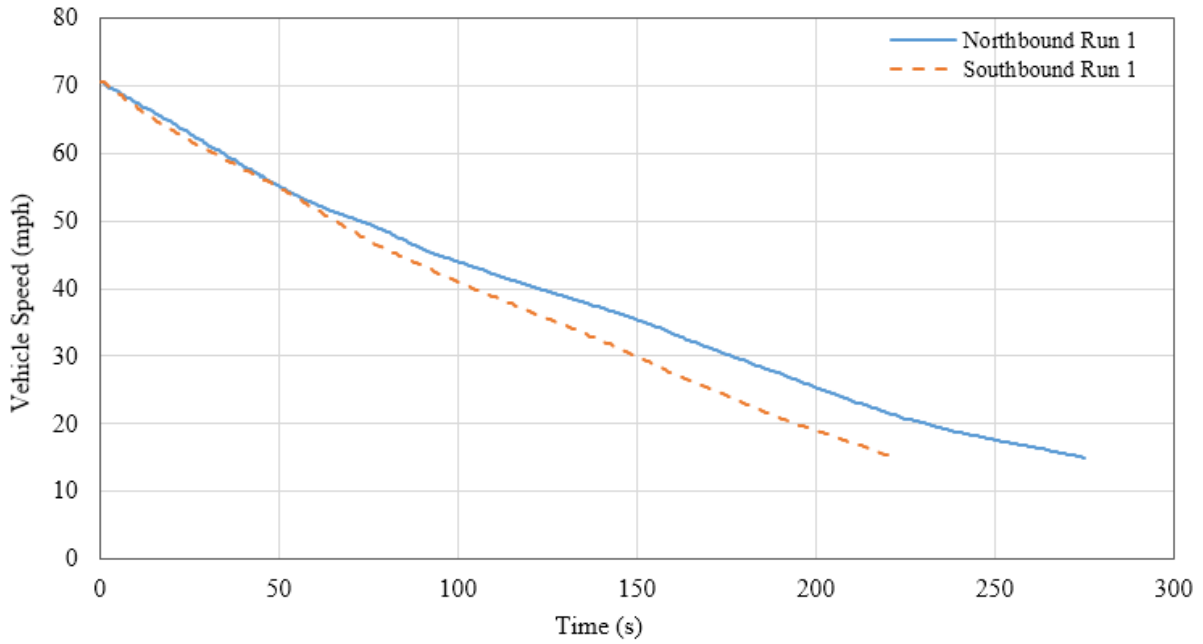


Figure 95. Graph. Velocity-Time Trace to Determine Drag Force Run 1 (Truck Loaded).

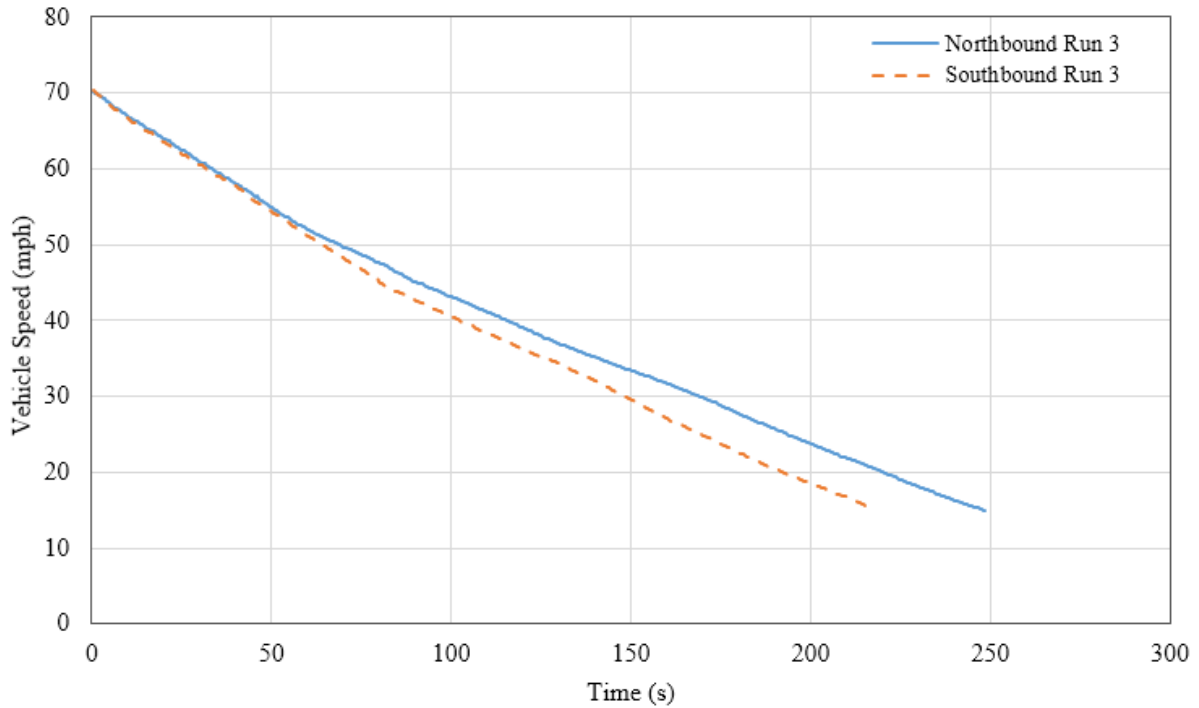


Figure 96. Graph. Velocity-Time Trace to Determine Drag Force Run 3 (Truck Loaded).

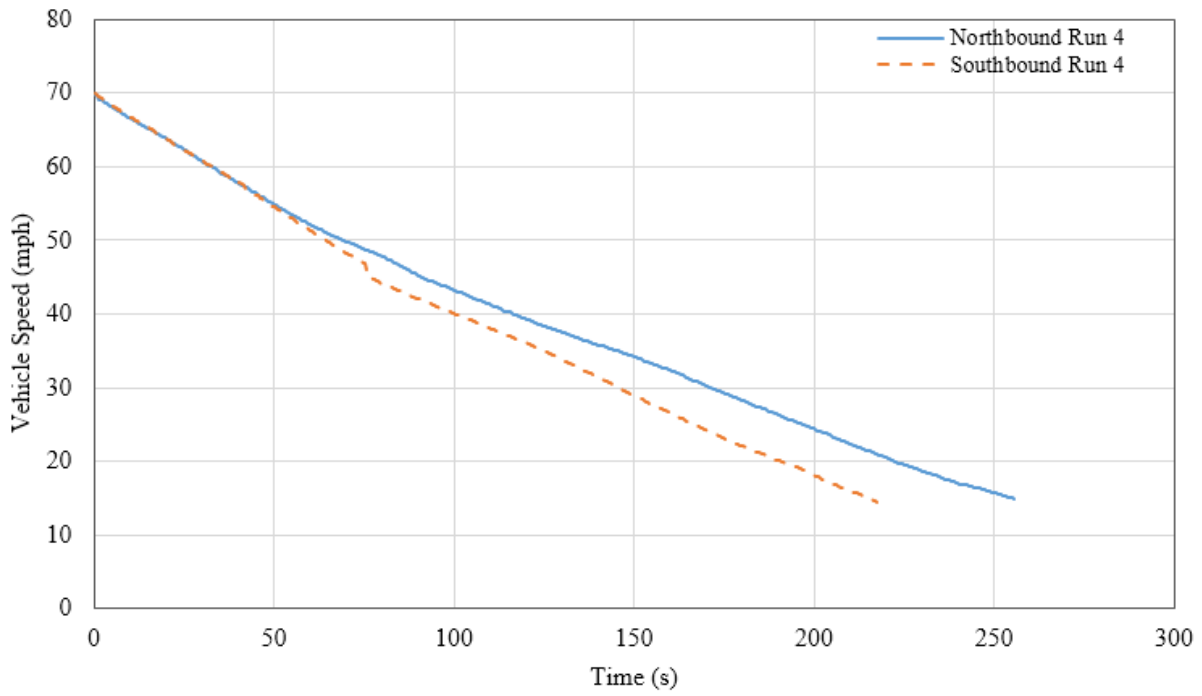


Figure 97. Graph. Velocity-Time Trace to Determine Drag Force Run 4 (Truck Loaded).

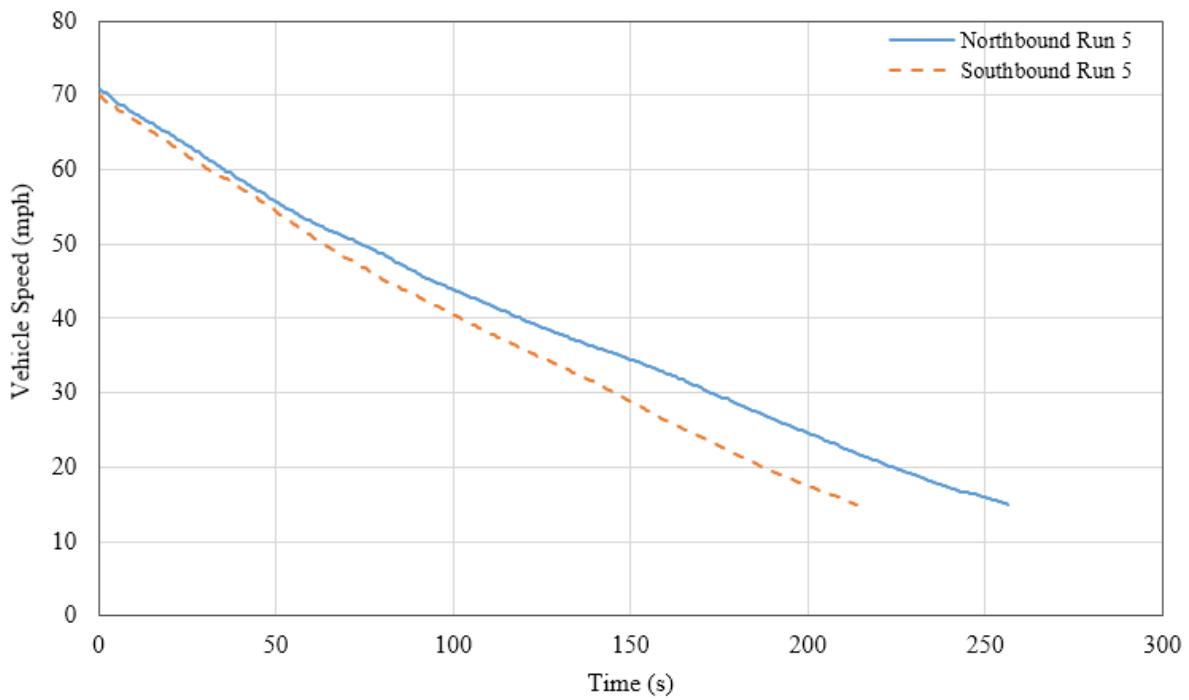


Figure 98. Graph. Velocity-Time Trace to Determine Drag Force Run 5 (Truck Loaded).

Coast-down Test Plots to Determine Drag Force (Truck Unloaded-No Jake Brake)

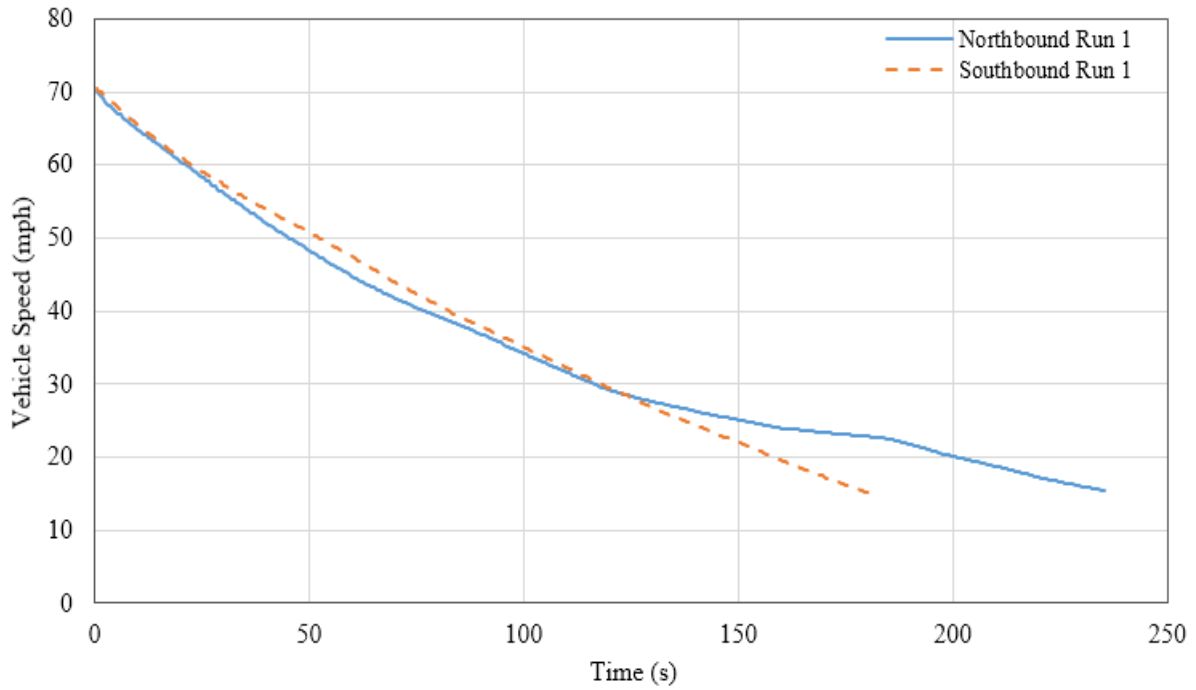


Figure 99. Plot. Velocity-Time Trace to Determine Drag Force Run 1 (Truck Unloaded).

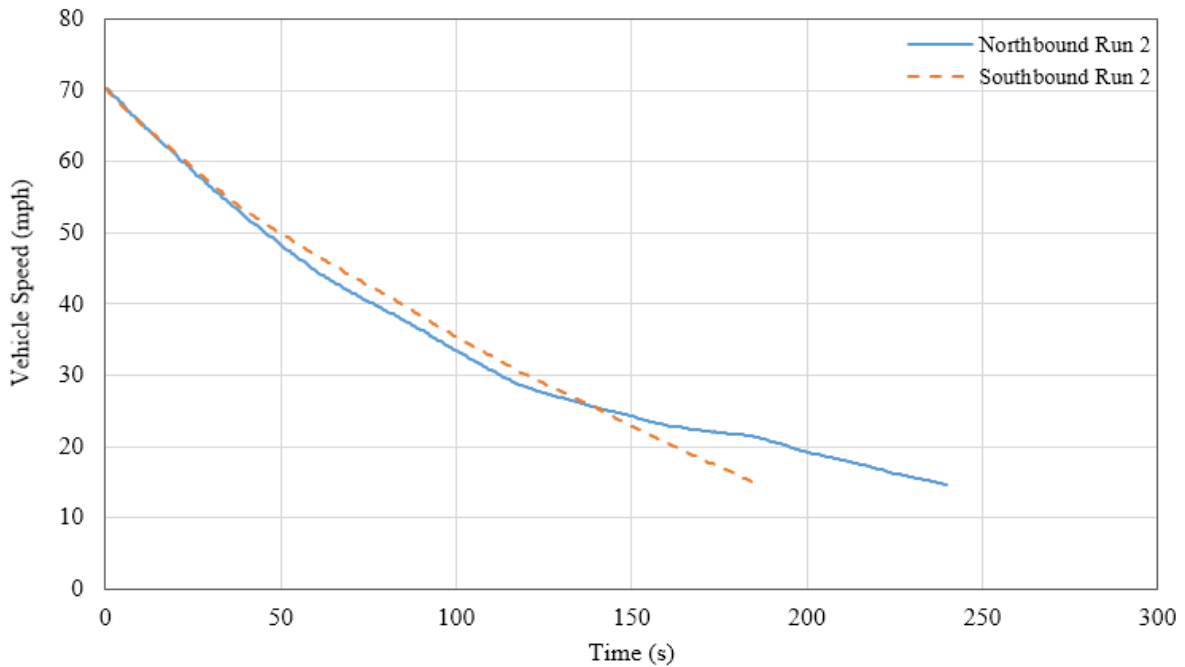


Figure 100. Graph. Velocity-Time Trace to Determine Drag Force Run 2 (Truck Unloaded).

Coast-down Test Plots to Determine Engine Brake Force (Truck Loaded - Full Jake)

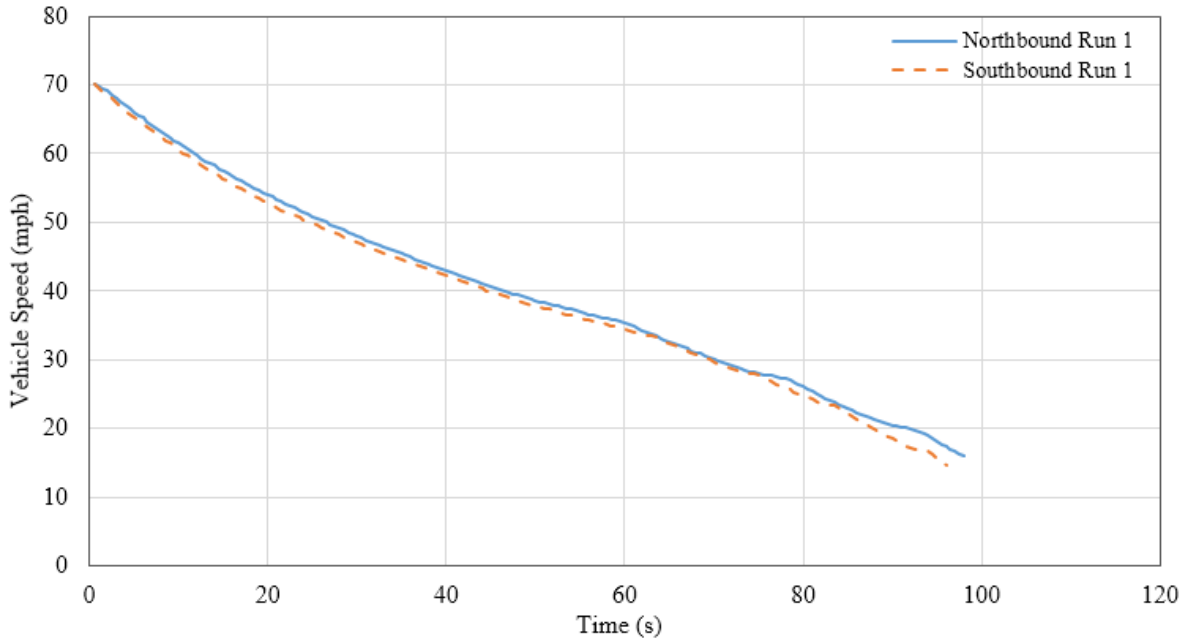


Figure 101. Graph. Velocity-Time Trace to Determine Engine Brake Force Run 1 (Truck Loaded).

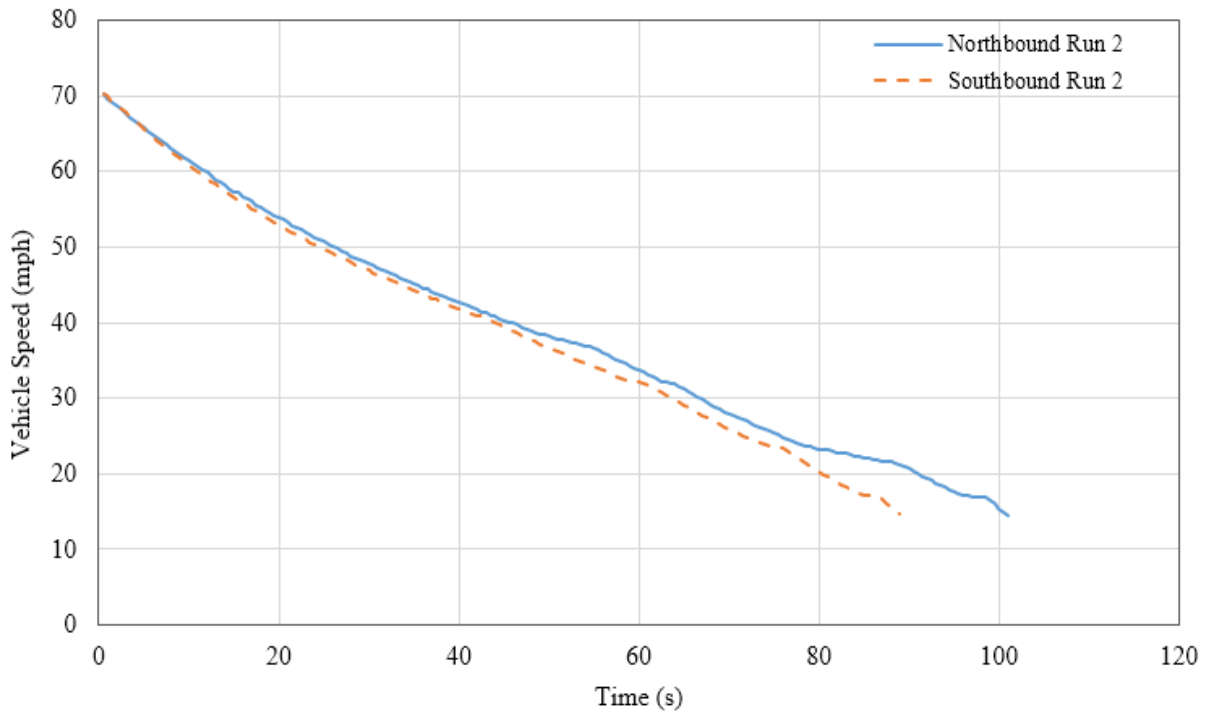


Figure 102. Graph. Velocity-Time Trace to Determine Engine Brake Force Run 2 (Truck Loaded).

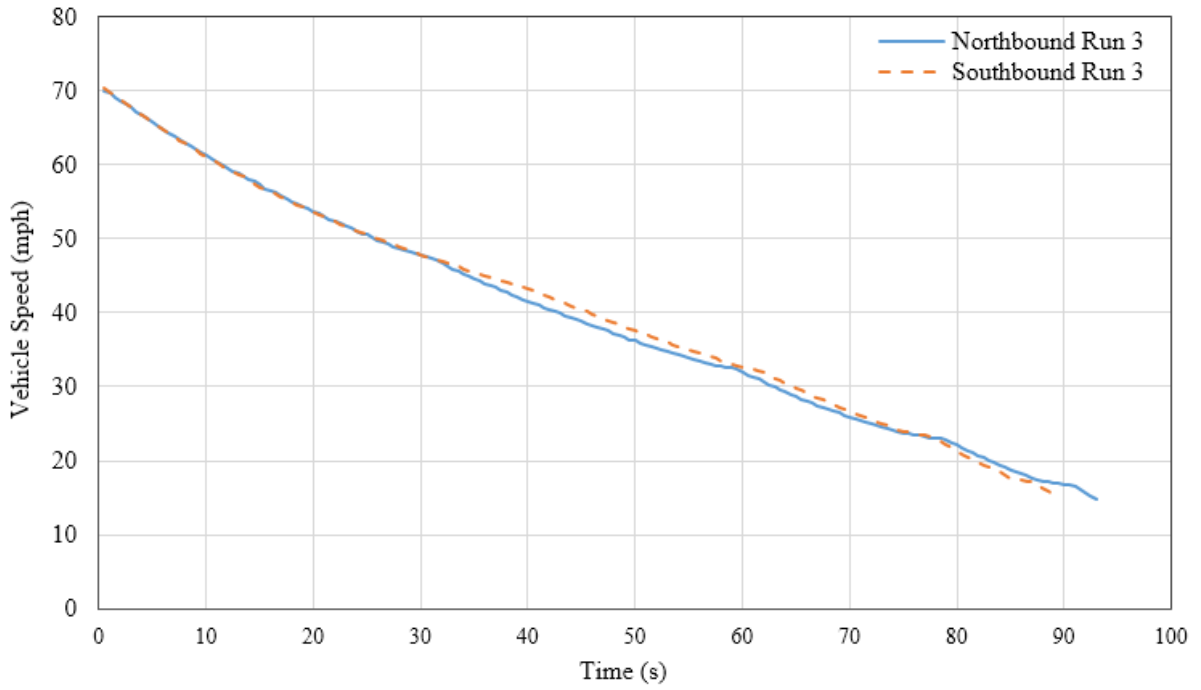


Figure 103. Graph. Velocity-Time Trace to Determine Engine Brake Force Run 3 (Truck Loaded).

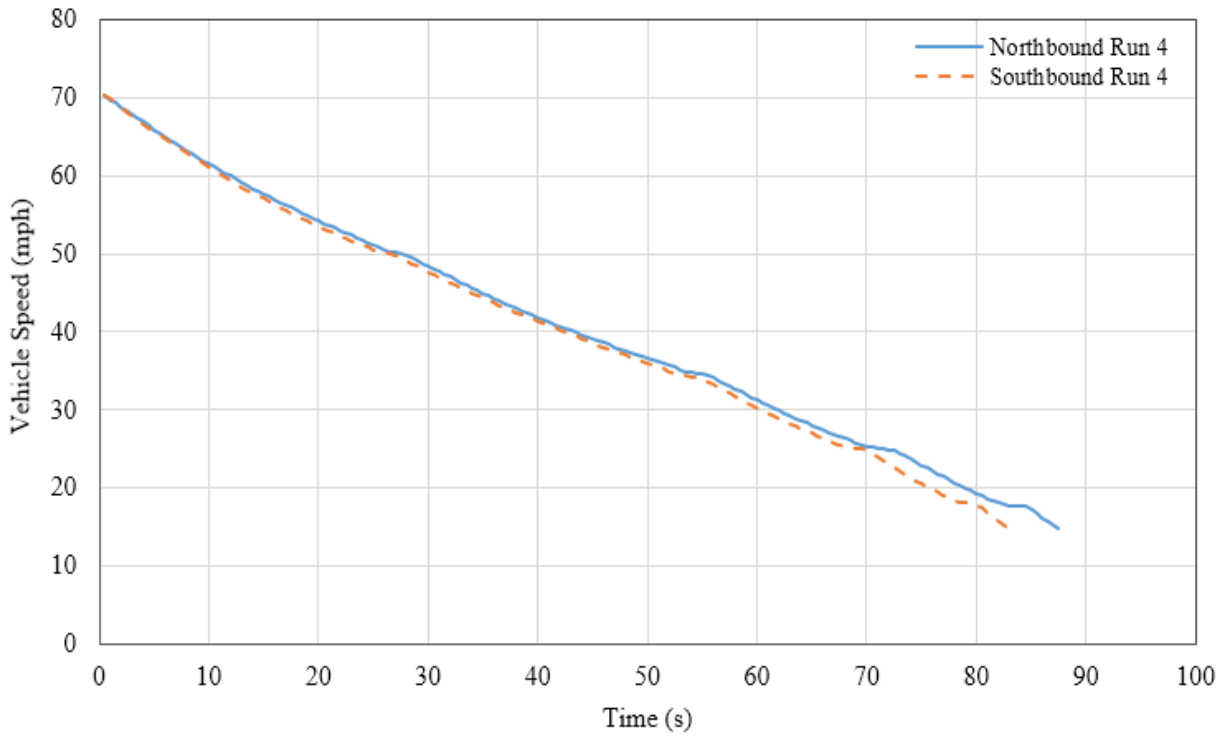


Figure 104. Graph. Velocity-Time Trace to Determine Engine Brake Force Run 4 (Truck Loaded).

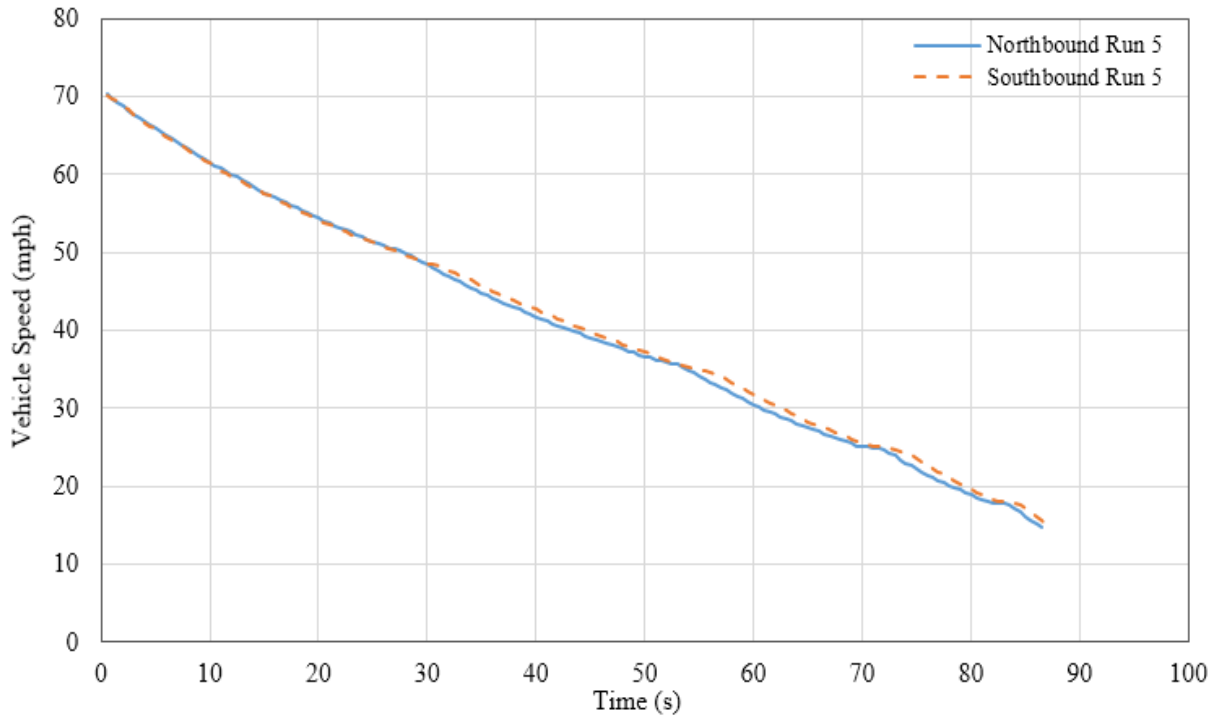


Figure 105. Graph. Velocity-Time Trace to Determine Engine Brake Force Run 5 (Truck Loaded).

Coast-down Test Plots to Determine Engine Brake Force (Truck Loaded – Half Jake)

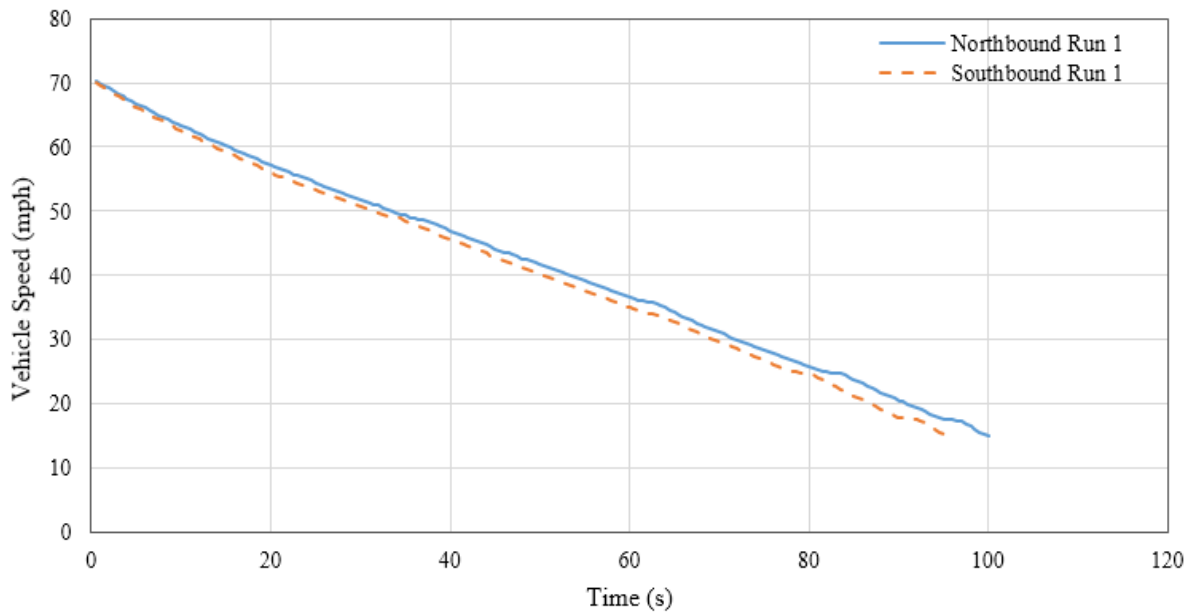


Figure 106. Graph. Velocity-Time Trace to Determine Engine Brake Force Run 1 (Truck Loaded).

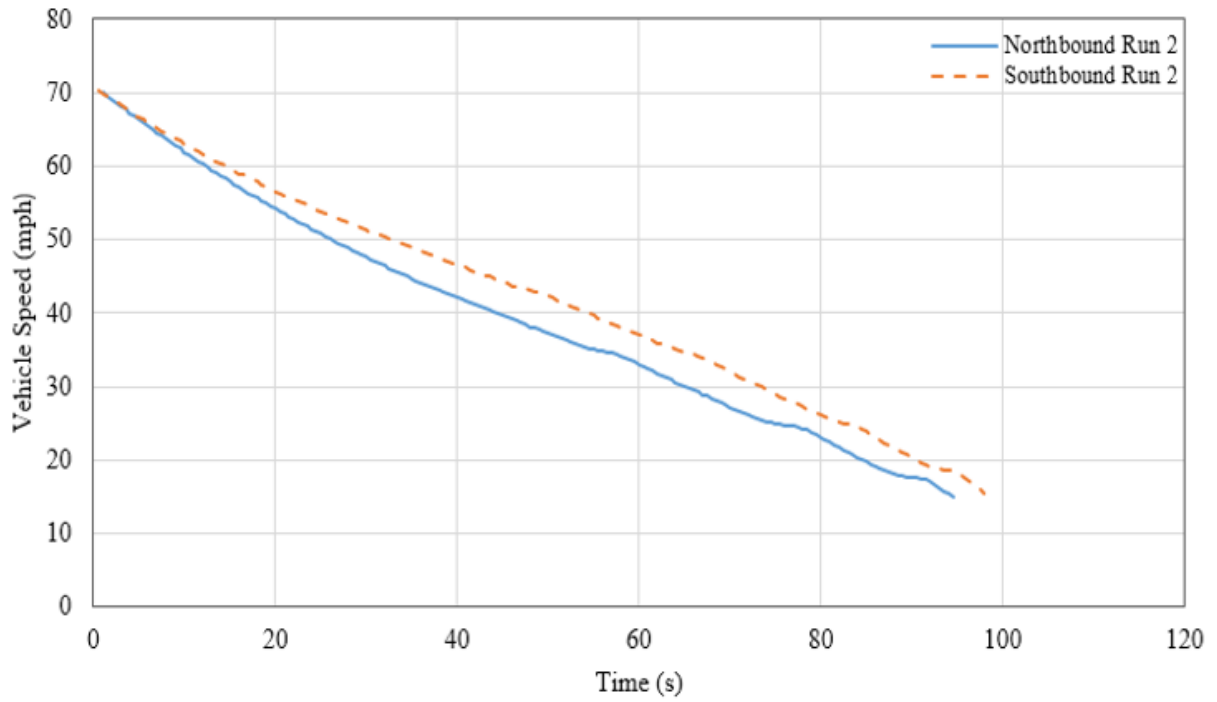


Figure 107. Graph. Velocity-Time Trace to Determine Engine Brake Force Run 2 (Truck Loaded).

APPENDIX 2: COOL-DOWN PLOTS

Extraction of Diffusivity Constant (K_1)

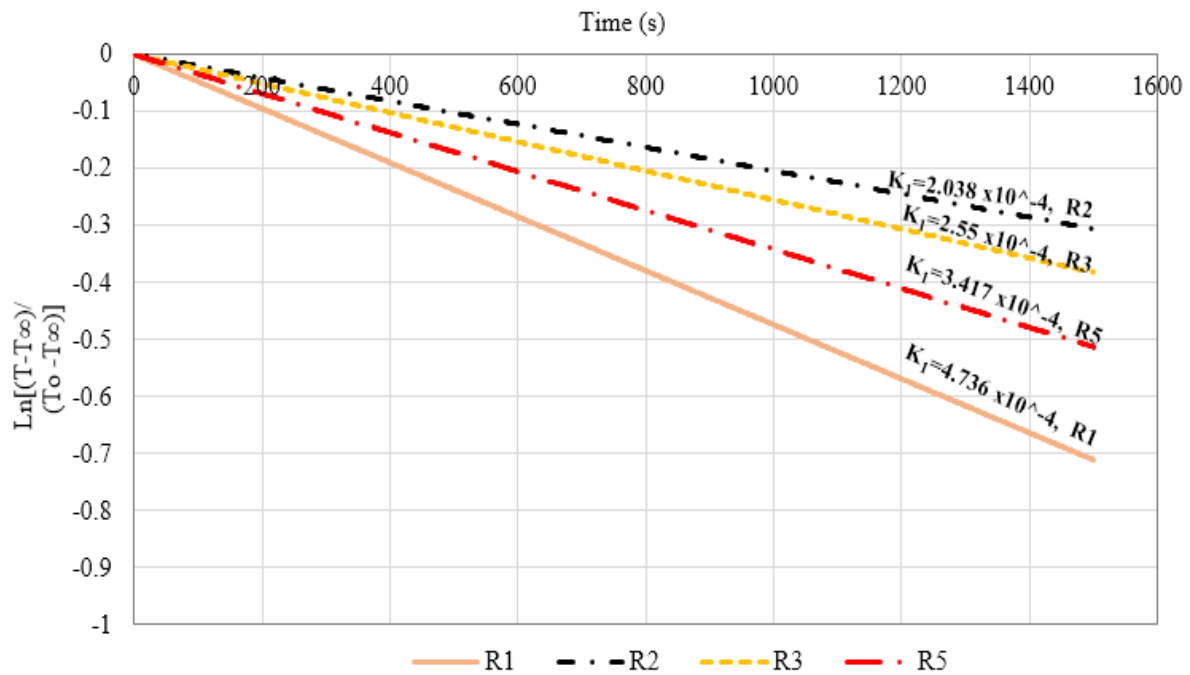


Figure 108. Graph. K_1 Extraction for $V = 0$ mph (Right Brakes).

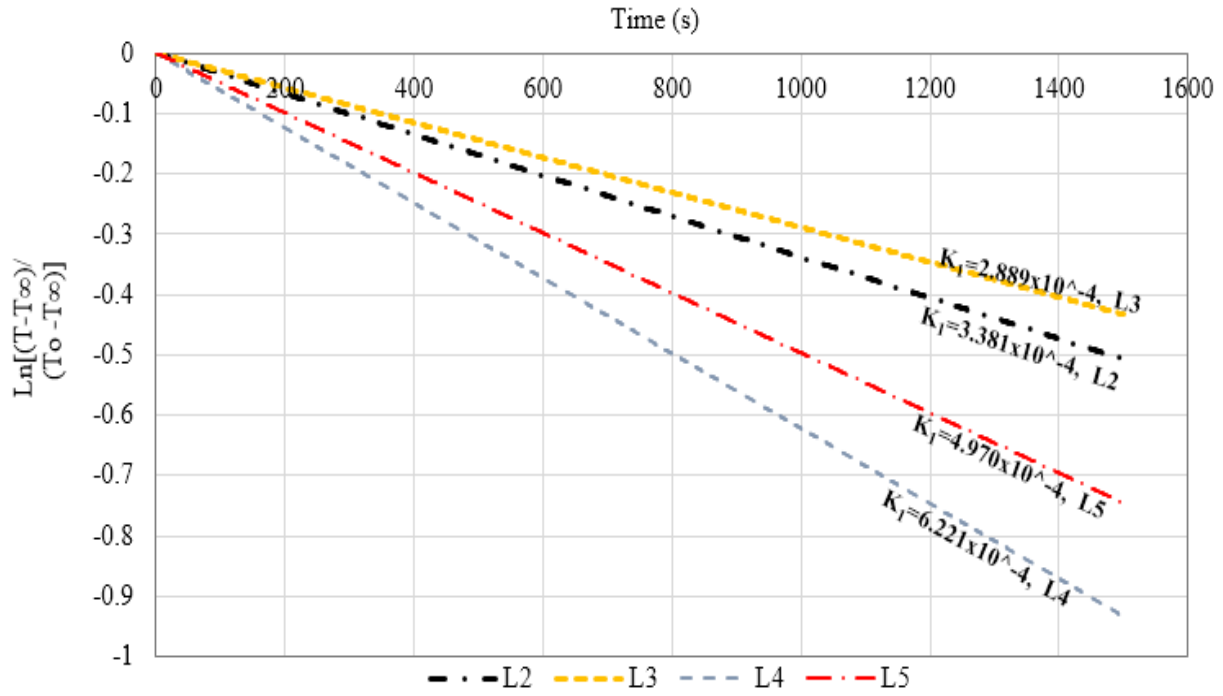


Figure 109. Graph. K_1 Extraction for $V = 20$ mph (Left Brakes).

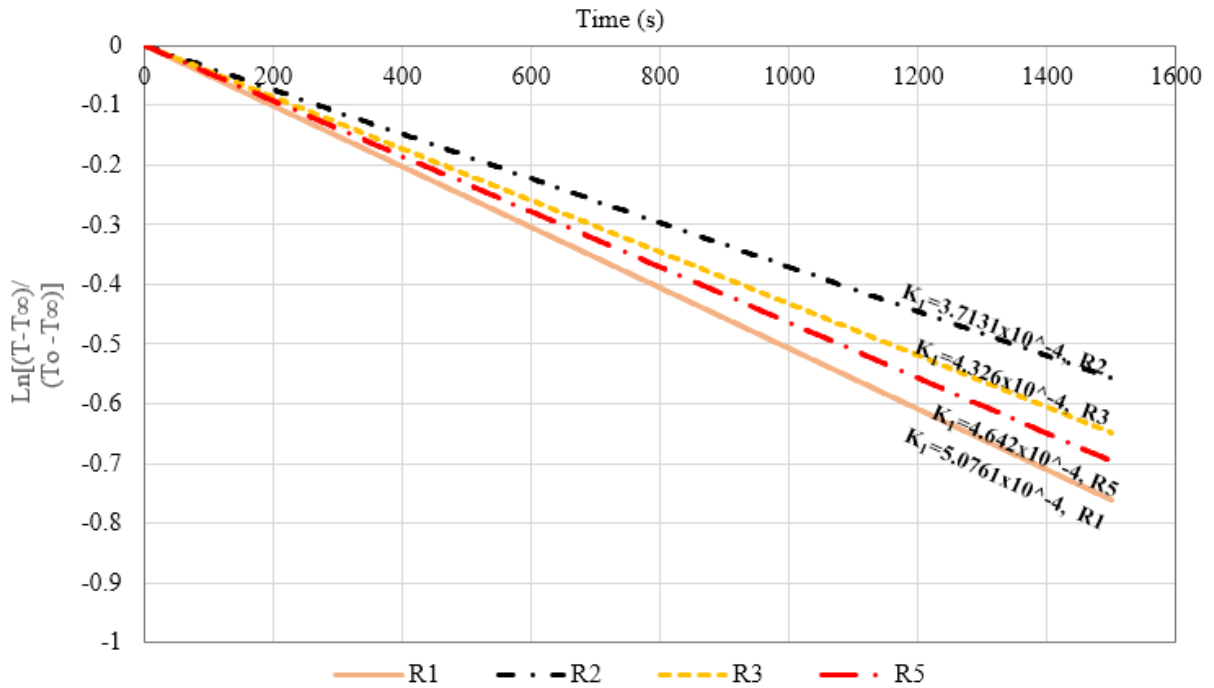


Figure 110. Graph. K_1 Extraction for $V = 20$ mph (Right Brakes).

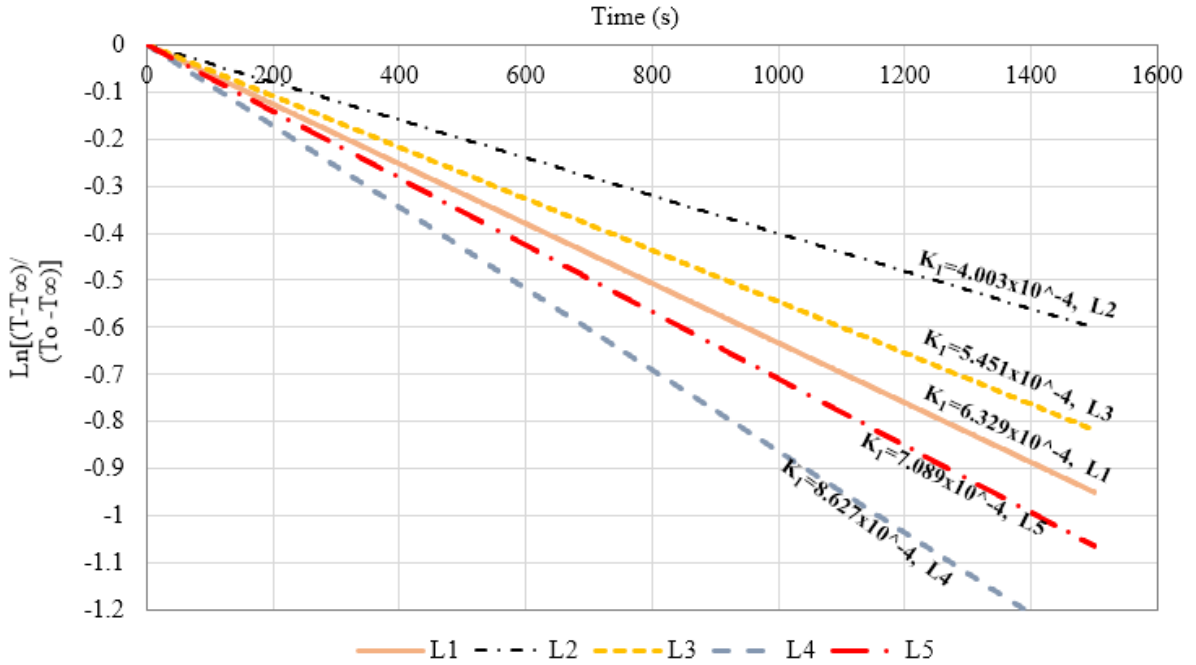


Figure 111. Graph. K_1 Extraction for $V = 30$ mph (Left Brakes).

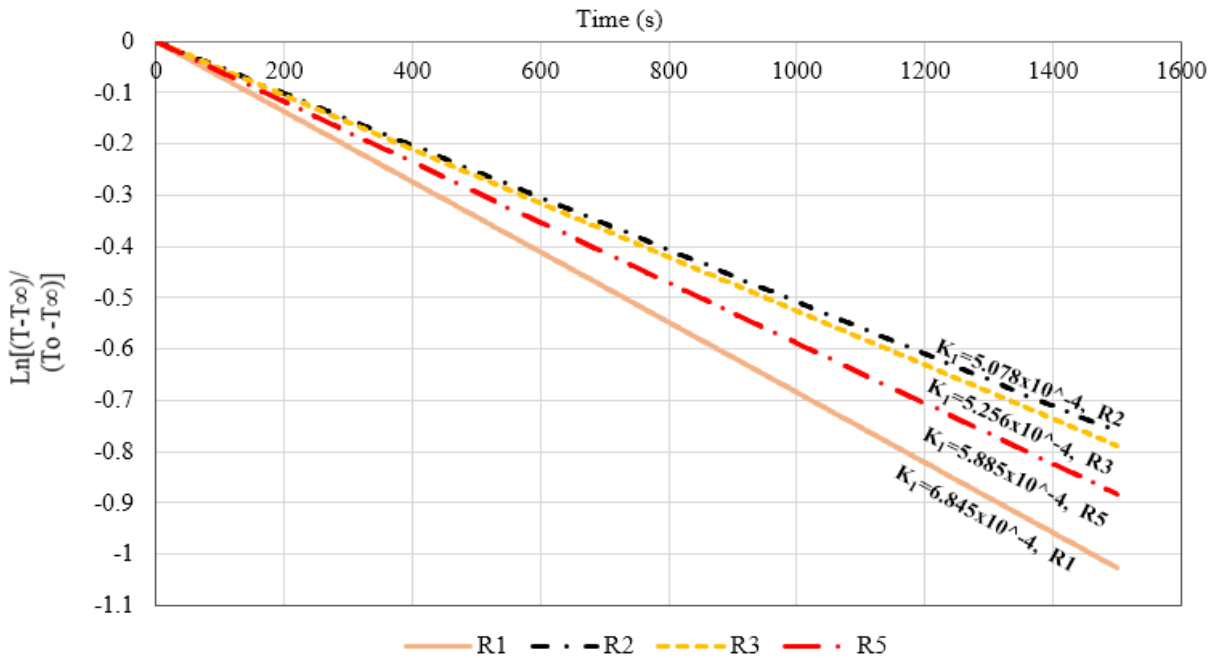


Figure 112. Graph. K_1 Extraction for $V = 30$ mph (Right Brakes).

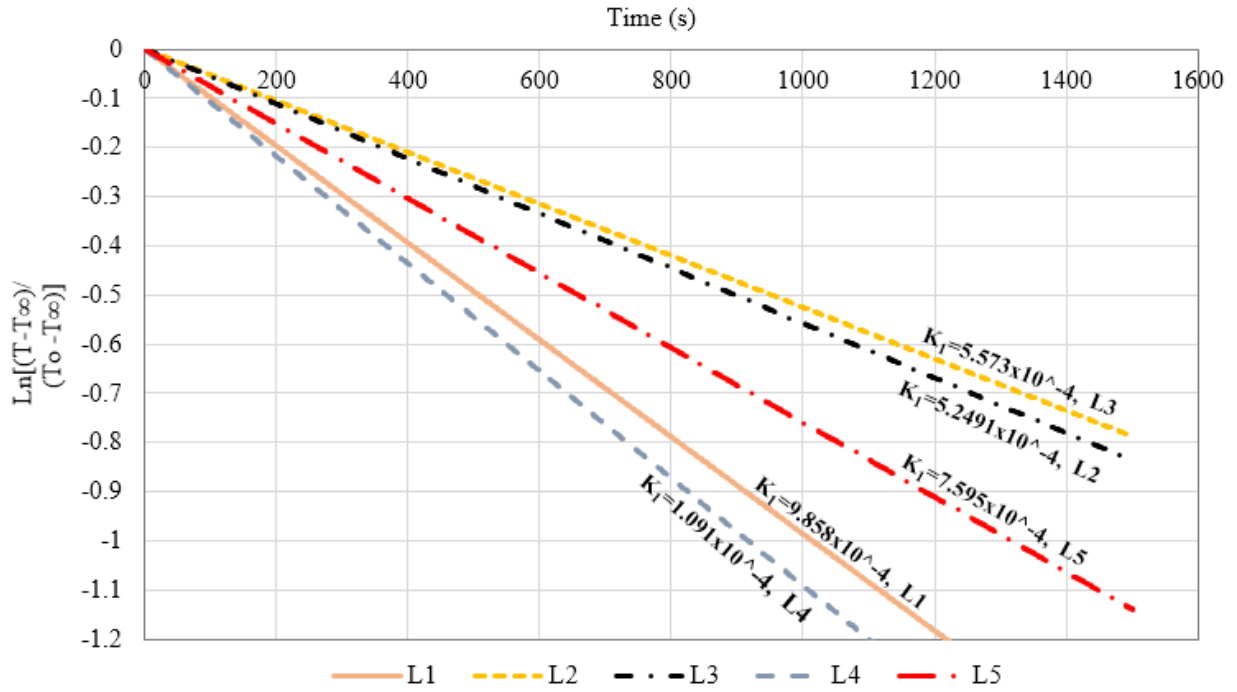


Figure 113. Graph. K_1 Extraction for $V = 45$ mph (Left Brakes).

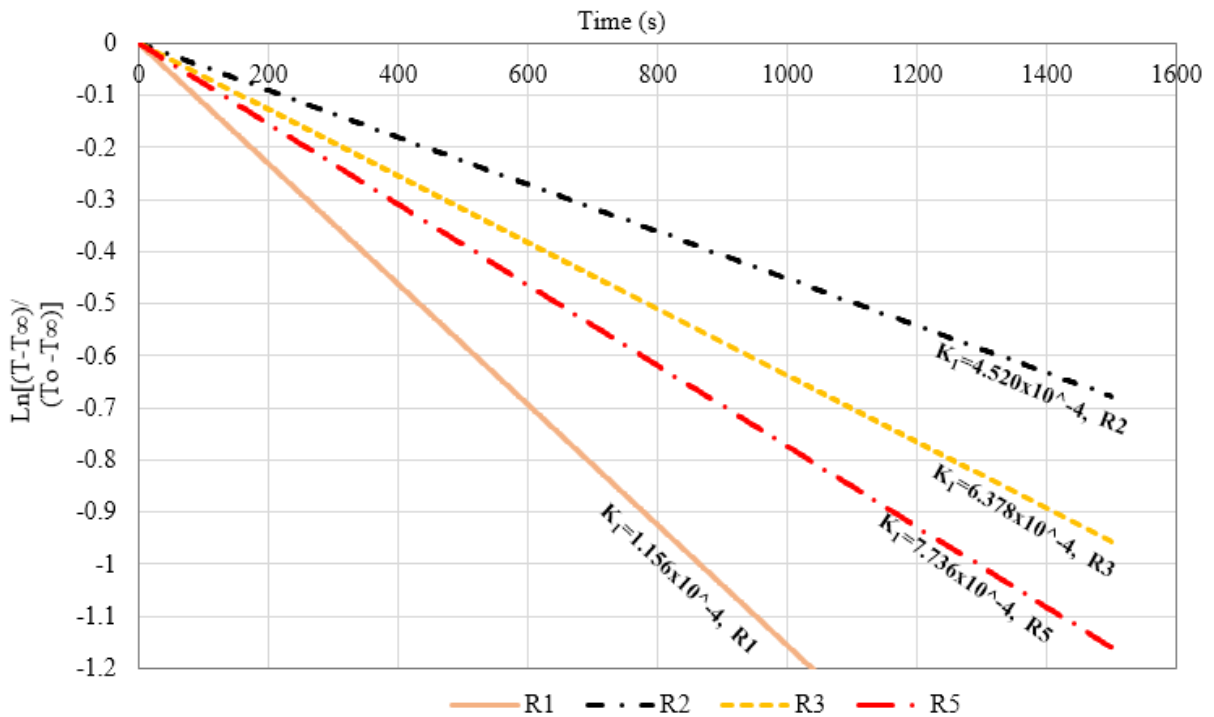


Figure 114. Graph. K_1 Extraction for $V = 45$ mph (Right Brakes).

APPENDIX 3: HILL DESCENT PLOTS

Plots of Power into the Brakes

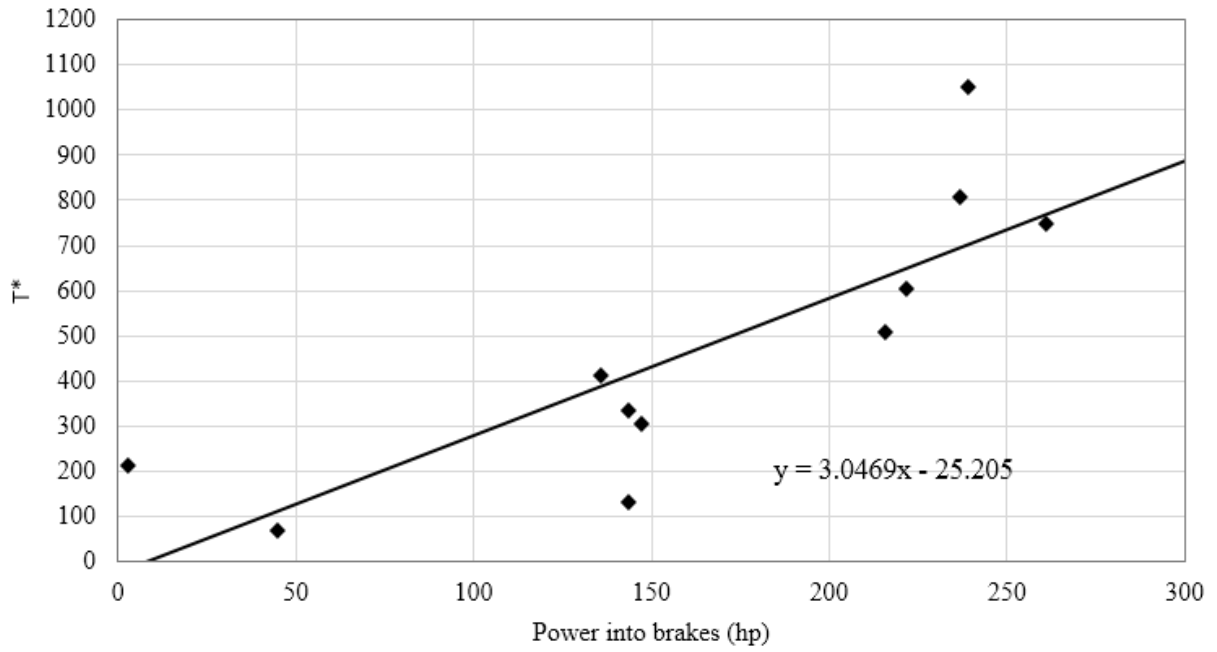


Figure 115. Graph. Plot of Temperature Parameters versus Power into Brakes at 21 mph.

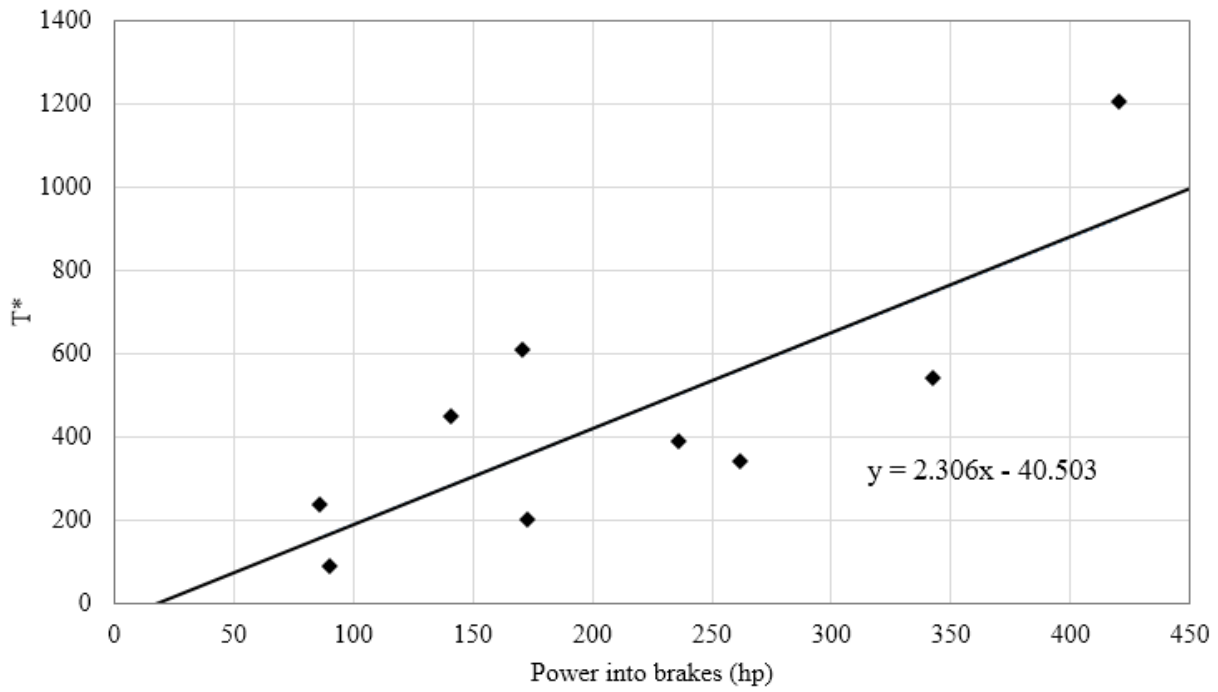


Figure 116. Graph. Plot of Temperature Parameters versus Power into Brakes at 31 mph.

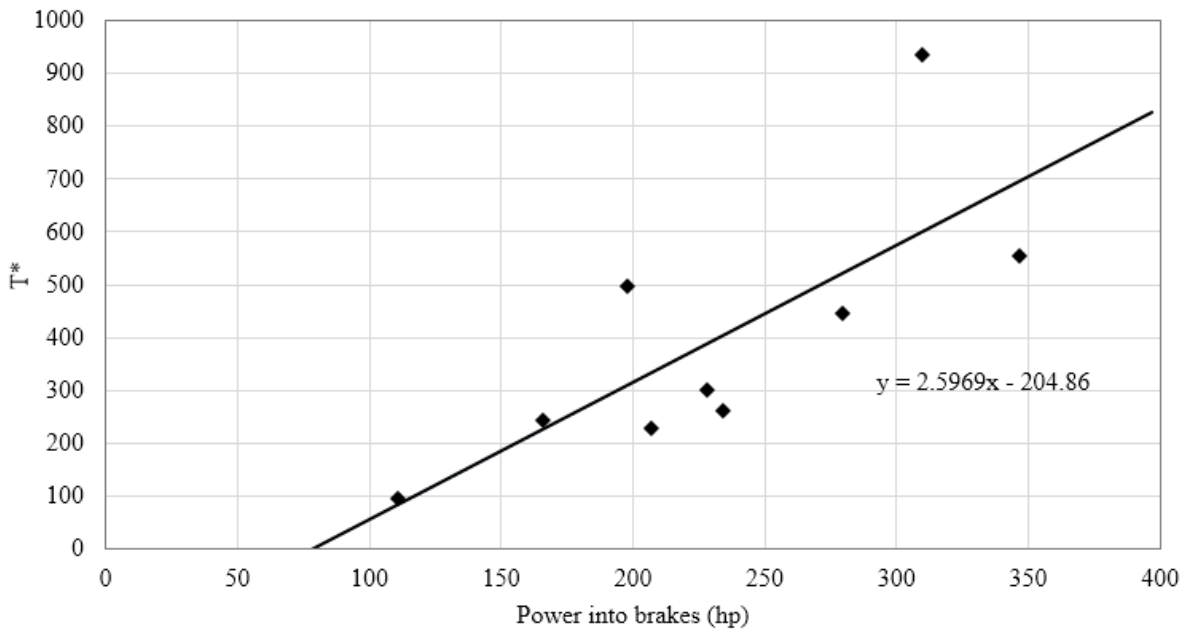


Figure 117. Graph. Plot of Temperature Parameters versus Power into Brakes at 36 mph.

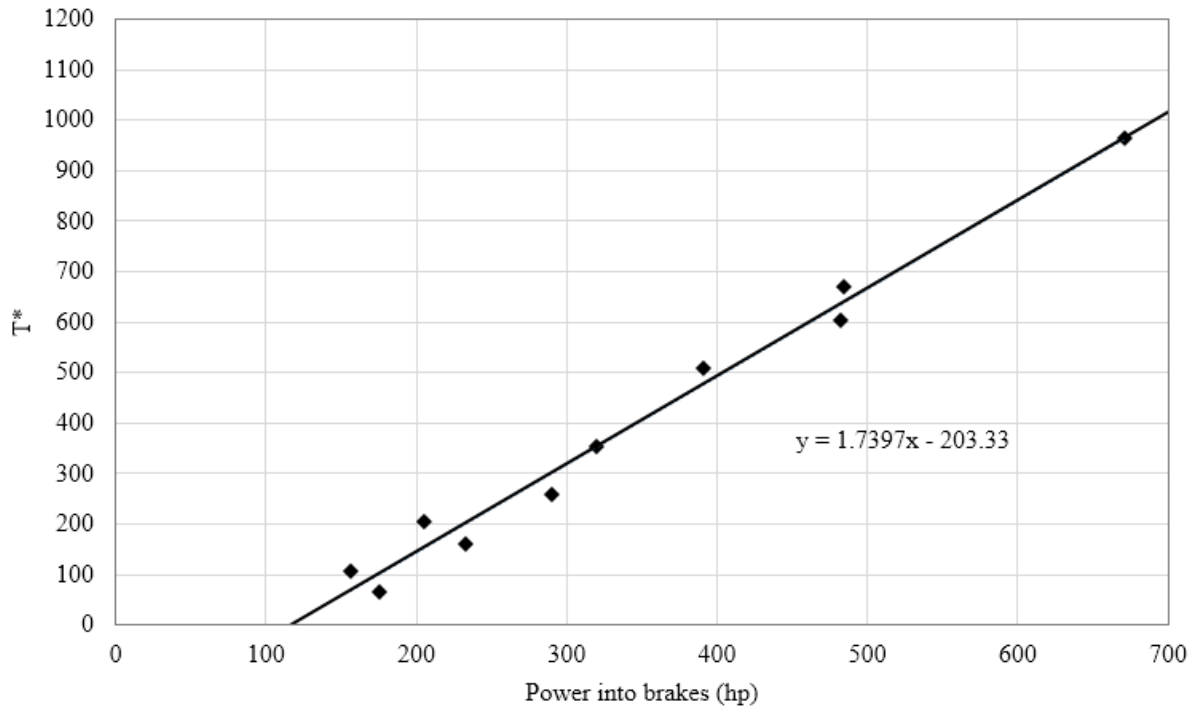


Figure 118. Graph. Plot of Temperature Parameters versus Power into Brakes at 50 mph.

APPENDIX 4: MAXIMUM SAFE SPEED PLOT

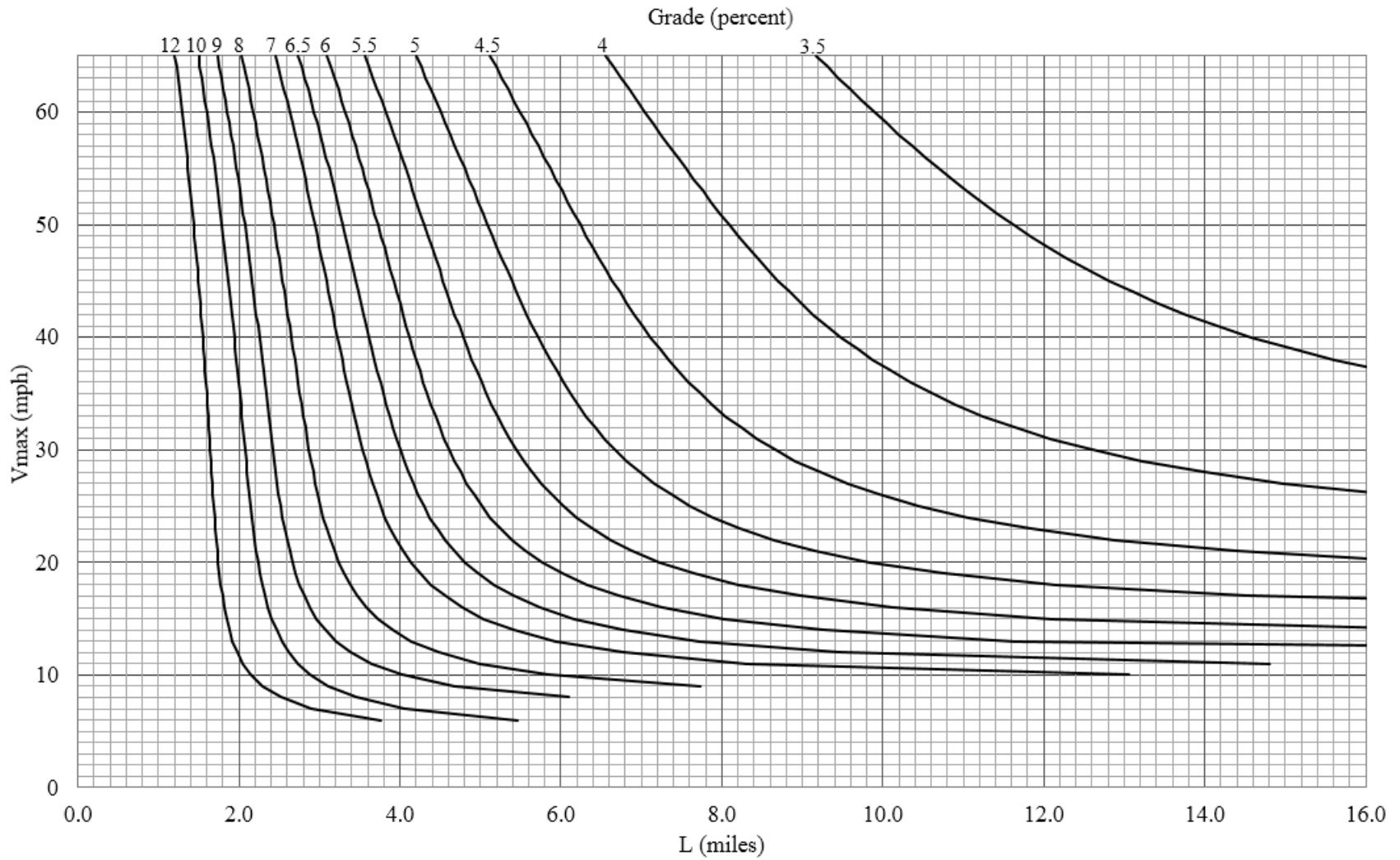


Figure 119. Graph. Maximum Safe Speed as a Function of Grade Length and Steepness for Truck Weight 95,000 lb.

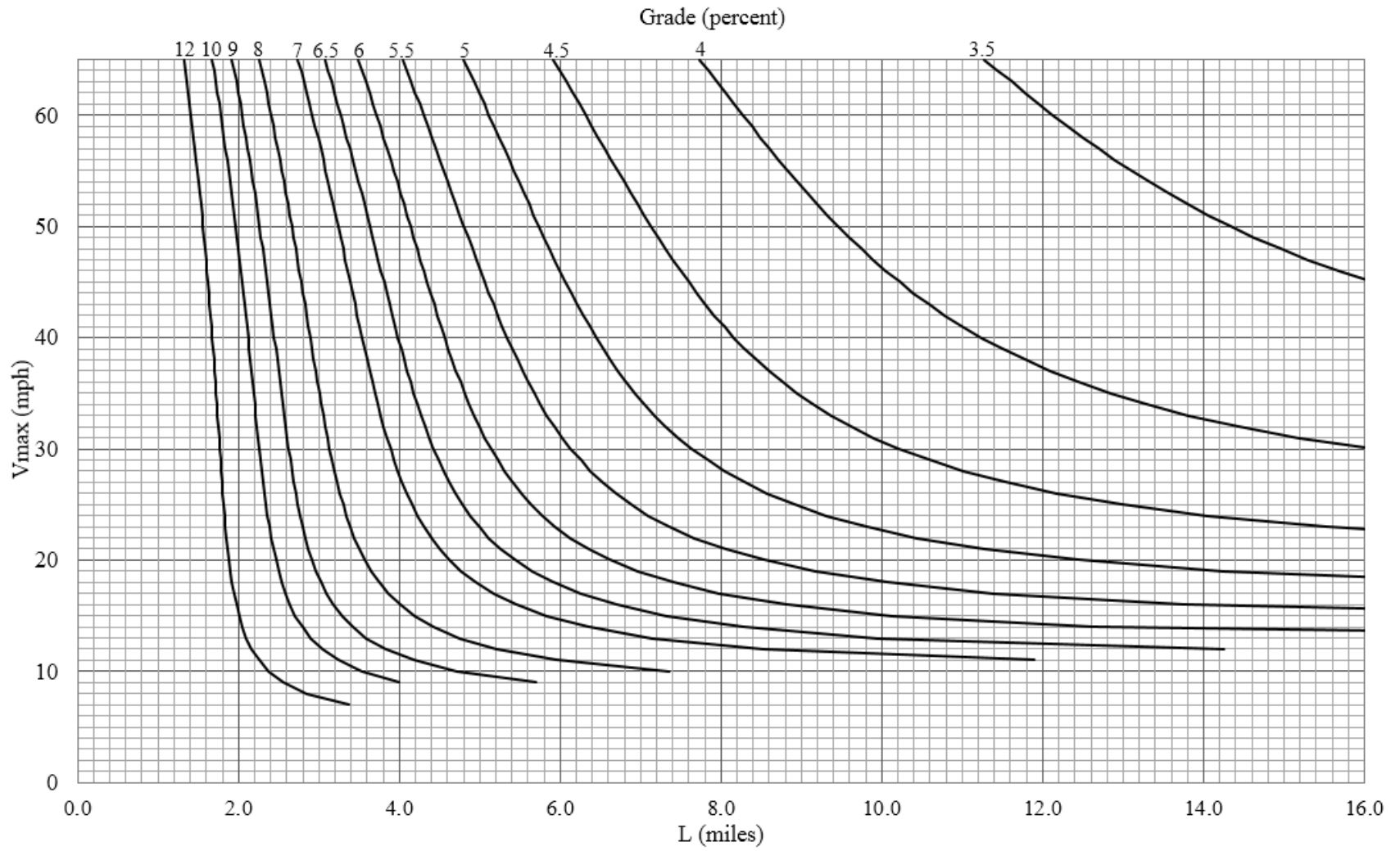


Figure 120. Graph. Maximum Safe Speed as a Function of Grade Length and Steepness for Truck Weight 90,000 lb.

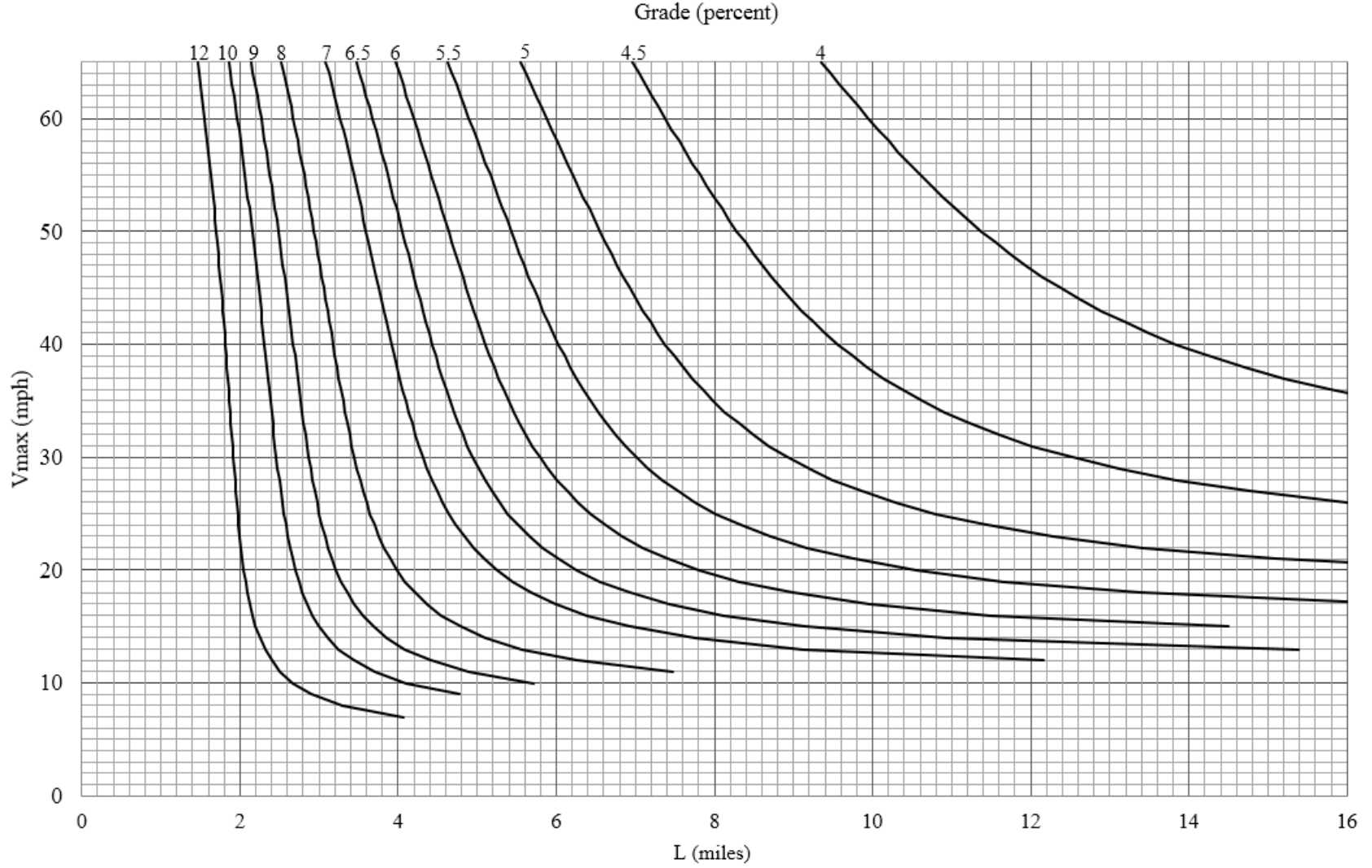


Figure 121. Graph. Maximum Safe Speed as a Function of Grade Length and Steepness for Truck Weight 85,000 lb.

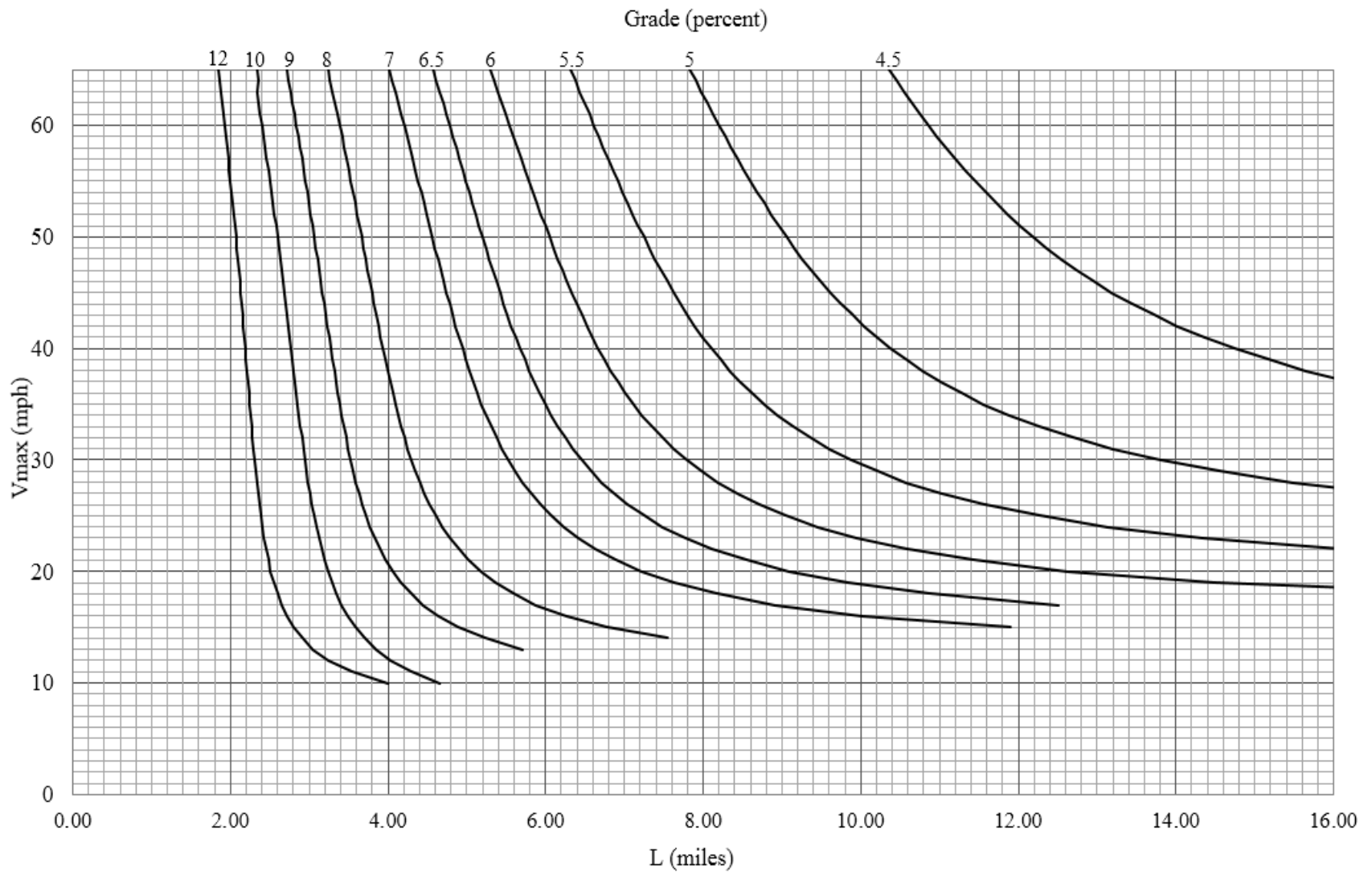


Figure 122. Graph. Maximum Safe Speed as a Function of Grade Length and Steepness for Truck Weight 75,000 lb.

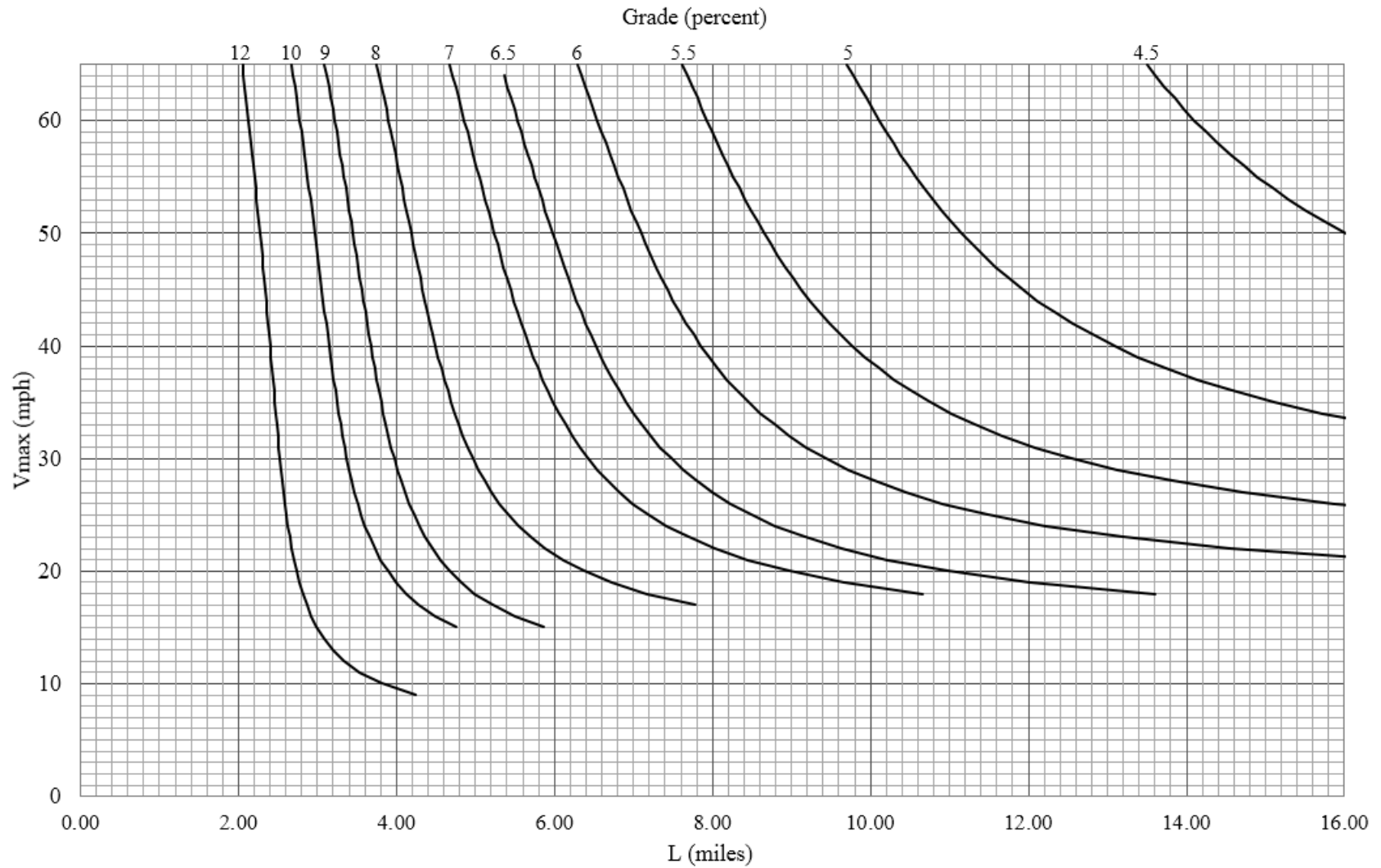


Figure 123. Graph. Maximum Safe Speed as a Function of Grade Length and Steepness for Truck Weight 70,000 lb.

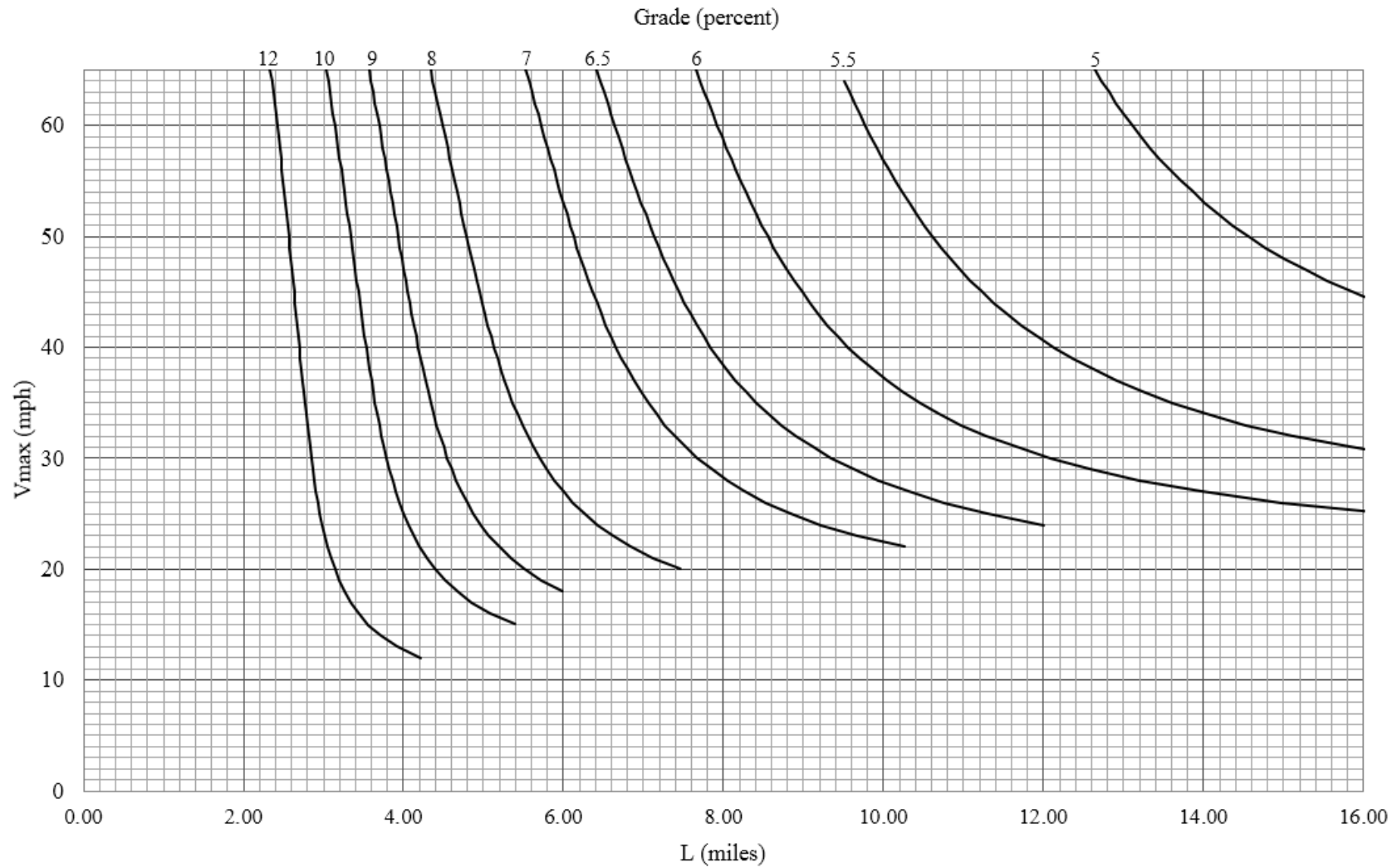


Figure 124. Graph. Maximum Safe Speed as a Function of Grade Length and Steepness for Truck Weight 65,000 lb.

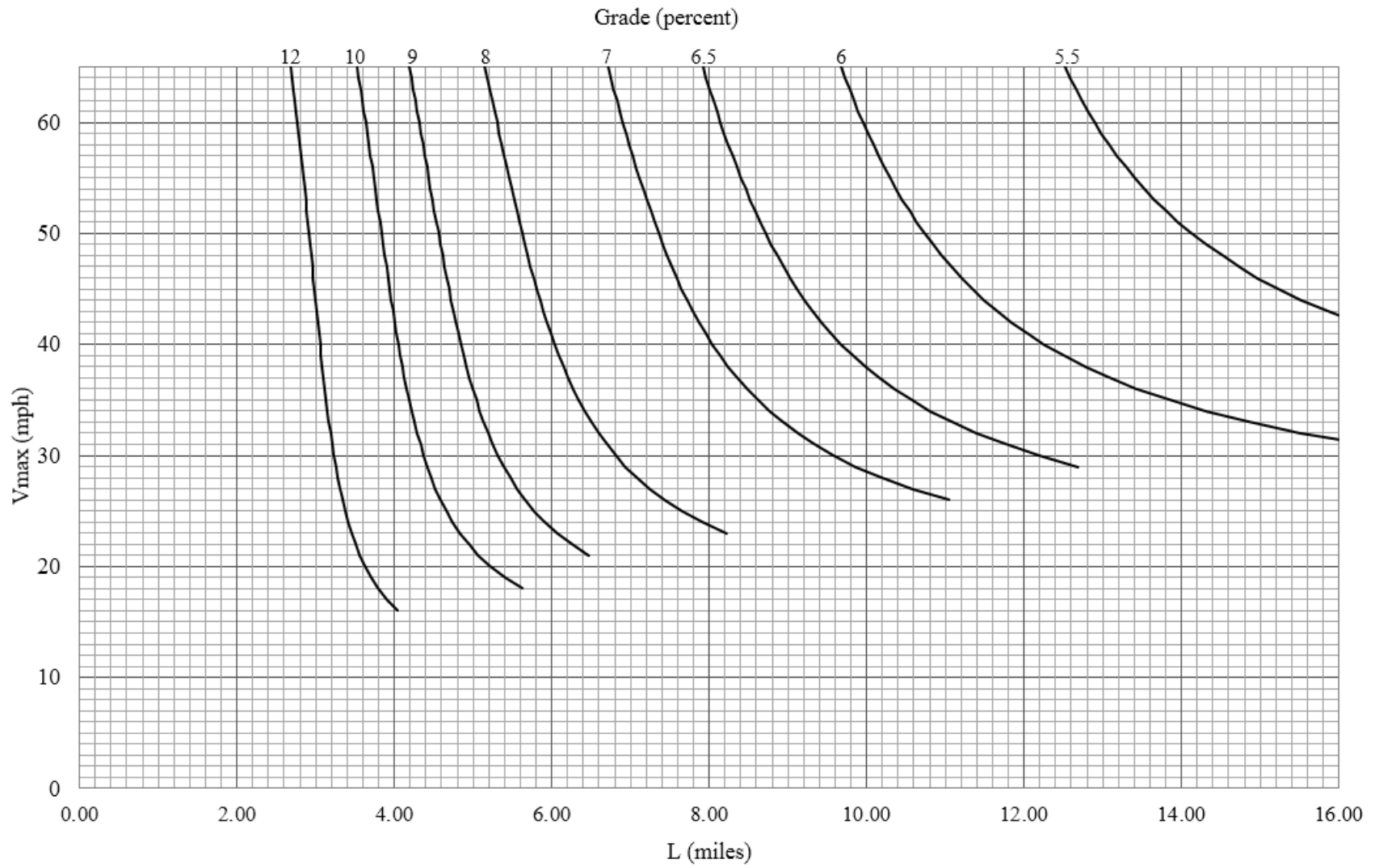


Figure 125. Graph. Maximum Safe Speed as a Function of Grade Length and Steepness for Truck Weight 60,000 lb.

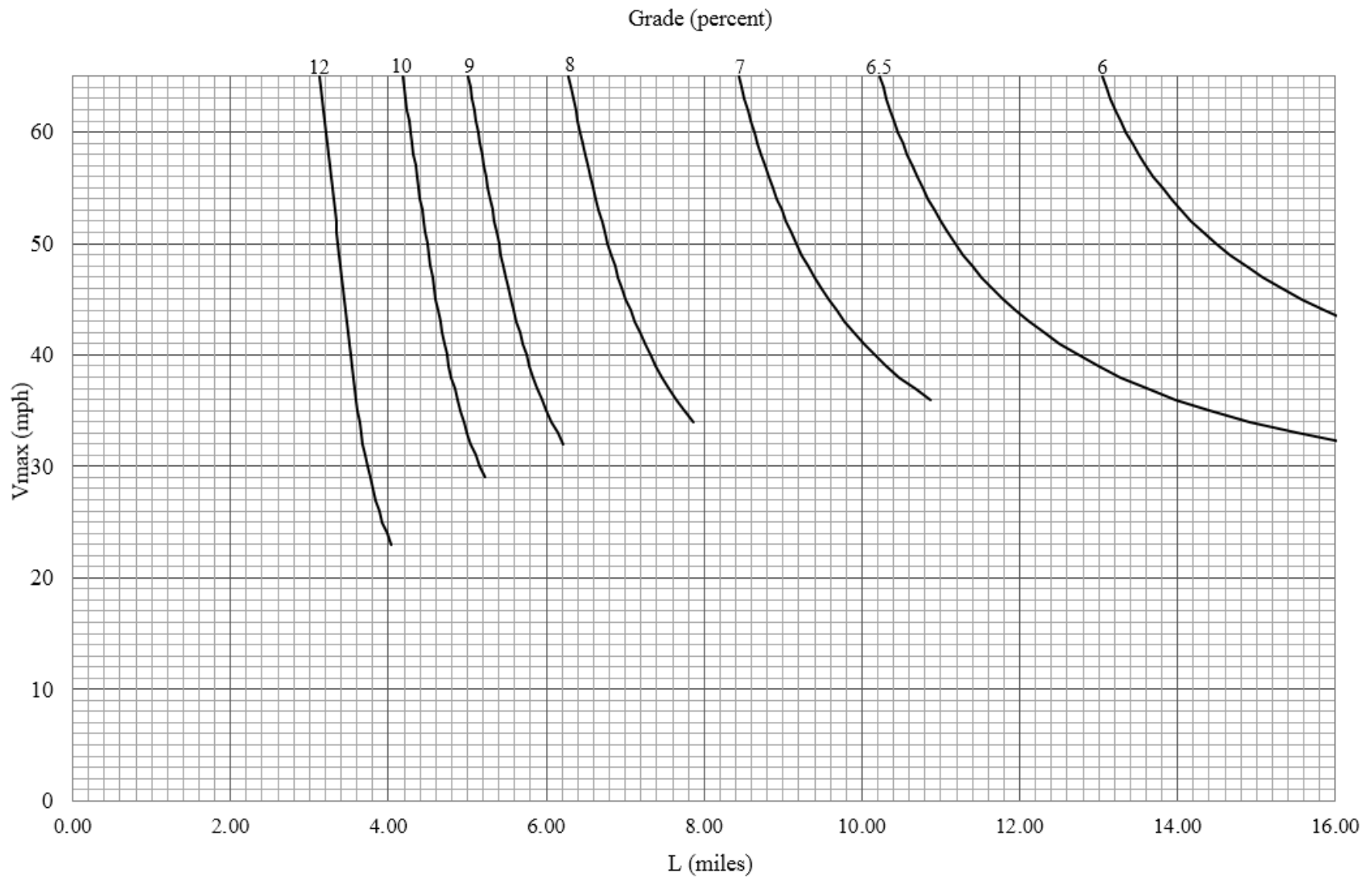


Figure 126. Graph. Maximum Safe Speed as a Function of Grade Length and Steepness for Truck Weight 55,000 lb.

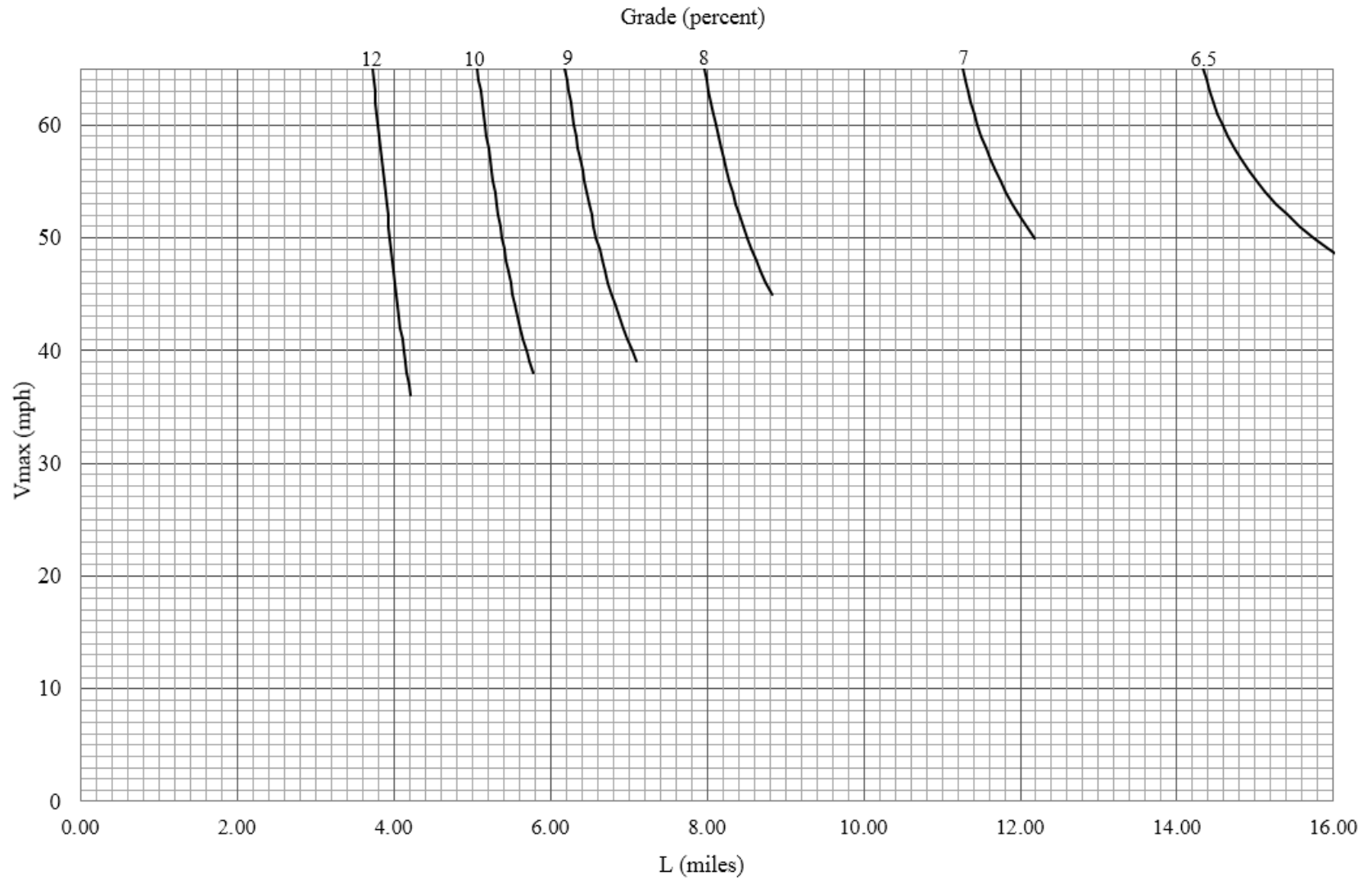


Figure 127. Graph. Maximum Safe Speed as a Function of Grade Length and Steepness for Truck Weight 50,000 lb.

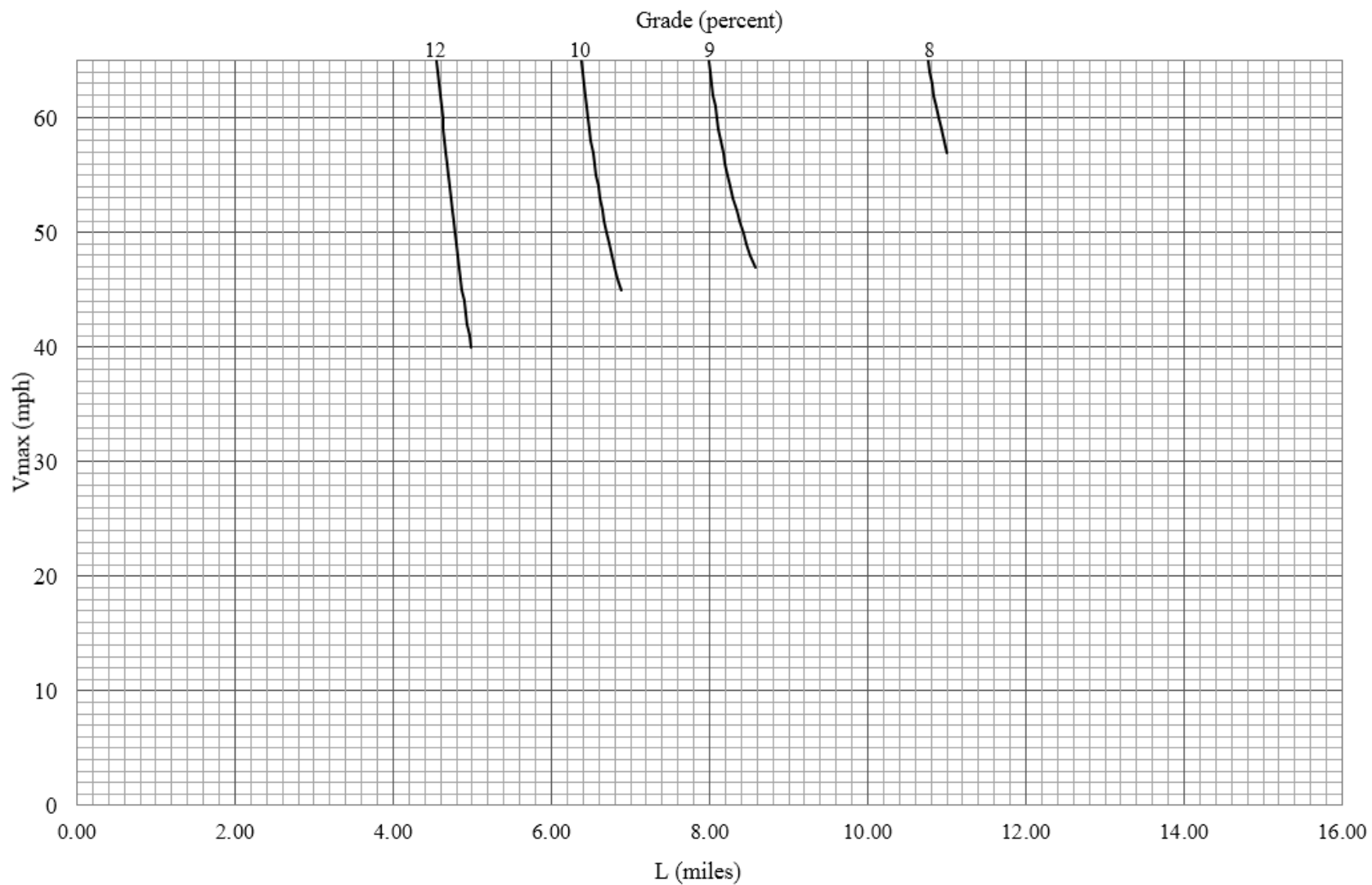


Figure 128. Graph. Maximum Safe Speed as a Function of Grade Length and Steepness for Truck Weight 45,000 lb.

APPENDIX 5: CASE STUDY 2

Case Study 2

This case study was taken from Johnson et al., 1982a. The parameters are as follows:

- Downgrade = 7.0 percent
- Braking length = 6.50 miles
- Maximum weight = 80,000 lb
- Speed limit = 55 mph

Maximum Safe Speeds from Old GSRs Model

Plots used for this case study for the old GSRs model were derived from the modified GSRs model by Johnson et al., 1982a.

1. From the V_{max} versus L plot, the highest integral multiple of 5,000 lb for which V_{max} is greater than 65 mph is 50,000 lb.
2.
$$N = \frac{80,000 - 50,000}{5,000}$$

 $N = 6$. $N > 5$, so the column of weights will begin with 50,000 lb and increase in 10,000 lb increments to 80,000 lb.
3. From the V_{max} versus L plots, the maximum truck weights and corresponding speeds are (Table 18):

Table 18. Maximum Truck Weights and Estimated Safe Speeds (Case Study 2 - Old GSRs).

Maximum Truck Weight (lb)	Maximum Safe Speed (mph)
80,000	12
70,000	14
60,000	23
50,000	55

The increments of truck weights and speeds to the nearest 5 mph are as shown below on Table 19.

Table 19. Maximum Truck Weights and Approximate Safe Speeds (Case Study 1 - Old GSRs).

Weight Increments (lb)	Maximum Safe Speed (mph)
51,000 - 60,000	25
61,000 - 70,000	15
71,000 - 80,000	10

Maximum Safe Speeds from Updated GSRS Model

For this case study, maximum safe speeds were derived from the updated GSRS model (

Table 11).

1. From the updated GSRS model the highest integral multiple of 5,000 lb for which V_{max} is greater than 55 mph is 60,000 lb.
2.
$$N = \frac{80,000 - 60,000}{5,000}$$

$$N = 4.$$
 $N < 5$, so the column of weights will begin with 60,000 lb and increase in 5,000 lb increments to 80,000 lb.
3. From the V_{max} versus L plots, the maximum truck weights and corresponding speeds are (Table 20):

Table 20. Maximum Truck Weights and Estimated Safe Speeds (Case Study 2 - Updated GSRS).

Maximum Truck Weight (lb)	Maximum Safe Speed (mph)
80,000	18
75,000	22
70,000	29
65,000	42
60,000	55

The increments of truck weights and speeds to the nearest 5 mph are as shown below on Table 21.

Table 21. Maximum Truck Weights and Approximate Safe Speeds (Case Study 2 - Updated GSRS).

Weight Increments (lb)	Maximum Safe Speed (mph)
61,000 - 65,000	40
66,000 - 70,000	30
71,000 - 75,000	25
76,000 - 80,000	20

APPENDIX 6: FIELD PICTURES



Figure 129. Photo. The ISX-15 Engine.



Figure 130. Photo. Hyundai Van Trailer.



Figure 131. Photo. Test Truck on a Weighing Scale.



Figure 132. Photo. Technician Adjusting Air Pressure to Brakes.



Figure 133. Photo. Truck Turning During Coast-down Testing.



Figure 134. Photo. Cool-down Testing.

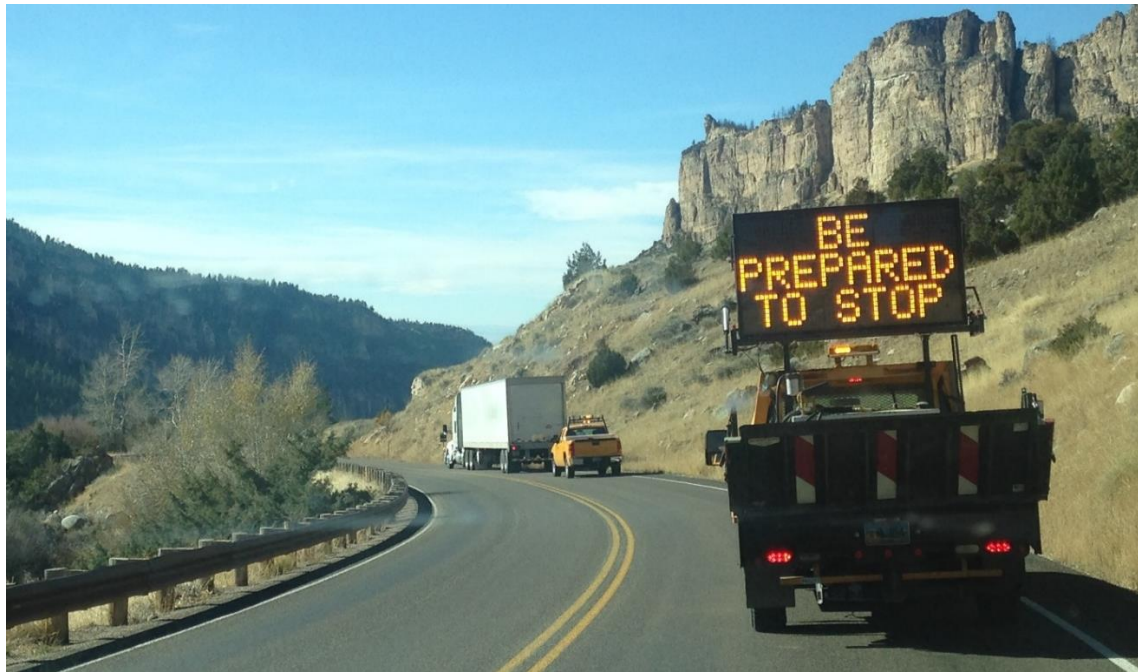


Figure 135. Photo. Hill Descent Testing.



Figure 136. Photo. Truck Brakes Cooling in between Testing.

ACKNOWLEDGEMENTS

The authors would like to thank the Wyoming Department of Transportation (WYDOT) and the Mountain Plains Consortium for financing and assisting with this project. Thanks to Admiral Transport Corporation for donating the test truck, loading facilities and assisting with the field tests. We would also like to thank James Evensen, John Hansen, Rich Hall, Joel Meena, Matt Carlson, and their teams for supporting this project.

The original picture shown in Figure 137 is the copyright property of YouTube and can be assessed from <https://www.youtube.com/watch?v=eQx57GzC2Rs>. The picture shows the forces acting on a truck on a downgrade.

The original picture shown in Figure 138 is the copyright property of Performance Review Institute and can be accessed from <https://p-r-i.org/>. (Performance Review Institute, 2018). The picture shows the components of a drum brake.

The original map shown in Figure 139 is the copyright property of Google® Earth™ and can be accessed from <https://www.google.com/earth>. (Google, 2018). The map overlays showing the track used in coast-down testing was developed as a result of this research project. The overlay is a red line showing the approximate centerline of the test track.